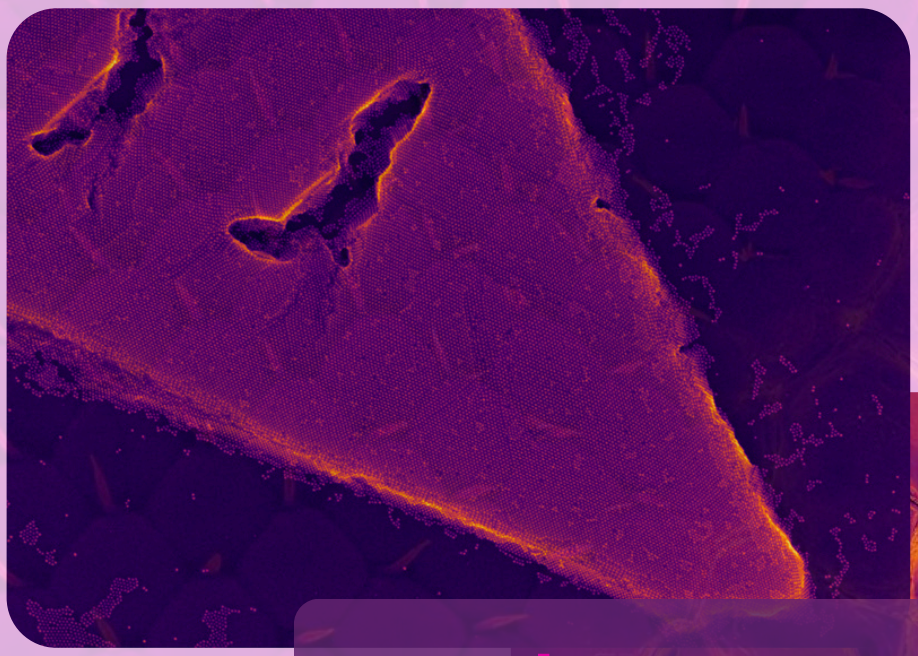

ASEM
Austrian Society for Electron Microscopy

# 16th ASEM Workshop

ISTA

April 20-21, 2026

CONFERENCE PROGRAM

ISTA

We thank our sponsors for their financial support to enable this event



















# Welcome!

On the occasion of the **16th ASEM Workshop 2026**, we are delighted to welcome you to the **Institute of Science and Technology Austria (ISTA)** in Klosterneuburg, hosting the ASEM Workshop here for the very first time.

Over the next two days, this campus becomes a meeting point for a community united by a shared fascination: revealing structure, organization, and composition far beyond the limits of the naked eye. The program spans life sciences and materials sciences alike—from the architecture of the mammalian respirasome and the ultrastructural organization of cells and tissues, to multimodal and ultrafast scanning electron microscopy, advanced analytical workflows such as EELS and EDX tomography, and investigations into the structure–property relationships of complex materials.

With around 175 participants, 32 talks, and more than 40 posters, we have aimed to put together a well-rounded program that showcases exciting research, methodological innovation, and practical experience across disciplines. At the same time, we have deliberately allowed space for what often matters just as much: catching up with friends and colleagues, engaging in interesting discussions during the poster session or over a bite to eat, and exchanging ideas and experience that inspire new directions long after the workshop ends.

The ASEM Workshop has always been a place where early-career researchers can present their work and meet on equal footing with seasoned experts, fostering meaningful interactions across generations and research fields – interactions that that often spark new ideas, fresh perspectives and maybe even lasting collaborations.

We hope you will use these two days to enjoy the talks, explore the posters, generously share your own experience, ask the questions you were saving for coffee breaks, and make the most of this rare opportunity to spend time with so many people who understand why a slightly better contrast transfer function can make your day!

We sincerely thank all our sponsors for their generous support in making this workshop possible and accessible for our EM community in Austria.

We wish you a rewarding and enjoyable workshop and invite you to join us in appreciating the art and science of electron microscopy that connects our community!

Your ASEM 2026 Organization Committee
Ludek, Leonid, Vanessa, and Bettina

# Content

# HITACHI
# FlexSEM 1000 II

VIDEKO
our vision: your success.

## ADVANCED PERFORMANCE IN COMPACT SHAPE

Wolfram

6x to 300.000x

0,3 - 20 kV

4 nm at 20 kV

**Detectors/Various Analyzers**
- Chamber Scope
- Optical Navigation Camera
- EDS analysis (Bruker / EDAX / Oxford)
- EBDS
- Everhart Thorney SE Detector
- Low KV Fast 5-segment high sensitivity BSE detector
- UVD – Variable Pressure SE detector
- UVD - Cathodoluminescence Detector
- UVD-STEM – High sensitivity STEM holder

**Software:**
- Hitachi map 3D – Surface reconstruction Software
- Large Area Imaging (Multi ZigZag)
- EM Flow Creator

**Automatic Image Controller:**
- Auto brightness & contrast control • Auto focus control • Auto astigmatism correction & focus
- Auto filament saturation
- Auto beam alignement
- Auto start

**Automatic axis alignment:**
- Auto beam adjustment
- Auto optical axis alignement
- Auto beam brightness control

**www.videko.at**

office@videko.at

EDWARDS HITACHI VAT PASSION. PRECISION. PURITY. JASCO THYRACONT Vacuum Instruments PINK

# Transportation

*Shuttle bus schedule*

MONDAY, 20 APRIL

**10:30** From SCHWEDENPLATZ (Night bus stop) Vienna to ISTA with a stop at Klosterneuburg Stadtplatz (at around 10:55)

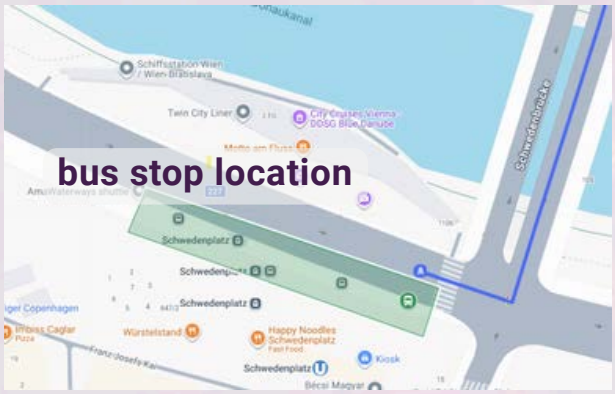


**18:20** From ISTA to Conference Dinner

**22:00** From Conference Dinner to SCHWEDENPLATZ Vienna

Conference dinner is at restaurant

"Mayer am Pfarrplatz"

Address: Pfarrplatz 2, 1190 Vienna

TUESDAY, 21 APRIL:

**08:00** From SCHWEDENPLATZ (Night bus stop) Vienna → ISTA with a stop at Klosterneuburg Stadtplatz (at around 08:25)

**16:30** From ISTA to SCHWEDENPLATZ Vienna

# ISTA Campus Map

# Floorplan Moonstone Seminar Center

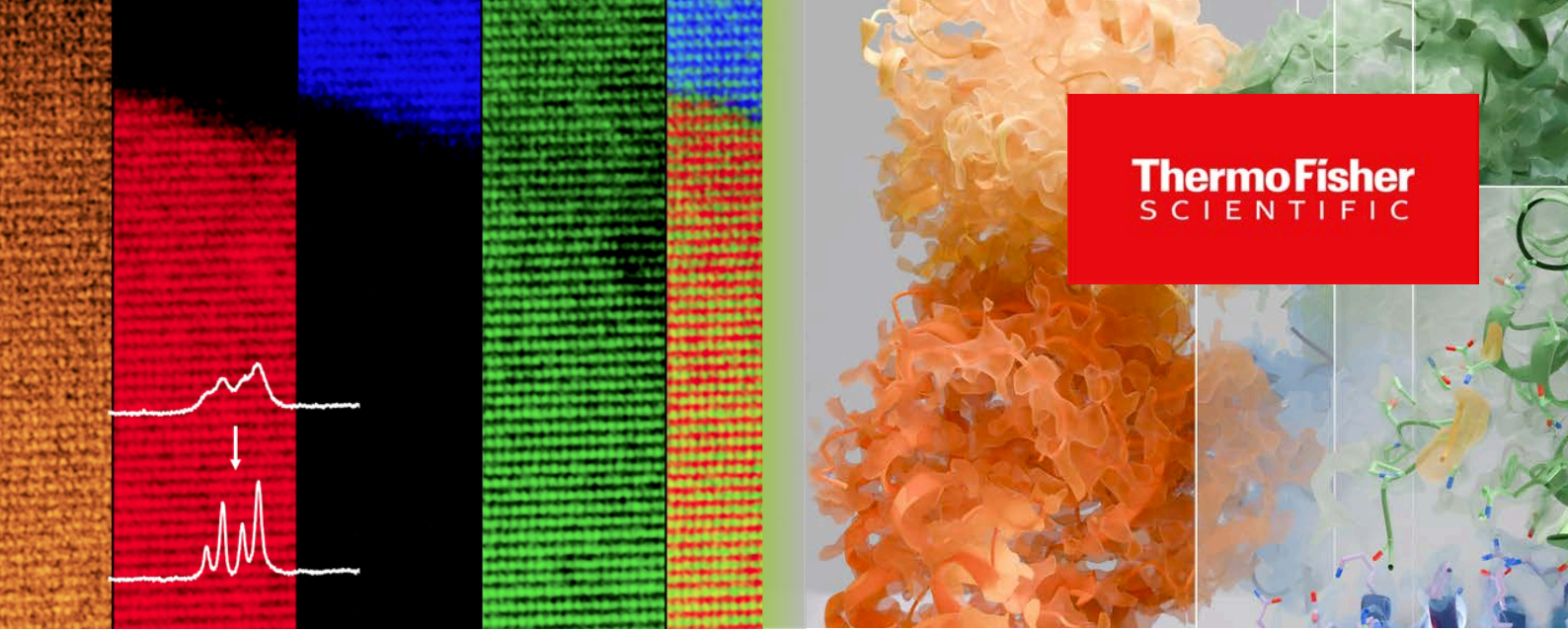


# Driving innovation in materials and life sciences with outstanding TEM performance

Accessible TEM and (S)TEM for every user with the Glacios™ cryo-TEM and Iliad™ (S)TEM

## Glacios™ cryo-TEM: The complete solution for high-resolution structure determination

Ideally suited for:

- Single particle analysis
- Cryo-electron microscopy
- Micro-electron diffraction

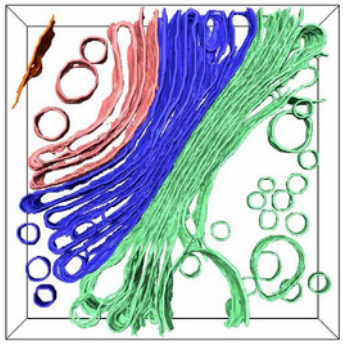

*3D visualization of Golgi apparatus from C, reinhardti using Glacios 2 Cryo-TEM. Sample prepared with Thermo Scientific ™ Aquilos™ Cryo-FIB.*

## Iliad™ S/TEM: Seamlessly integrated EELS and EDS

- Advanced EELS and EDS spectroscopy
- NanoPulser Beam Blanker for dose optimization
- Quick voltage switching (30-300 kV).
- Velox Software for data processing
- AutoScript TEM for customized workflows

Learn more at the presentation

## Ice to data

with our electron microscopy specialist
Javier Fernandez-Collado

To learn more, visit thermofisher.com/em

thermo scientific

# Program

## MONDAY, APRIL 20TH

| TIME | |
|---|---|
| **09:30** | Registration |
| **12:00** | Opening |
| **12:15** | **Invited Speaker Gerhard Sommer:** From Forces to Fibers: Multiscale Visualization of Mechanical Effects on Arteries |
| **12:45-13:35** | **Clara Kofler:** From four t(w)o three: An exploration of interferometric 4D-STEM for measuring 3D variations in twisted bilayer graphene |
| | **Elias Pescoller:** Towards Quantum Computing Enhanced Electron Microscopy |
| | **Philip Steiner:** Immunogold Live-Cell CLEM for the ultrastructural localization of TPC1 in J774 macrophages |
| | Sponsor presentation by Martin Slama (**Tescan**) |
| **13:35** | Coffee break |
| **14:00** | Fritz Grasenick Award ceremony |
| **14:10** | **Grasenick Award lecture by Antonin Jaros:** Sensing Spin Precession with Free Electrons |
| **14:30** | **Grasenick Award lecture by Irene Vercellino:** SCAF1 drives the compositional diversity of mammalian respirasomes |
| **14:50** | Sponsor presentation by Javier Fernandez Collado (**Thermo Fisher**) |
| **15:00** | Coffee break |
| **15:30-16:40** | **Murat Sivis:** Multimodal Ultrafast Scanning Electron Microscopy |
| | **Peter Kirchweger:** Advanced cryo-STET imaging: targeting the mtDNA in situ |
| | **Tatiana Kormilina:** Accessible workflows for EELS and EDX tomography through automated acquisition and multimodal reconstruction |
| | **Yong Huang:** Multi-scale investigations on the strengthening and toughening of highly nanotwinned transition metal nitride film |
| | Sponsor presentation by Wolfgang Schwinger (**Zeiss**) |
| | Sponsor presentation by Mikhail Lazarev (**Bruker**) |
| | **Conference Group Photo** |
| **16:40-18:10** | **Poster session 1** |
| **19:00** | **Conference dinner** |

# Program

## TUESDAY, APRIL 21ST

| TIME | |
|---|---|
| **8:30** | Morning Coffee |
| **09:00** | **Invited Speaker Daniel Knez:** Atomic-Scale Insights into Matter via Multi-Modal STEM: From Structure to Function |
| **9:30-10:20** | **Johannes Liesche:** TEM-tomography for structure-function modeling of cell connections in plant tissues |
| | **Zhuo Chen:** Direct observation of Schottky-vacancy clusters and their mechanical response in MoN/TiN superlattice |
| | **Bernadette C. Ortner:** Electron Microscopy Analysis for the Optimization of Perovskite–Organic Tandem Solar Cells |
| | Sponsor presentation by Fengfa Yao (**CIQTEK**) |
| **10:20** | Coffee break |
| **10:45** | **Special Guest presented by ISTA: Charles Roques-Carmes** Electron Microscopy as a Platform for Nanophotonics and Quantum Optics |
| **11:15-12:00** | **Alexey Minenkov:** Plasma FIB Tomography of Mast Cells: Challenges and Solutions |
| | **Umair Javed:** Origin of pores in electron irradiated hexagonal boron nitride |
| | Sponsor presentation by Lars Jansen (**Schaefer Scientific**) |
| | Sponsor presentation by Georg Raggl (**Jeol**) |
| **12:00** | **Poster session 2 & Lunch break** |
| **13:30** | **General Assembly** (incl. Poster Prize and Image Competition Ceremony) |
| **14:45** | Coffee break |
| **15:00-16:00** | **Sergei Bogdanov:** Ghost Imaging with Free Electron-Photon Pairs |
| | **Lena Wiesbauer:** Advanced multimodal Electron Microscopy for Characterization of Two-Pore Channels in Macrophages **Lukas** |
| | **Lobenwein:** Optimization of dopant detection in wide band gap semiconductors using STEM EELS |
| | Sponsor presentation by Sajjad Tollabimazraehno (**Videko/Hitachi**) |
| | Sponsor presentation by Bas ter Mull (**Protochips**) |
| **16:00** | Closing & Lab tours |

## Introducing the new

# Crossbeam 750

## For Scientific & Industrial Research

ZEISS new high-end FIB/SEM system with **Gemini 4 column** for the most challenging imaging and milling tasks.


- better & faster imaging
- precise end-pointing
- improved field-of-view
- high precision 6” & 8” stage
- 4 mm coincidence point
- 1.2 nm at 1 keV with DCV*

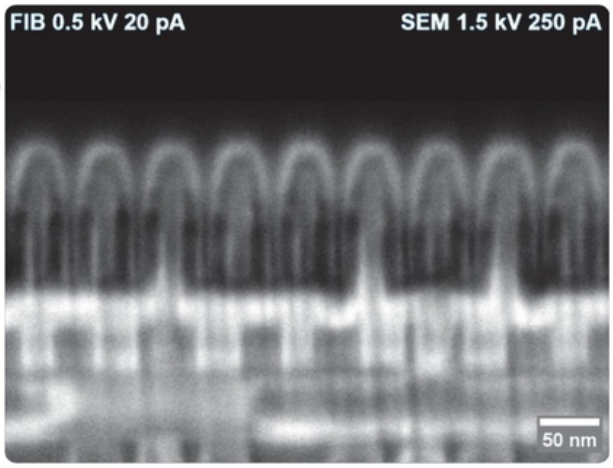


*DCV = image deconvolution

# Poster Program

# A SECOND LIFE FOR YOUR SEM

**We modernize your SEM with new electronics, software and controls.**


your **End of Support** solution

## SUPPORT

**Extend microscope service** with 10 years spare part guarantee.

## PERFORMANCE

Increase **efficiency** with the most **powerful and versatile** scan generator and image acquisition, including cutting-edge **automation.**

## RESSOURCES

Use **resources sustainably** and reduce power consumption by up to 70%.

Learn more about our SEM Modernization:
**www.pointelectronic.com**

point electronic

# Talk Abstracts

## From Forces to Fibers: Multiscale Visualization of Mechanical Effects on Arteries

Gerhard Sommer[1], Anna Pukaluk[2], Melanie Pranger[3], Lisa Wallinger[1], Dagmar Kolb[3,4], Gerd Leitinger[3], Christian Viertler[5], Gerhard A. Holzapfel[1,6]

[1]*Institute of Biomechanics, Graz University of Technology, Austria*
[2]*Helmholtz Pioneer Campus, Helmholtz Zentrum München, Neuherberg, Germany*
[3]*Gottfried Schatz Research Center, Medical University of Graz, Austria*
[4]*Core Facility Ultrastructure Analysis, Medical University of Graz, Austria*
[5]*Diagnostic and Research Institute of Pathology, Medical University of Graz, Austria*
[6]*Department of Structural Engineering, Norwegian University of Science and Technology, Norway*

Altered arterial tissue properties in diseases such as atherosclerosis arise from remodeling processes that modify the composition and organization of the vessel wall across multiple length scales. These changes affect extracellular matrix components, including collagen fibrils, elastic fibers, and interfibrillar proteoglycans (PGs), which strongly influence the mechanical behavior of arterial tissue. At the same time, coronary stent implantation (CSI), a widely used treatment for coronary artery disease, may induce vascular injury during deployment and is closely associated with restenosis. Understanding how arterial micro- and ultrastructure respond to mechanical loading is therefore essential for improving stent design and for gaining deeper insight into vascular remodeling.
In these studies, biomechanical testing was combined with high-resolution electron microscopy to investigate load-dependent micro- and ultrastructural changes in arterial tissues and to analyze coronary artery damage induced by simulated stent deployment. Unloaded and mechanically loaded samples were fixed with glutaraldehyde and prepared for structural analysis. Vessel surfaces were examined using SEM, while collagen fibrils and smooth muscle cells (SMCs) were imaged by TEM, and proteoglycans (PGs), together with collagen fibrils, were analyzed using electron tomography (ET).

ASEM showed that surface damage after simulated stenting was more pronounced with longitudinal than with circumferential stent-strut orientation, reflecting the predominantly circumferential alignment of collagen fibers in the tunica media, which provides greater mechanical resistance. Nevertheless, severe endothelial injury occurred beneath and around the indented region regardless of orientation, suggesting that endothelial removal may contribute to restenosis after stent implantation. TEM further revealed that the mechanical impact extended beyond the intima into the tunica media. SMCs beneath the indentation exhibited substantial structural damage, whereas collagen fibrils largely maintained their integrity. In contrast, PGs showed pronounced rearrangement within the collagen network. ET reconstructions revealed clustering of PGs beneath the indented region, where they were displaced by the dense collagen structure (Fig. 1)

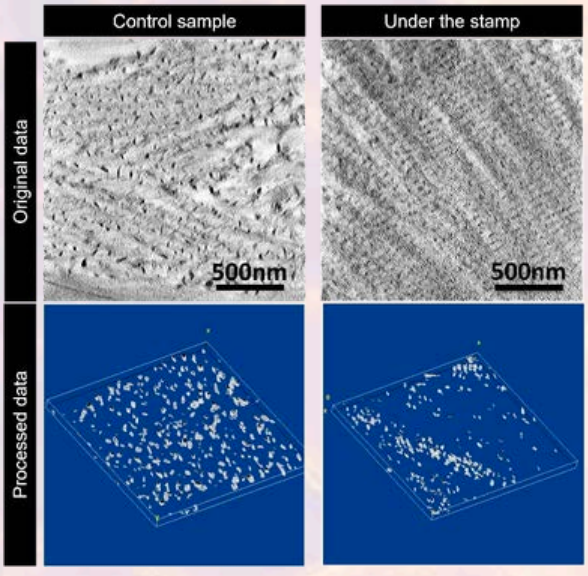


Fig 1: Representative ET reconstructions showing PG organization in an uninjured control sample (left) and in tissue beneath the stent strut (right).

Overall, the combination of biaxial mechanical testing and electron microscopy techniques enables visualization and quantification of load-dependent structural changes in arterial tissues. These findings contribute to a better understanding of vascular injury mechanisms and extracellular matrix remodeling and may support the development of improved stent designs aimed at reducing vascular damage and restenosis.

# From four t(w)o three: An exploration of interferometric 4D-STEM for measuring 3D variations in twisted bilayer graphene

Clara Kofler[1,2], Florian Libisch[3], Toma Susi[1], Jani Kotakoski[1]

[1]*Faculty of Physics, University of Vienna, Boltzmanngasse 5, 1090 Vienna, Austria;*
[2]*Vienna Doctoral School in Physics, University of Vienna, Boltzmanngasse 5, 1090 Vienna, Austria;*
[3]*Institute for Theoretical Physics, TU Vienna, Wiedner Hauptstrasse 8-10/136, 1040 Vienna, Austria;*
*Corresponding author: clara.kofler@univie.ac.at*

Four-dimensional (4D) scanning transmission electron microscopy (STEM) has become an almost routine procedure in high-level electron microscopy now that modern pixellated direct electron detectors are able to quickly collect, and computers are able to handle the massive amount of diffraction data characteristic of this method. However, computational power is merely the muscle, and cannot achieve much without solid theory and steadfast thought behind the employed analysis. Therefore, a lot of effort has gone into developing ways to coax novel information from 4D-STEM datasets, and while some methods, like ptychography or center of mass imaging, are by now well established, others are more obscure.

Here, we want to discuss interferometric 4D-STEM, a method still in its adolescence, that could shed light on a property well hidden from conventional STEM, the three-dimensional (3D) structure of thin specimen, in particular twisted bilayer graphene. There, the overlap of the identical but twisted layers can lead to the formation of periodic moiré patterns, superstructures that cause the emergence and change of different properties -- among them the distance between the layers, which varies depending on the local stacking order [1].

By analyzing interference patterns formed in the overlap regions of diffraction disks originating from the separate layers when probed with a defocused beam, as shown in Figure 1, it should be possible to reconstruct the subtle interlayer distance variations and provide a spatially resolved distance map over the whole moiré pattern. Building upon the works by Latychevskaia [2] and
Zachman [3], who established the foundation of this method, we examine whether, to what extent, with which resolution, and under what conditions interferometric 4D-STEM gives sensible results, by systematically testing it for simulated data of increasing complexity.

This systematic study should not only lay the groundwork for hypothetical future experimental work, but also provide a useful starting point for people interested in doing similar work, hopefully saving them some time and hardship. With the nature of data and also of science itself changing in the wake of technological advances, it is more important than ever to share our work and support one another in our quest for good, reliable, and open research.

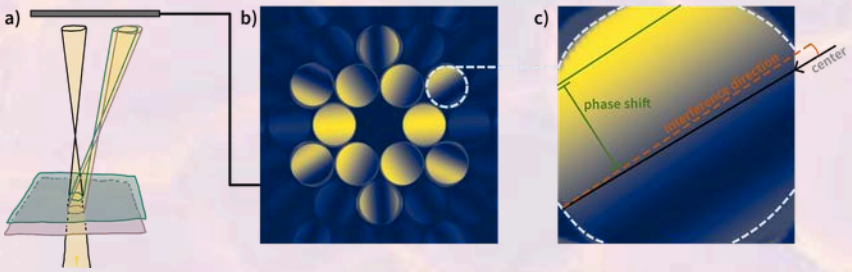


**Figure 1:** Interferometric 4D-STEM. a) The defocused electron beam (coming from below) is scattered on the two layers seperately leading to two diffraction disks for each scattering direction. b) The overlap regions of the diffraction disks show interference features. c) The phase shift and interference direction in the overlap region contain 3D information.

[1] Uchida et al., Phys. Rev. B 90, 155451 (2014)
[2] Latychevskaia et al., Ultramicroscopy 219, 113020 (2020)
[3] Zachman et al., Small 17, 2100388 (2021)

# Towards Quantum Computing Enhanced Electron Microscopy

Elias Pescoller[1,2,*], Santiago Beltrán Romero[2,3], Sebastian Egginger[4], Dominik Hornof[2,3], Nicolas Jungwirth[5], Martino Zanetti[6,7,2], Michael S. Seifner[2,3], Iva Březinová[1], Philipp Haslinger[2,3], Thomas Juffmann[6,7], Johannes Kofler[4], Dennis Rätzel[2,3,8], Philipp Schindler[7]

[1]*Institute for Theoretical Physics, TU Wien, Wiedner Hauptstraße 8-10/136, 1040 Vienna, Austria*
[2]*Vienna Center for Quantum Science and Technology, Atominstitut, TU Wien, Stadionallee 2, 1020 Vienna, Austria*
[3]*University Service Centre for Transmission Electron Microscopy, TU Wien, Stadionallee 2, 1020 Vienna, Austria*
[4]*Johannes Kepler University, 4040 Linz, Austria*
[5]*University of Innsbruck, 6020 Innsbruck, Austria*
[6]*University of Vienna, Faculty of Physics, Vienna Center for Quantum Science and Technology, 1090 Vienna, Austria*
[7]*University of Vienna, Max Perutz Labs, 1030 Vienna, Austria*
[8]*ZARM, University of Bremen, Am Fallturm 2, 28359 Bremen, Germany*

Advanced imaging techniques such as microscopy have long been a foundation for scientific discovery, enabling the visualization and understanding of microscopic objects. The development of electron microscopy has overcome the resolution limit of optical microscopy, pushing the size of resolvable objects down to the nanoscale. Still, traditional electron microscopes rely on classical intensity measurements, absorbing electrons upon detection and thereby greatly limiting the way information can be extracted from them.
Quantum computing enhanced electron microscopy aims to supplement the classical detectors with the coherent interaction with a quantum computer consisting of a trapped ion lattice. We present a protocol that, by preparing the trapped ions in non-classical states of motion, realizes a conditional Pauli-X gate on the qubits, depending on the presence of a probe electron [1]. This leads to entanglement between the quantum computer and the state of the electron, which may be used to transfer information about a specimen to the quantum computer, allowing for coherent information processing and readout using arbitrary projective measurements. Multiple electrons can become entangled through their interaction with the quantum computer, enabling sensing schemes that go beyond the standard quantum limit and may pave the way to dose-efficient electron microscopy.

**References**

[1]: Elias Pescoller, Santiago Beltrán-Romero, Sebastian Egginger, Nicolas Jungwirth, Martino Zanetti, Dominik Hornof, Michael S. Seifner, Iva Březinová, Philipp Haslinger, Thomas Juffmann, Johannes Kofler, Philipp Schindler, and Dennis Rätzel. Coupling free electrons to a trapped-ion quantum computer. arXiv: 2601.11446 [quant-ph].

**Acknowledgements**

This research is funded in part by the Gordon and Betty Moore Foundation Grant GBMF12992, by the Austrian Science Fund (FWF) through Grant No. 10.55776/COE1, Y1121, P36041, P35953 and the FFG-project AQUTEM.

*elias.pescoller@tuwien.ac.at*

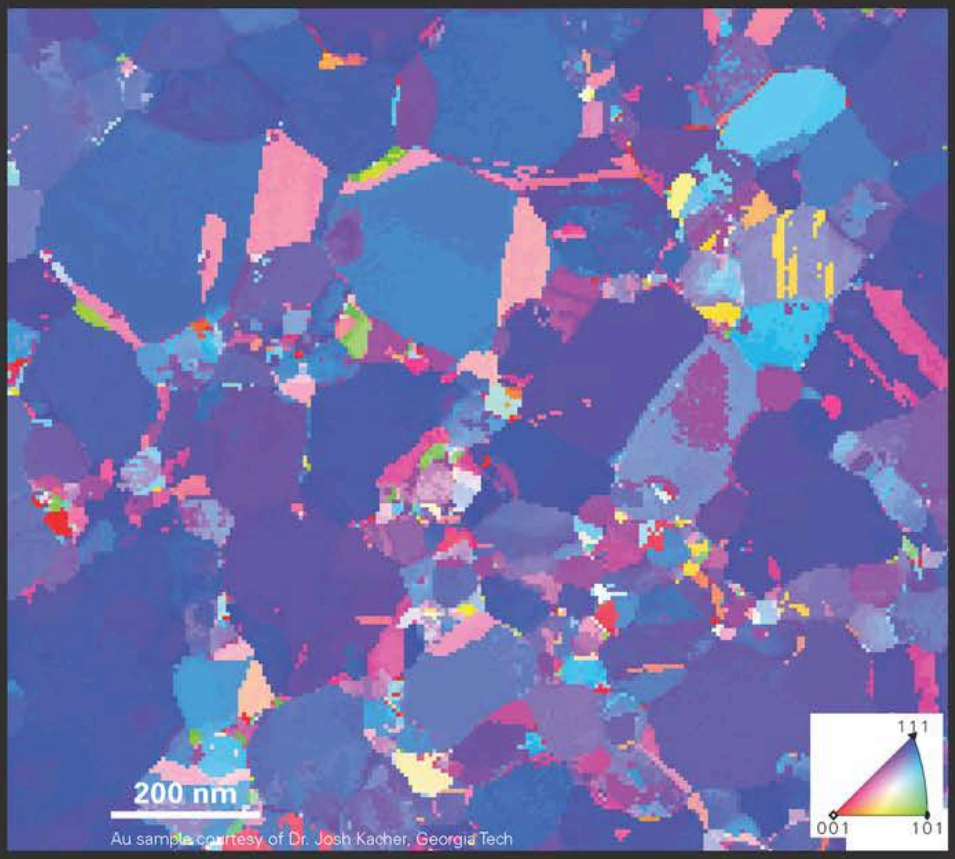


## 4D STEM orientation analysis

STEMx® OIM features in DigitalMicrograph® use an automated template-matching approach to index patterns and generate orientation maps. Orientation map data generated by STEMx OIM can be imported into EDAX® OIM Analysis™ for further processing or linked with EELS, EDS, and other 4D STEM analysis data thanks to eaSI™ technology in DigitalMicrograph.

To learn more, visit gatan.com.

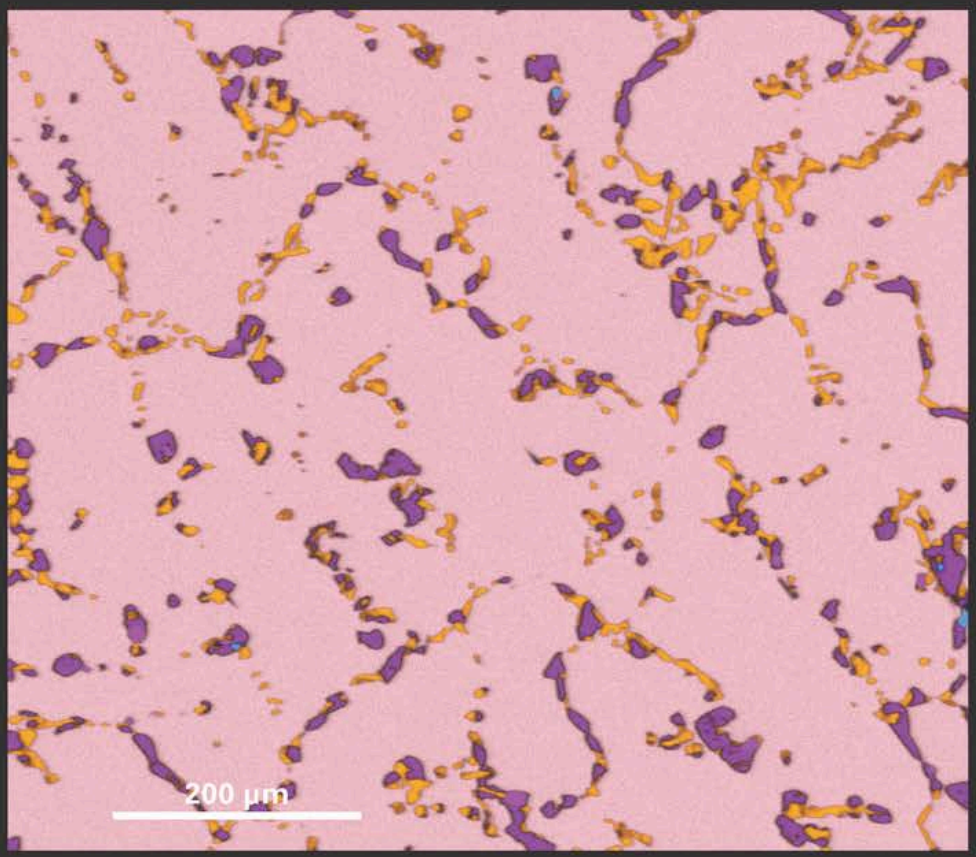


## Introducing the EDAX Octane Elite Ultra EDS System

The EDAX® Octane Elite Ultra energy dispersive x-ray spectroscopy (EDS) system provides revolutionary compositional analysis in the scanning electron microscope. The windowless 160 $mm^2$ EDS detector delivers superior sensitivity to light and heavy elements and provides accurate analytical results at accelerating voltages up to 30 kV.

To learn more, visit edax.com.

GATAN + EDAX
AMETEK

# Immunogold Live-Cell CLEM for the ultrastructural localization of TPC1 in J774 macrophages

Philip Steiner[1], Lena Wiesbauer[1], Emma Punzenberger[1], Julia Schatz[1], Ancuela Andosch[2,3], Yuliia Nazarenko[1], Robert Mallmann[4], Norbert Klugbauer[4], Heiko Groiss[5], Alexey Minenkov[5], and Susanna Zierler[1,6,7]

*1 Institute of Pharmacology, Faculty of Medicine, Johannes Kepler University Linz, Austria*
*2 Department of Biosciences and Medical Biology, Paris Lodron University Salzburg, Austria*
*3 CF Imaging, Center for Medical Research, Faculty of Medicine, Johannes Kepler University Linz, Austria*
*4 Institute of Experimental and Clinical Pharmacology and Toxicology, University Freiburg, Germany*
*5 Center for Surface and Nanoanalytics, Johannes Kepler University Linz, Austria*
*6 Walther Straub Institute of Pharmacology and Toxicology, Ludwig-Maximilians-Universität München, Germany*
*7 Clinical Research Institute for Inflammation Medicine, Johannes Kepler University Linz, Austria*

Two-pore channels (TPCs) are endolysosomal cation channels that play a central role in the regulation of endolysosomal and autophagolysosomal remodeling, as well as cytosolic $Ca^{2+}$ homeostasis [1]. The intracellular localization of the two isoforms TPC1 and TPC2 plays an important role in biomedical research. The prevailing hypothesis is that TPC1 is predominantly located in endosomes and TPC2 predominantly in lysosomes [2]. However, high-resolution ultrastructural data for precise localization under physiological conditions are currently lacking. In this study, an Immunogold Live-Cell CLEM (correlative light and electron microscopy) workflow was established for the first time to ultrastructurally localize TPC1 in J774 macrophages. This correlative method combines live-cell imaging with high-pressure freeze-fixation (HPF), thereby enabling the preservation of physiological states while maintaining excellent ultrastructure. Crucially, the unambiguous differentiation between endosomes, endolysosomes, and autophagolysosomes was only possible through the correlation of fluorescence and electron microscopy in the CLEM approach. Using CLEM, TEM tomography and optimized immunogold labeling, TPC1 could be qualitatively detected in these compartments, with the highest abundance observed in endosomes. The presented methodology represents an innovative approach for subcellular protein localization and will be used in the future for quantifying TPC distribution as well as for AI-assisted volume electron tomography of whole cells.

**References**

1. Steiner, P.; Arlt, E.; Boekhoff, I.; Gudermann, T.; Zierler, S. Two-pore channels regulate inter-organellar $Ca^{2+}$ homeostasis in immune cells. Cells 2022, 11, 1465–1475, doi:10.3390/cells11091465
2. Morgan, A.J.; Martucci, L.L.; Davis, L.C.; Galione, A. Two-pore channels: going with the flows. Biochem. Soc. Trans. 2022, 50, 1143–1155, doi:10.1042/BST20220229.

# Balancing Resolution and Throughput Through Ion Beam Profile Control

Martin Slama[1]

[1]*Tescan Group, Brno, Czech Republic*

In focused ion beam–scanning electron microscopy (FIB-SEM), the spatial current density distribution and stability of the ion beam critically determine milling accuracy, surface integrity, and process reproducibility. Beam tails, profile asymmetries, and current-dependent broadening directly influence lamella thickness control in TEM specimen preparation, tip geometry in atom probe tomography (APT), redeposition behavior in cross-sectioning, and milling efficiency during large-volume 3D characterization.

Systematic optimization of beam profile characteristics across the full current range directly affects both precision and throughput. At low beam currents, improved probe definition and reduced peripheral intensity enhance spatial resolution, enable more precise site-specific navigation, and improve control over fine geometries during TEM and APT specimen preparation. At high beam currents, stable and well-defined beam shapes support increased material removal rates while maintaining cross-section fidelity and minimizing geometric distortions. Together, these improvements reduce process variability, limit corrective steps, and shorten overall workflow time in routine laboratory operations.

This contribution examines the relationship between beam profile parameters and measurable performance indicators in daily FIB-SEM applications, spanning high-precision specimen preparation to large-area cross-sections and volumetric 3D analysis.

The discussed beam engineering principles are implemented in recent plasma and Ga FIB column developments, including the Mistral™ plasma FIB and the second-generation Orage™ Ga FIB, integrated in the AMBER X 2 and AMBER 2 platforms, respectively, enabling application-oriented selection without compromising between precision and throughput.

# Localized Detection of Electron Spin Precession with Free Electrons

Antonín Jaroš,[1,2] Michael S. Seifner,[1,2] Johann Toyfl, [1,2] Benjamin Czasch,[1,2] Santiago Beltrán-Romero,[1,2] Isobel C. Bicket,[1,2] Philipp Haslinger[1,2]

*[1]USTEM, TU Wien, Stadionallee 2, 1020 Wien, Austria*
*[2]VCQ, Atominstitut, TU Wien, Stadionallee 2, 1020 Vienna, Austria*

Spin is a fundamental quantum property of matter, intrinsically linked to the electronic and chemical environment. Spin states can be coherently manipulated using microwave (MW) radiation, and spectroscopic methods such as electron spin resonance (ESR) and nuclear magnetic resonance (NMR) have provided profound insights into spin systems [1,2]. However, these conventional approaches typically probe the ensemble-averaged response of spins and therefore lack spatial resolution, limiting their ability to access local spin information within heterogeneous specimens

Here, we present SPINEM (Spin Electron Microscopy), a technique that integrates MW spectroscopy with transmission electron microscopy (TEM) to enable localized detection of spin excitations using a free-electron probe. Spin polarization is provided by the magnetic field of the pole piece ($B_0$ ≈ 170 mT). A custom-designed microresonator, implemented in a dedicated TEM holder [3], drives spin transitions at ≈ 5 GHz and induces a synchronous modulation of the electron beam (see Figure 1). This modulation enables phase-locked detection, isolating spin-precession-induced beam deflections with sensitivities down to the picoradian scale. By sweeping the polarizing $B_0$ field across the resonance condition of the specimen, spatially resolved SPINEM spectra can be acquired with a lateral resolution of 30 µm [4].

By uniting spin physics with high-resolution electron optics, SPINEM establishes a new platform for quantum electron microscopy. The technique enables sensitive and quantitative detection of spin excitations and opens a pathway toward spatially resolved mapping of spin excitations, providing access to local spin information beyond the reach of conventional methods.

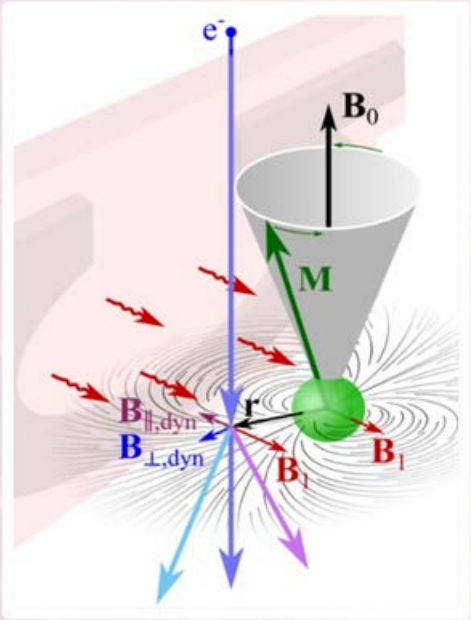


**Figure 1:** SPINEM spectra are recorded by sweeping the static polarizing magnetic field ($B_0$) through the resonance condition while keeping the driving magnetic field ($B_1$) constant to preserve a stable phase reference. When resonance is reached, the sample's magnetization (M) starts to precess, generating time-varying magnetic fields ($B_{dyn}$) that deflect the electron beam.

## References

[1] A. Bienfait, et al. Nat. Nanotechnol. 2016, 11, 253.
[2] B. Reif, S. E. Ashbrook, L. Emsley, M. Hong Nat. Rev. Method. Prim. 2021, 1, 2.
[3] A. Jaroš, J. Toyfl, A. Pupić, B. Czasch, G. Boero, I. C. Bicket, P. Haslinger Ultramicroscopy 2025, 278, 114224.
[4] A. Jaroš, M. S. Seifner, J. Toyfl, B. Czasch, S. Beltrán-Romero, I. C. Bicket, P. Haslinger ACS Nano 2026, 20, 3443.


# ANALYZERS FOR ELECTRON MICROSCOPY

## Discover Bruker's QUANTAX Family

Bruker's unique range of analytical tools for electron microscopes enables researchers to analyze the composition and structure of materials on the micro- and nanoscale. The QUANTAX measurement systems include **EDS** for SEM, T-SEM, TEM and STEM, as well as **EBSD** (also on-axis TKD), **WDS**, and **micro-XRF on SEM**. Seamless integration of each tool within the comprehensive ESPRIT software suite allows easy combination of data obtained across these complementary techniques. The QUANTAX family empowers researchers to see the whole picture and achieve the best results.

**For more information please visit www.bruker.com/quantax**

## SCAF1 drives the compositional diversity of mammalian respirasomes

Irene Vercellino[1], Leonid Sazanov[2]

*[1]Forschungszentrum Jülich, ER-C-3, Wilhelm-Johnen Strasse, 52425, Jülich, Germany*
*i.vercellino@fz-juelich.de*
*[2]Institute of Science and Technology Austria, Am Campus 1, 3400, Klosterneuburg, Austria*
*sazanov@ist.ac.at*

Supercomplexes of the respiratory chain are established constituents of the oxidative phosphorylation system, but their role in mammalian metabolism has been hotly debated. Although recent studies have shown that different tissues/organs are equipped with specific sets of supercomplexes, depending on their metabolic needs, the notion that supercomplexes have a role in the regulation of metabolism has been challenged. However, irrespective of the mechanistic conclusions, the composition of various high molecular weight supercomplexes remains uncertain. Here, using cryogenic electron microscopy, we demonstrate that mammalian (mouse) tissues contain three defined types of 'respirasome', supercomplexes made of CI, CIII2 and CIV. The stoichiometry and position of CIV differs in the three respirasomes, of which only one contains the supercomplex-associated factor SCAF1, whose involvement in respirasome formation has long been contended. Our structures confirm that the 'canonical' respirasome (the C-respirasome, CICIII2CIV) does not contain SCAF1, which is instead associated to a different respirasome (the CS-respirasome), containing a second copy of CIV. We also identify an alternative respirasome (A-respirasome), with CIV bound to the 'back' of CI, instead of the 'toe'. This structural characterization of mouse mitochondrial supercomplexes allows us to hypothesize a mechanistic basis for their specific role in different metabolic conditions.

## Ice to Data: The Future of Cryo-EM Workflow Integration

Javier Fernandez Collado, PhD

*Thermo Fisher Scientific*

Cryo-electron microscopy (cryo-EM) has become a widely adopted technique in structural biology, enabling high-resolution structure determination of macromolecular complexes. As the field continues to expand, researchers increasingly rely on advanced, multi-instrument workflows for their research.

Both single-particle cryo-EM (SPA) and cryo-electron tomography (cryo-ET) require coordinated use of multiple systems. In SPA, screening is often performed on a more accessible transmission electron microscope (TEM) before high-resolution data acquisition. Cryo-ET is inherently multi-modal, combining lamella preparation with a focused ion beam (FIB) and TEM for tomographic acquisition, as well as light microscopy for target identification.

An integrated workflow spanning from sample preparation to data analysis where hardware and software are designed to operate as a unified ecosystem is essential for maximizing throughput and reproducibility. Such integration streamlines daily operations and reduces complexity for users.

Furthermore, integrated solutions allow laboratories to implement advanced workflows progressively. Facilities can expand capabilities by adding complementary instruments and software modules without compromising the performance of existing systems.

In this presentation, we will highlight recent technological advances that enhance integration, automation, and connectivity within of Thermo Fisher Scientific instruments and software, which together underpin modern cryo-EM and cryo-ET workflows.

# Multimodal Ultrafast Scanning Electron Microscopy

Leon Kroß[1], Benjamin Schröder[1], Niklas Wemheuer[1], Claus Ropers[1,2] and Murat Sivis[1,2]

*[1]Max Planck Institute for Multidisciplinary Sciences, Göttingen, Niedersachsen, Germany*
*[2]University of Göttingen, 4th Physical Department, Göttingen, Niedersachsen, Germany*

We present a newly-developed multimodal ultrafast scanning electron microscope (USEM), which enables the simultaneous measurement of different electron probe signals using electron energies ranging from 100 eV to 30 keV in both transmission and reflection (cf. Fig. 1a). As a first proof of concept, we study the structure and dynamics of the charge-density-wave (CDW) compound 1T-$TaSe_2$. By raster-scanning a focused electron probe across the sample and recording a diffraction pattern (cf. bottom inset) at each scan position, we realize a four-dimensional scanning transmission electron microscopy (4D-STEM) modality, which allows for the reconstruction of different material contrasts via digital k-space filtering. In addition to the direct and scattered beams used for bright- and dark-field imaging (cf. insets), respectively, diffraction reflexes associated with the crystalline lattice of 1T-$TaSe_2$, as well as superstructure reflections arising from the commensurate room-temperature CDW (cf. zoom-in), can be exploited to spatially map more complex structural changes. Furthermore, operating the USEM in pulsed mode enables the investigation of ultrafast material dynamics, such as the suppression of CDW peaks upon optical excitation of the sample with femtosecond laser pulses at a wavelength of 1030 nm (cf. Fig. 1b). The timescale of this suppression is currently limited by the ~2 ps space-charge-limited electron pulse duration employed. By optimizing the electron-gun and photoemission conditions, we anticipate achieving electron pulse durations comparable to the ~200 fs reported for UTEMs.

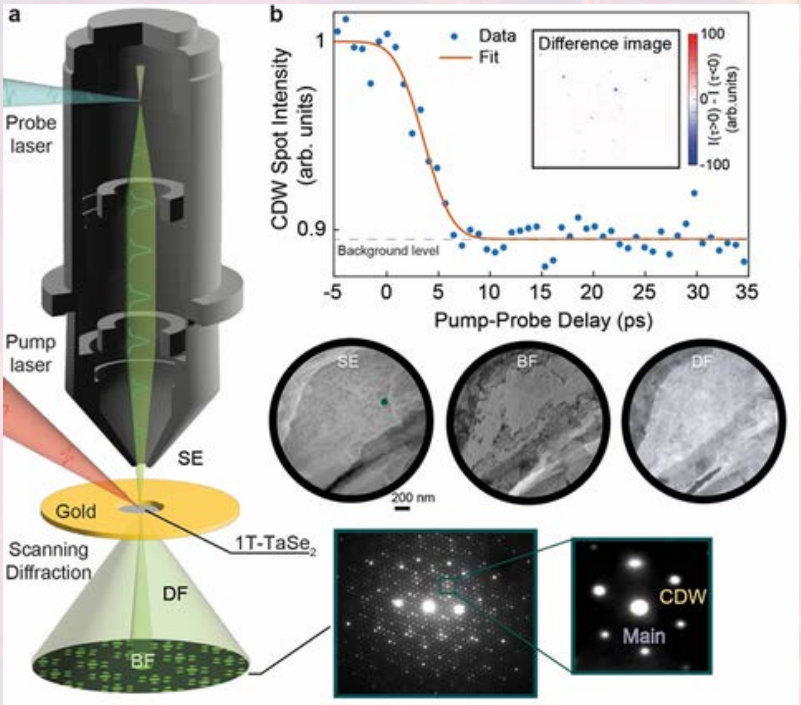


**F**ig. 1 a) Schematic of the laser-driven USEM and experimental setup, including secondary-electron (SE), bright- and dark-field (BF and DF) images (insets) of the TaSe2 thin film (< 50 nm) at 20 keV electron energy. Exemplary diffracted primary electron pattern in transmission at the point marked in the SE image, showing main-lattice (Main) and charge-density wave (CDW) spots. b) Pump-probe measurement of the commensurate (C) to incommensurate (IC) phase transition. Inset shows a difference image of the diffraction patterns after and before time zero.

# Advanced cryo-STET imaging: targeting the mtDNA in situ

Peter Kirchweger [1], Shahar Seifer[1], Lev Melnikovsky[1], and Michael Elbaum[1]

[1]*Department of Chemical and Biological Physics, Weizmann Institute of Science, Israel*

Cryo-Scanning Transmission Electron Tomography employs a focused electron probe that is rastered across a vitrified specimen while scattered electrons are recorded by bottom-mounted pixelated or area detectors [1, 2]. Tomographic data acquisition is performed using SerialEM [3]. Using the pixelated Dectris ARINA detector, we established 4D cryo-STET [4] and recently expanded the methodology by implementing shadow-montage reconstruction [5]. Shadow-montage stitches together many tiny shadow images produced in the diffraction plane during scanning with a defocused electron beam, enhancing spatial resolution while maintaining a large field of view. By adjusting how those shadows are aligned it can also reconstruct different depths of the sample. For azimuthal-segmented area detectors, we developed cryo-STET methods based on parallax-corrected bright-field (pBF) and parallax-filtered integrated differential phase contrast ($\pi$DPC) imaging [6, 4, 7].

In addition, I will present recent developments in three-dimensional deconvolution (3dcon), which we developed for cryo-STET [8, 9] and TEM-based cryo-electron tomography [10]. This approach reduces structural “salt-andpepper” noise and partially compensates for the missing wedge in tomographic reconstructions. Applications of 3dcon to both TEM-based cryo-ET and cryo-STET datasets will be shown.

I will briefly introduce the principles of shadow-montage reconstruction, pBF, and $\pi$DPC imaging, and demonstrate their application to targeting mitochondrial genome (mtDNA) in situ. The mtDNA has been a deeply studied topic for some time, including by cryo-ET [11]. Direct visualization with cryo-ET was not possible due to the radiation sensitivity of the mtDNA [11]. The mitochondrial genome serves here as a representative example demonstrating the potential of cryo-STET for studying macromolecular organization within intact cellular environments.

**References**

1. Wolf, S. G. et al. Nature methods 11 (Apr. 16, 2014).
2. Kirchweger, P. et al. en. Journal of visualized experiments: JoVE (June 23, 2023).
3. Mastronarde, D. N. Microscopy and microanalysis: the official journal of Microscopy Society of America, Microbeam Analysis Society, Microscopical Society of Canada 9 (Aug. 24, 2003).
4. Seifer, S. et al. en. Microscopy and microanalysis: the official journal of Microscopy Society of America, Microbeam Analysis Society, Microscopical Society of Canada 30 (July 4, 2024).
5. Seifer, S. et al. bioRxiv (Sept. 11, 2025)
6. Seifer, S. et al. Microscopy and microanalysis: the official journal of Microscopy Society of America, Microbeam Analysis Society, Microscopical Society of Canada 27 (Dec. 11, 2021).
7. Kirchweger, P. et al. bioRxiv (Nov. 29, 2025).
8. Waugh, B. et al. Proceedings of the National Academy of Sciences of the United States of America 117 (Nov. 3, 2020).
9. Kirchweger, P. et al. en. Journal of Structural Biology 215 (Sept. 30, 2023).
10. Croxford, M. et al. Proceedings of the National Academy of Sciences 118 (Dec. 14, 2021)
11. Kukat, C. et al. en. Proceedings of the National Academy of Sciences of the United States of America 112 (Sept. 8, 2015).

# Accessible workflows for EELS and EDX tomography through automated acquisition and multimodal reconstruction

TatianaKormilina[a b], Georg Haberfehlner [a], Thomas Mairhofer (Radlinger) [a], Ferdinand Hofer [a], Gerald Kothleitner [a b]

[a]*Graz Centre for Electron Microscopy (ZFE), Steyrergasse 17, 8010, Graz, Austria*
[b]*Institute of Electron Microscopy and Nanoanalysis (FELMI), Graz University of Technology, Steyrergasse 17, Graz, Austria*

In the modern days scanning transmission electron microscope (STEM) is not just an imaging tool, but a powerful analytical instrument that can be fitted with a plethora of detectors for chosen angular ranges or phase contrast imaging, as well as spectroscopic techniques that can reveal elemental composition or even chemical bonding and electronic properties of the specimen. At the same time 3D investigations become more common and accessible, rendering specimen tilt property of TEM measurements very promising for 3D reconstructions. This creates a potent field, where various STEM modalities can be acquired at several tilt angles and tell about the properties of the sample in question in three dimensions. While being often reported on and readily accessible at most microscopes, the path to harvesting this information is rather trackless. There is a lack of affordable software assistance in acquiring such tilt series in effective manner at as well as a thorny and unclear task of processing the emerging low SNR data.

We demonstrate three accessible approaches to high-quality multimodal tomographic data reconstruction, including a universal automatization approach of secondary (e.g. spectroscopic) signal tilt series acquisition using open-source scripting language AutoHotKey, combination of multimodal tomography data acquired (e.g. on different microscopes) with different field of view, pixel size and tilt range parameters, and finally, improving SNR and fidelity of a reconstruction using total variation minimization with Frobenius norm signal coupling available in open-source GAPTOR application.

These approaches are used to characterize elemental compositions of Cu alloy materials.

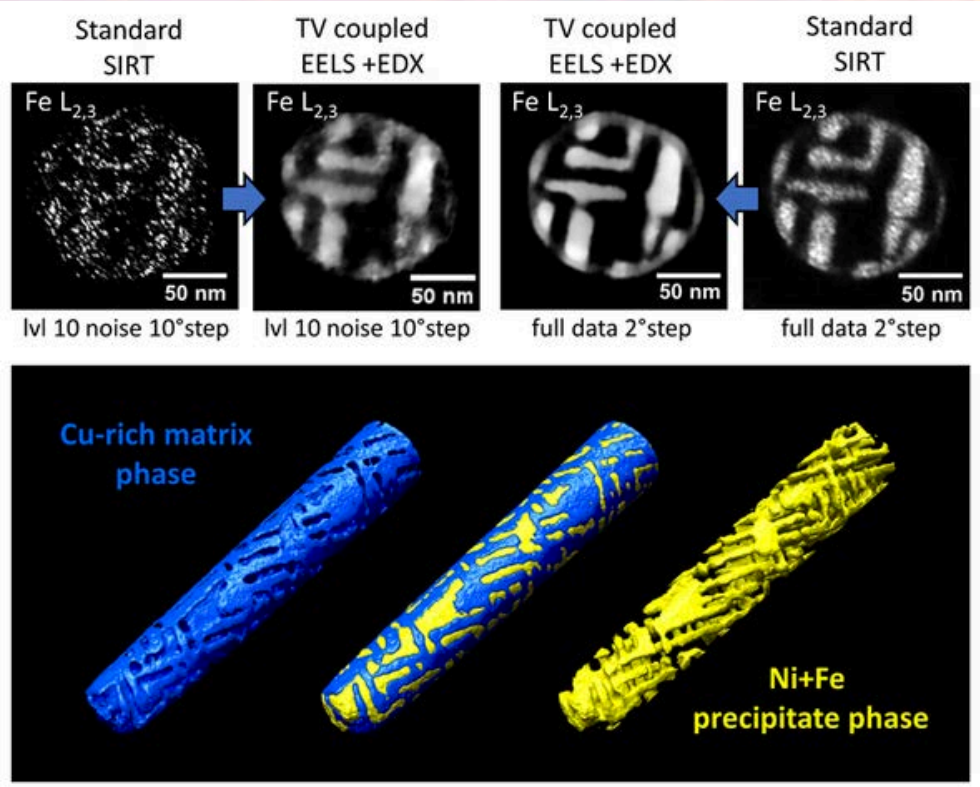

CIQTEK

# Advanced EM Solutions


www.ciqtekglobal.com
info@ciqtek.com

# Multi-scale investigations on the strengthening and toughening of highly nanotwinned transition metal nitride film

Yong Huang[1*], Zhuo Chen[1], Zaoli Zhang[1]

[1] *Erich Schmid Institute of Materials Science, Austrian Academy of Sciences, Jahnstraße 12, Leoben, A-8700, Austria*

**yong.huang@oeaw.ac.at*

Achieving simultaneous high hardness and fracture toughness in ceramic coatings is a long-standing challenge. This study presents a nano-twinned TaN/TiN (nt-TaN/TiN) multilayer thin film that overcomes this trade-off via a hierarchical twin boundary network. Synthesized by magnetron sputtering, the film features a columnar architecture rich in coherent (CTB) and incoherent (ITB) twin boundaries.

Mechanical testing reveals a remarkable hardness of ~39 GPa and an outstanding fracture toughness of ~4.1 MPa√m, establishing a new benchmark for transition metal nitrides (TMNs). Atomic-scale TEM reveals that the negative stacking fault energy of TaN activates slip systems, enabling rare intragranular plasticity in rock-salt ceramics.

The exceptional performance originates from synergistic mechanisms:

- Strengthening: Twin boundaries act as potent barriers to dislocation motion.
- Toughening: The hierarchical network suppresses intergranular fracture, while frequent orientation changes across CTBs force a highly tortuous transgranular crack path, dissipating fracture energy.

These findings demonstrate that nano-twinned architectures offer a scalable strategy for designing next-generation superhard, tough protective coatings for extreme applications

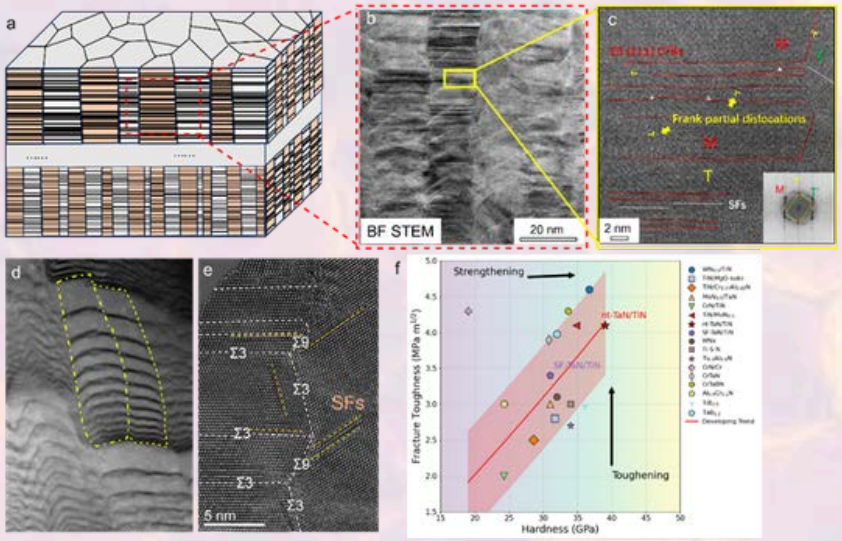


Figure 1. (a) Schematic of the hierarchical nano-twin architecture. (b) Cross-sectional STEM image showing high-density nano-twins. (c) HRTEM image identifying coherent twin boundaries (CTBs), stacking faults (SFs), and Frank partial dislocations. (d) Post-deformation STEM image showing grain shearing and bending. (e) HRTEM view of post-deformation CSL grain boundaries and emitted SFs. (f) Comparison of hardness vs. fracture toughness for various transition metal nitrides.

**References**

[1] Huang, Y. et al. Highly nanotwinned transition metal nitride film enabled by negative stacking fault energy. Acta Materialia 299, 121475, doi:https://doi.org/10.1016/j.actamat.2025.121475 (2025).

# ZEISS EMToolkit - Visual Workflow Builder for Automatization of EM Control, Image Recognition, Analysis and Metrology

Wolfgang Schwinger*[,1,] Manoj Mathew[2]

*Corresponding Author: wolfgang.schwinger@zeiss.com
[1]Carl ZEISS GmbH, Laxenburgerstr. 2, 1100 Wien
[2]Carl Zeiss Microscopy GmbH, Kistlerhofstraße 75, Munich

ZEISS Solutions Lab will soon launch a new and innovative software tool for easy automatization of imaging workflows on ZEISS electron microscopes by using the standard API interface of the ZEISS EM control software SmartSEM. This user-centric graphical interface allows not only efficient microscope control but also image recognition, image analysis and metrology through easy to learn visual programming.
This solution empowers any user of ZEISS electron microscopes to boost productivity, throughput and efficiency for any repetitive image acquisition and analysis workflow especially for routine work like in failure analysis, quality assurance and quality control.
The user can built workflows using drag-and-drop building blocks, eliminating the need for time consuming coding (although parallel phyton scripting is available). AI-based detection algorithms significantly enhance accuracy and repeatability compared to labour-intensive manual processes. Simply annotate and train AI models and plug them into EMToolkit. New auto-functions and customizable measurement capabilities ensure precise and reliable correlation between metrology data statistics and processing conditions. Logics and conditional loops allow for simple setup even of complex and demanding analytical workflows.

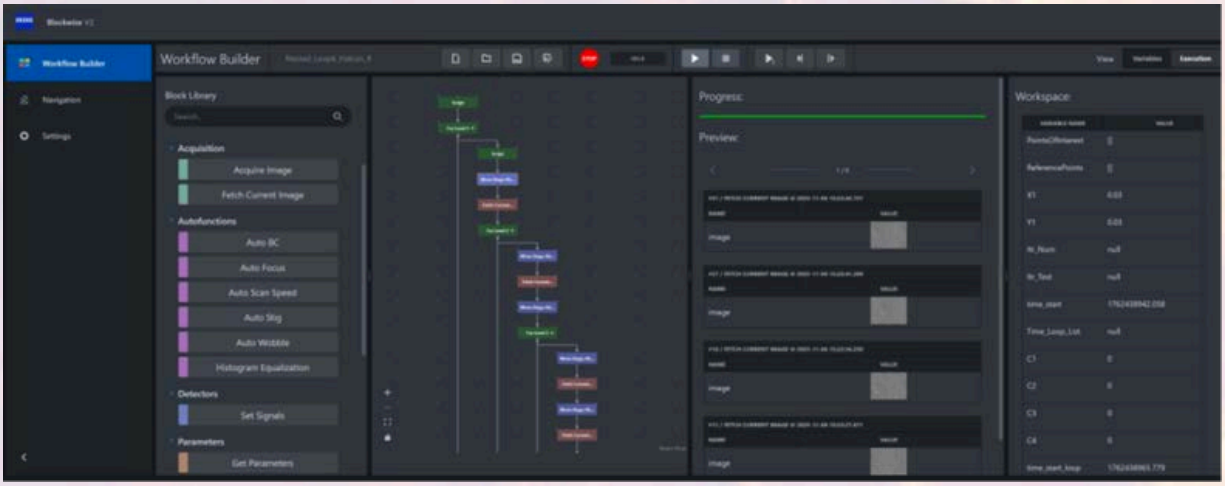


Figure 1. Modern, simple to learn user interface with visual workflow builder is at the core of ZEISS EMToolkit.

# XFlash® FlatQUAD – Maximum Efficiency in X-ray Detection

Mikhail Lazarev, Bruker Nano GmbH, Am Studio 2D, 12489 Berlin, Germany


## Mastering challenging tasks in EDS analysis

Elemental analysis with EDS in SEM can be challenging when dealing with complex and difficult samples, such as beam-sensitive materials, biological and life science thin sections, semiconductor devices, battery materials, FIB/TEM lamellae, nanoparticles, and samples with topographical features or heavy surface charge (i.e., glass and ceramics). QUANTAX FlatQUAD is the EDS system based on the revolutionary XFlash® FlatQUAD detector. The XFlash® FlatQUAD is an EDS micro- and nano-analysis detector that performs where conventional systems reach limitations. Maximum signal collection is ensured by its annular four independent SDD segments design, the placement under the pole-piece, and the high take-off angle. Extremely fast mapping at the highest output count rate (OCR) can be achieved with moderate beam currents.

The XFlash® FlatQUAD enables unmatched sensitivity, even at low (< 3 kV) voltages and ultra-low probe currents (< 50 pA). These beam conditions are required for challenging samples and cannot be achieved with conventional single or even multiple large area EDS detectors with inclined geometry.

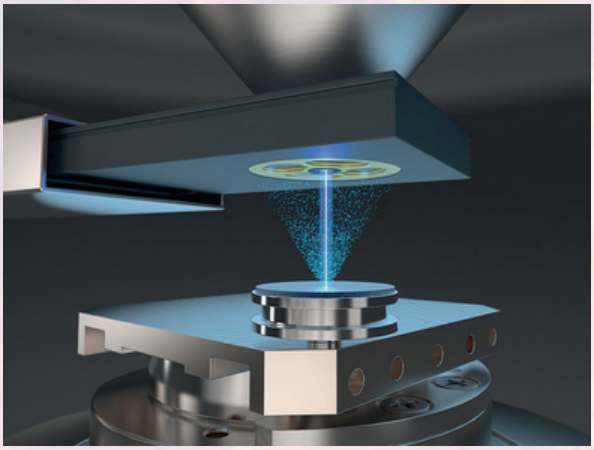

**For further information, please visit www.bruker.com/flatquad or contact mikhail.lazarev@bruker.com.**

# Atomic-Scale Insights into Matter via Multi-Modal STEM: From Structure to Function

Daniel Knez*[,1], Evelin Fisslthaler[2], Philipp Christ[1], Nikola Šimić[2], Michael Oberaigner[2], Harald Plank[1,2], Robert Winkler[1], Martina Dienstleder[2], Verena Reisecker[1], Michelle Brugger-Hatzl[2], Elena Unterleutner[1], Tatiana Kormilina[2], Georg Haberfehlner[1], Werner Grogger[1,2], Ferdinand Hofer[1,2], Gerald Kothleitner[1,2]

* *daniel.knez@felmi-zfe.at;* [1]*Institute of Electron Microscopy and Nanoanalysis (FELMI), Graz University of Technology, Steyrergasse 17, 8010, Graz, Austria;*
[2]*Graz Centre for Electron Microscopy, Steyrergasse 17, 8010 Graz, Austria*

The development of next-generation technologies, from energy conversion to quantum information, is increasingly limited by our ability to study and control matter at the atomic scale. Bridging the gap between synthesis and application requires a detailed understanding of how local structural motifs and electronic states govern macroscopic functionality. Scanning transmission electron microscopy (STEM) has emerged as an indispensable approach for this purpose. By leveraging a rich diversity of simultaneous signals, it provides a unique multi-modal platform to correlate structural, chemical, and physical properties. While scanning probe techniques offer comparable resolution for surface analysis, STEM remains essentially unmatched for accessing information from within the bulk.

In this talk, I will present research highlights from our group demonstrating the versatility of modern STEM across a wide range of material systems and research questions. These include the investigation of single dopant atoms in complex materials [1] and the exploration of the interplay between structural and electronic properties in oxide heterostructures. Utilizing atomic-resolution electron energy-loss spectroscopy (EELS) and integrated Differential Phase Contrast (iDPC) imaging, we study two-dimensional electron gas (2DEG) formation, correlating oxygen defect distribution with metallic states at the interface [2]. Furthermore, we demonstrate the quantitative mapping of lithium distribution and structural evolution in battery materials by harnessing low-dose imaging and diffraction techniques [3].

Our multi-modal approach extends to beam-sensitive systems, where Cryo-STEM is utilised to reveal elusive structure-property relationships, such as the dielectric response in organic photovoltaics (OPV) and the structure of cellulose nanocrystals [4]. Possibilities enabled by novel direct electron detectors for in situ EELS elemental mapping will also be discussed, illustrated by phase evolution studies in aluminium alloys [5].

Finally, I will provide an outlook on how simulation-informed ptychography and machine-learning-assisted analysis may circumvent current constraints in the detection and interpretation of atomic-scale phenomena.

## References

[1] D. Knez et al. (2024), Commun Mater 5 (1), 19
[2] M. Oberaigner et al. (2023), arXiv-ID: 2310.03863v1.
[3] N. Šimić et al. (2024), Adv. Energy Mater. 14 (34), 2304381.
[4] D. Knez et al. (2025), Small 21 (25), e2500351.
[5] E. Fisslthaler et al. (2025), Adv. Eng. Mater. 27 (21), 2500716.

## Acknowledgements

Funding from the EU's Horizon 2020 Programme (grant no. 823717, project "ESTEEM3"), the Austrian Cooperative Research (project "INSIGHT", grant no. SP-2021-04), the Austrian Science Fund (FWF, project "Chain Game", No. 10.55776/PIN7297824 and project "AtomDensityMap", No. 10.55776/PIN1180625), as well as the COMET-K2 Center "IC-MPPE" (Project No. 886385, ASSESS) is acknowledged.

## TEM-tomography for structure-function modeling of cell connections in plant tissues

Stefan Möstl, Johannes Liesche

*University of Graz*

Plasmodesmata (PD) are nano-scale membrane-lined channels that mediate symplastic connectivity between plant cells. PD coordinate growth, development, and stress responses by regulating the exchange of ions, metabolites, RNAs, and proteins. Despite their central role, a quantitative structure–function framework for PD has remained elusive due to their sub-50 nm dimensions, structural heterogeneity across tissues and conditions, and dynamic regulation of permeability. Here, we present an optimized TEM tomography workflow that yields data on ultrastructural features used in predictive transport models of PD function.

Using our new ThermoFisher Talos L120C (installed early 2026), our approach combines high-tilt, low-dose TEM tomography with fiducial-assisted alignment and robust 3D reconstruction to resolve PD architecture at nanometer resolution across representative tissue volumes. We extract morphometrics essential for modeling and couple them to biophysical descriptions of diffusional and convective flux. Sampling PD populations across developmental zones and treatments reveals continuous structural trajectories that map onto graded shifts in predicted size-exclusion limits and effective permeability, moving beyond the binary open/closed paradigm.

Methodological developments focus on specimen preparation preserving PD ultrastructure with enhanced contrast, tilt-series strategy optimization, and semi-automated segmentation/parameter extraction scalable to thousands of PD.

## Direct observation of Schottky-vacancy clusters and their mechanical response in MoN/TiN superlattice

Zhuo Chen[1], Yong Huang[1] , Zaoli Zhang[1]

*[1]Erich Schmid Institute of Materials Science, Austrian Academy of Sciences A-8700 Leoben, Austria*

A deeper understanding of vacancy-induced effects in ceramics may lead to optimized material design and improved mechanical properties. However, current research primarily focuses on the impact of vacancies on the intrinsic mechanical properties of materials, lacking direct experimental validation of their mechanical response behavior. In this study[1], we closely investigate the influence of Schottky-vacancy defects introduced during the deposition process on the mechanical behavior of MoN/TiN superlattice. In the as-deposited coating, Schottky vacancies are found to be distributed inside MoN as clusters. By coupling FIB with cross-sectional TEM observation, we further reveal Schottky vacancies evolution under loads at the atomic level and their significant impact on superlattice deformation. These Schottky vacancies promote superlattice intermixing and weaken the interface-strengthening effect. However, they are also beneficial to dislocation nucleation and increase the nitride plastic deformability. These findings provide a new perspective on the impact of point defects on the mechanical properties of ceramic materials.

**References**

[1] Z. Chen, Y. Huang, Z. Gao, Y. Zheng, P.H. Mayrhofer, Z. Zhang, Direct observation of Schottky-vacancy clusters and their mechanical response in MoN/TiN superlattice, Acta Materialia 283 (2025) 120551.

DECTRIS

## Explore our products


### ARINA
Ultrafast 4D STEM


### QUADRO
Fast Electron Diffraction


### ELA
Electron Energy Loss
Spectroscopy


### SINGLA
Cryo-EM Single Particle Analysis

### DECTRIS CLOUD
The Science Platform for
Collaborative Discovery

www.dectris.com

# Electron Microscopy Analysis for the Optimization of Perovskite–Organic Tandem Solar Cells

Bernadette C. Ortner*[,a,b], Georg Haberfehlner[a], Gerald Kothleitner[a,c], Thomas Rath[b], Markus C. Scharber[d], Gregor Trimmel[b]

**Corresponding Author: bernadette.ortner@felmi-zfe.at, [a] Institute of Electron Microscopy and Nanoanalysis, NAWI Graz, Graz University of Technology, Steyrergasse 17, 8010, Graz, Austria; [b]Institute for Chemistry and Technology of Materials (ICTM), NAWI Graz, Graz University of Technology, Stremayrgasse 9, 8010, Graz, Austria; [c]Graz Centre for Electron Microscopy, Steyrergasse 17, Graz, 8010, Austria; [d]Linz Institute for Organic Solar Cells (LIOS), Institute of Physical Chemistry, Johannes Kepler University Linz, Altenbergerstrasse 69, 4040 Linz, Austria*

Perovskite–organic tandem solar cells offer a promising route toward high-efficiency photovoltaics by combining complementary absorber materials. While both sub cells show strong standalone performance, their integration into efficient tandem devices requires precise control of morphology and interfacial layers.[1] Moreover, achieving spectrally complementary absorption regions while maintaining high electrical performance remains a central challenge in device design. Donor dilution in organic bulk heterojunction solar cells provides an effective route to increase visible light transmission and tailor the absorption profile of the organic sub cell, thereby improving its spectral compatibility with the perovskite counterpart. However, increasing dilution typically leads to reduced power conversion efficiency. To investigate the morphological origins of this performance loss, we investigate D18:L8-BO solar cells with donor-to-acceptor weight ratios ranging from 1:1.5 to 1:100. Because donor and acceptor phases exhibit low intrinsic mass contrast, scanning transmission electron microscopy combined with electron energy loss spectroscopy (STEM-EELS) is employed to differentiate domains via variations in sulfur and nitrogen content. Elemental mapping reveals a progressive disruption of the percolating donor network with increasing dilution. While charge carrier mobilities remain largely unaffected, exciton dissociation and charge collection efficiencies decrease significantly, identifying network continuity as the limiting factor.[2] Furthermore, cross-sectional specimens of perovskite–organic tandem devices are prepared with a focused ion beam and transferred under inert conditions into the microscope. This enables direct analysis of interlayer formation, interfaces, and perovskite layer quality, all of which require careful adjustment. Overall, this work demonstrates how electron microscopy provides critical insights across multiple length scales, supporting the rational optimization of tandem solar cell architectures.

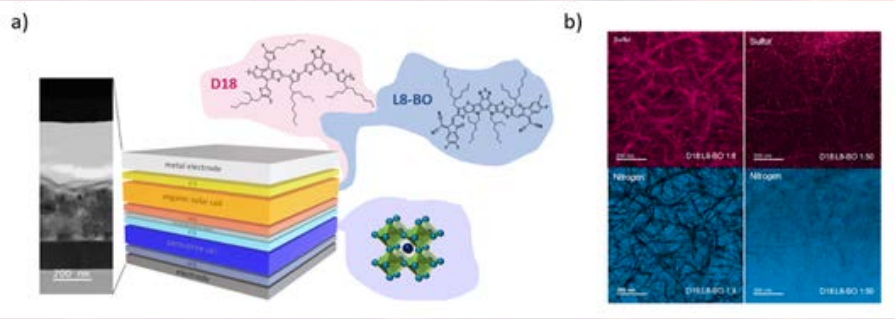


Figure 1: a) Cross-section and a scheme of the device architecture of a perovskite–organic tandem solar cell combining the wide bandgap perovskite FA0.8Cs0.2PbI1.6Br1.4 sub cell and an organic sub cell based on D18:L8-BO. b) Elemental ratio maps of N (blue) and S (red) based on STEM-EELS measurements of D18:L8-BO films with donor: acceptor ratios of 1: 8 and 1 : 50 (w : w).

This work was funded by FFG Austria as part of the PEROPTAM project, (FO999896686/44474121) which is conducted in a collaboration of JKU & TUG.

**References**

[1] Zhang, Z.; Chen, W.; Jiang, X. et al.Suppression of phase segregation in wide-bandgap perovskites with thiocyanate ions for perovskite/organic tandems with 25.06% efficiency, Nat. Energy 2024, 9, 592–601.

[2] Ortner, B. C.; Binter, K.; Hönigsberger, J. et al. Donor dilution in D18: L8-BO organic solar cells: visualization of morphology and effects on device characteristics, J. Mater. Chem. C 2025, 13, 18981–18990.

# Unlocking the Power of Unique High-Speed Scanning Electron Microscopy with No Compromise of Superb Imaging Resolution at Low kV for Large Scale Volume Microscopy Applications from CIQTEK

Dr. Fengfa Yao*

**CIQTEK Co., Ltd.*

Volume electron microscopy (vEM) aims to reconstruct three-dimensional biological and materials architectures at nanometre-scale detail across millimetre-scale fields of view. In practice, conventional FE-SEMs often force a compromise among spatial sampling, field coverage, acquisition time, and dose, especially when thousands of tiles are required to survey heterogeneous specimens or large serial-section arrays. This limits the routine use of vEM and cross-scale “overview-to-detail” studies in both life-science and materials laboratories.

Here we present HEM6000, a single-beam Schottky FE-SEM developed by CIQTEK and configured for high-throughput, large-area imaging with strong performance at low accelerating voltages. The platform combines an immersion electromagnetic–electrostatic objective lens and a deceleration mode (100 V–6 kV) to enhance low-kV signal collection and contrast, while maintaining a broad operating range up to 30 kV. A multi-stage electrostatic deflection architecture supports stable scanning across large areas, including a large-FOV imaging mode up to 1 mm × 1 mm, and a high-resolution large-FOV mode enabling 4 nm/pixel sampling over 64 μm × 64 μm. The detection suite includes low-angle BSE detection (retractable, model-dependent) and optional in-column electron detection, targeting robust material and ultrastructural contrast at low kV. To enable unattended, reproducible acquisition, HEM6000 incorporates an automation layer featuring automatic sample recognition, automatic imaging-area selection, automatic brightness/contrast, autofocus, and automatic astigmatism correction. The specimen handling workflow is further supported by fully automatic sample exchange with a typical exchange time <15 minutes, accommodating samples up to 4 inches (optional 6 inches). Optional software modules provide large-area stitching (AutoMap) and 3D reconstruction, and the system can be coupled to downstream quantitative pipelines, including denoising, segmentation, and statistical analysis. We demonstrate the vEM-oriented workflow on resin-embedded serial sections of mouse brain, where low-kV BSE imaging provides sufficient contrast to resolve key ultrastructural features (e.g., membranes, mitochondria, synaptic regions) while enabling large-area mosaics composed of many tiles. We further discuss transfer of the same acquisition strategy to heterogeneous functional materials and semiconductor structures, where cross-scale mapping accelerates discovery of sparse defects and rare process anomalies and supports volume reconstruction when combined with serial sectioning or complementary preparation approaches.

Overall, HEM6000 provides a practical route to reducing the traditional throughput–coverage–resolution trade-off in large-area electron microscopy by integrating low-kV-optimized optics, large-FOV imaging modes, automation, and workflow-ready software on a single-column platform.

# Electron Microscopy as a Platform for Nanophotonics and Quantum Optics

Charles Roques-Carmes[1]

[1] *Institute of Science and Technology, Austria (ISTA), Klosterneuburg, Austria*

Over the past decades, nanophotonics has emerged as a transformative platform for controlling light-matter interactions, enabling novel light sources, detectors, and devices that tailor the polarization, spectral, and angular properties of optical fields. Central to this progress is the design of nanostructured materials – such as metasurfaces, photonic crystals, and nanoresonators – that reshape electromagnetic modes at the nanoscale and engineer emission from atoms, molecules, and solid-state systems.

In parallel, electron microscopy has evolved into a powerful platform for investigating nanophotonic structures, offering broadband, deeply subwavelength excitation and direct access to optical near fields with nanometer spatial resolution [1]. Free electrons interacting with nanophotonic environments not only serve as versatile probes of optical modes, but also constitute quantum objects whose interactions with photons and other quantum systems, including bound electronic states and spins, can be engineered and coherently controlled [2].

In this talk, I will present a general framework to model, tailor, enhance, and optimize radiation from free electrons interacting with engineered nanophotonic structures. Using this approach, I will demonstrate nanophotonic enhancement and control of both coherent and incoherent cathodoluminescence [3], [4], and show how structured photonic environments reshape electron-induced radiation processes. I will further show how this framework enables the design of nanophotonic systems that reach the regime of strong coupling between single free electrons and photonic modes, for example via ponderomotive guiding in photonic microfibers [5]. This regime opens pathways toward heralded macroscopic nonclassical light generation, deterministic single-photon sources, and quantum gates mediated by free-electron–photon interactions.

Finally, I will outline how quantum sensing technologies can be integrated directly into electron beam lines, positioning electron microscopy as a hybrid quantum-nanophotonic platform for probing, controlling, and interfacing quantum systems at the nanoscale [6].

**References**

[1] C. Roques-Carmes, S. E. Kooi, Y. Yang, N. Rivera, P. D. Keathley, J. D. Joannopoulos, S. G. Johnson, I. Kaminer, K. K. Berggren, and M. Soljačić, “Free-electron–light interactions in nanophotonics,” Appl. Phys. Rev., vol. 10, no. 1, 2023.

[2] R. Ruimy, A. Karnieli, and I. Kaminer, “Free-electron quantum optics,” Nat. Phys., pp. 1–8, 2025.

[3] Y. Yang, C. Roques-Carmes, S. E. Kooi, H. Tang, J. Beroz, E. Mazur, I. Kaminer, J. D. Joannopoulos, and M. Soljačić, “Photonic flatband resonances for free-electron radiation,” Nature, vol. 613, no. 7942, pp. 42–47, 2023.

[4] C. Roques-Carmes, N. Rivera, A. Ghorashi, S. E. Kooi, Y. Yang, Z. Lin, J. Beroz, A. Massuda, J. Sloan, N. Romeo, and others, “A framework for scintillation in nanophotonics,” Science, vol. 375, no. 6583, p. eabm9293, 2022.

[5] A. Karnieli, C. Roques-Carmes, N. Rivera, and S. Fan, “Strong Coupling and Single-Photon Nonlinearity in Free-Electron Quantum Optics,” ACS Photonics, July 2024, doi: 10.1021/acsphotonics.4c00908.

[6] J. Grzesik, D. Catanzaro, C. Roques-Carmes, E. I. Rosenthal, G. van de Stolpe, A. Karnieli, G. Scuri, S. Biswas, K. Leedle, D. Black, R. L. Byer, I. Kaminer, R. J. England, F. Fan, Shanhui, O. Solgaard, and J. Vuckovic, “Quantum sensing of electron beams with solid-state spin qubits,” ArXiv Prepr. ArXiv250813112.

attolight™

# ALLALIN

## SEM- Spectroscopic platform

- SEM
- Cathodoluminescence
- Photoluminescence
- Nanoprobes
- EBIC
- Time-resolved analyses
- Cryo measurements

- Electronics & Optoelectronics
- Photovoltaic cells
- Light emitting diodes
- 2D materials
- Plasmonic
- Nanomaterials
- Ceramics, minerals
- Organic, polymer, biological samples

# Plasma FIB Tomography of Mast Cells: Challenges and Solutions

Alexey Minenkov,[1][1] Sara Hirner,[1] Lena Wiesbauer,[2] Ancuela Andosch,[3] Philip Steiner,[2] Heiko Groiss[1]

[1]*Center for Surface and Nanoanalytics, Johannes Kepler University Linz, Austria*
[2]*Institute of Pharmacology, Faculty of Medicine, Johannes Kepler University Linz, Austria*
[3]*CF Imaging, Center for Medical Research, Faculty of Medicine, Johannes Kepler University Linz, Austria*

In this contribution, we address the development and optimization of a practical, high-quality workflow for large-volume plasma focused ion beam–scanning electron microscopy (PFIB-SEM) tomography using mast cells as a suitable test object. Beyond their classic roles in allergic diseases such as asthma and anaphylaxis, mast cells are vital for tissue homeostasis, repair, and defence. Despite extensive research, mast cell ontogeny and functions in cancer and cardiovascular health are still far from full comprehension.

Further advances demand reliable refinement of the cells' ultrastructure with the highest fidelity. Manual segmentation of numerous distinct granules (vesicles) is extremely time-consuming. Thus, we aim to extend the established correlative light and electron microscopy (CLEM) ultrastructural workflow by integrating AI-based segmentation. Since the reliability of an AI model depends not only on imaging quality but also requires an immense amount of data for training, PFIB tomography is a marvellous tool for collecting the needed datasets in a reasonable time. For that, we utilized a Xe PFIB TESCAN Amber X augmented with a rocking stage.

The cells were prepared via high-pressure freezing (HPF) followed by cryo-substitution, and then embedded in epoxy resin. In this regard, the primary technical challenge of PFIB tomography is the mitigation of charging and thermal damage in insulating embedding media, ensuring an artifact-minimized surface, coupled with high-contrast, high-resolution SEM imaging. We systematically modified the epoxy resin by adding conductive carbon nanoparticles, finding that a carbon concentration of 5% yielded the best reduction of charging artifacts while maintaining workable viscosity for embedding. After thorough optimization, the FIB preset of 10 nA at 30 kV, combined with stage rocking of ±7°, ensured the smoothest cuts with minimal curtaining. For SEM imaging, 300 pA at 5 keV with a low-energy backscattered electron (LE BSE) detector provided superior image readout with the highest signal-to-noise ratio, enhancing contrast of ultrastructural features within the resin matrix. Using these settings, reconstructions containing ca. 1000 slices with isotropic voxels of 7 nm were achieved (Figure 1). More details on the workflow implementation and optimization, together with the first AI segmentation findings, will be provided and discussed.

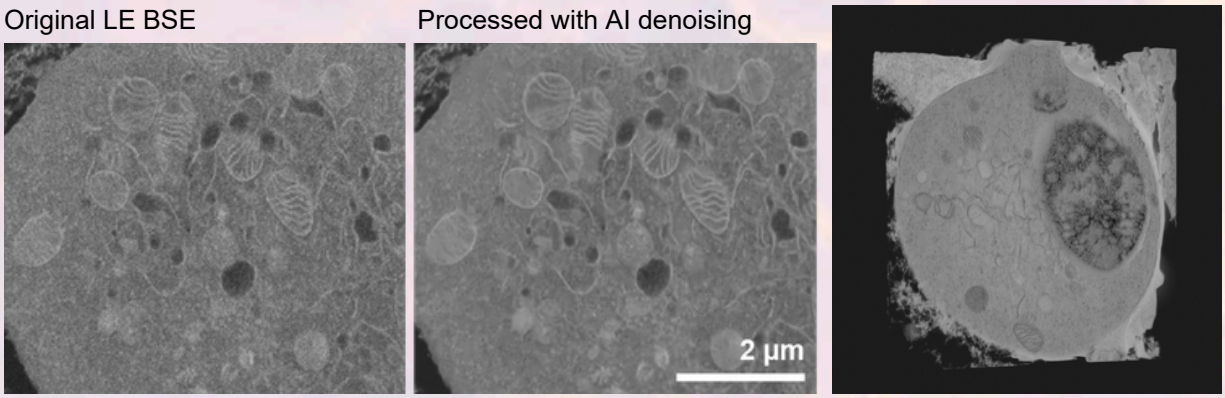


Figure 1. Exemplary imaging and FIB-SEM tomography results.

[1] Corresponding author: oleksii.minienkov@jku.at

# Origin of pores in electron irradiated hexagonal boron nitride

Umair Javed[1], Manuel Längle[1], Vladmir Zobac[1], Alexander Markavich[1], Clara Kofler[1], Martin Paul[1], Darwin Lorber[1], Nandhini Ravindran[1], Clemens Mangler[1], Toma Susi[1], Jani Kotakoski[1]

[1]*University of Vienna, Faculty of Physics, Vienna, Austria*

For nearly two decades, it has been known that electron irradiation of hexagonal boron nitride (hBN) leads to formation of triangular pores with nitrogen-terminated edges. The broadly accepted explanation was that boron is easier to displace than nitrogen, owing to their different displacement cross section resulting from their mass difference and different displacement threshold energies. It had also been speculated that the residual vacuum in the microscope column could play a role in preferred removal of boron atoms, but this hypothesis was not tested until now.

In this study [1], we used Nion UltraSTEM 100 in Vienna which operates at the base pressure of 1e-10 mbar (which is three orders of magnitude lower than typical microscopes). Due to customization it is also possible to introduce a controlled gas atmosphere around the sample while keeping the imaging conditions up to 1e-6 mbar. We studied the electron-beam-induced pore growth in hBN at oxygen partial pressures from 1e-10 mbar to 3e-8 mbar with electron energies of 60 keV and 80 keV.

In contrast to previous high-vacuum experiments, we show that electron irradiation at 1e-10 mbar leads to circular pores with no preference to either boron or nitrogen terminated edges (Fig. 1(a)), whereas even small amounts of oxygen in the atmosphere during the experiment changes the pore shapes into triangles with nitrogen-terminated edges (Fig. 1(b)). These results hold for both 60 and 80 keV electron energies. Although pore growth at 60 keV is generally slower than at 80 keV, at the highest pressure the growth rate appears independent of the electron energy. This indicates, that at higher pressures, the pore growth is dominated by a beam-assisted chemical process rather than direct electron-beam damage (Fig. 1(c)).

We turn to ab initio simulations to elucidate the underlying reasons for this observation. They show that oxygen atoms, created from O2 by the electron beam, attach preferentially to B at pore edges. From this configuration, it is easier to remove the O and B together rather than just O with the electron beam, whereas the opposite is true for N atoms at the edge. This explains the prevalence of nitrogen edges at higher oxygen pressures, and therefore also the observed triangular pores.

Our observations show that damage in hBN under electron irradiation is a combination of physical damage caused by electrons in the form of knock-on damage or radiolysis, and chemical damage caused by oxygen radicals, which affect boron significantly more than nitrogen. This opens up the possibility for defect-engineering of materials with desirable edges or atomic-scale defects by controlling both physical and chemical effects during particle irradiation.

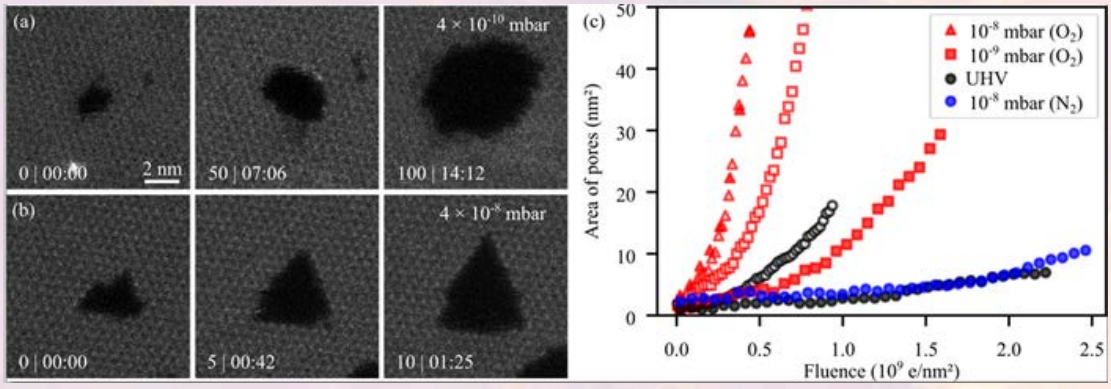


Figure 1: (a) Series of STEM-MAADF images of pore growth at 4e-10 mbar. (b) Series of STEM-MAADF images of pore growth at 4e-8 mbar oxygen partial pressure. (c) Pore growth for different acceleration voltages and atmospheres. Open symbols represent data recorded at 80 keV, whereas filled ones represent 60 keV.

## References

1. U. Javed et al., arXiv:2507.13180 (2025)

# Surface-Sensitive Imaging at Low Acceleration Voltages: When Less Can Be More

Sascha Reh, Lars Jansen*, Karl Kersten

Standard sample preparation for transmission electron microscopy (TEM) is time consuming and tedious: fixation, dehydration, embedding, ultrathin sectioning, and heavy metal staining, just to name a few. On top of that, high-end TEM systems are expensive to buy and maintain. This puts them out of reach for many labs, especially when all you need at first is a quick check of sample quality, particularly with delicate biological specimens or non-conductive materials.

Low-kV scanning electron microscopy on compact desktop instruments offers a much simpler and faster alternative for surface-sensitive imaging with very little preparation. Operating at low acceleration voltages keeps the interaction volume small, boosts surface contrast and drastically reduces beam damage to sensitive samples. This makes it especially useful for negatively stained cells, thin tissue sections, or polymer-based materials, where conventional high-kV imaging or block staining can easily introduce artifacts or simply isn't practical for rapid screening.

In this talk we show how low-kV SEM can act as an efficient pre-screening step before investing time in high-resolution TEM. Using the Thermo Scientific™ Phenom Pharos™ G2 FEG SEM with its built-in STEM detector, you can carry out quick morphological checks and collect TEM-compatible bright-field and annular dark-field images, all in the same instrument. The STEM images give complementary information based on mass-thickness contrast and surface sensitivity. This helps you quickly to locate regions that are worth for further in-depth TEM examination. As a result, the approach saves preparation time, reduces sample consumption, and avoids unnecessary high-resolution work on unsuitable areas.

We present examples from biological and materials samples (negatively stained cells, thin tissue slices, and polymer matrices) to illustrate how low-kV SEM and STEM can deliver useful, structural detail with minimal handling effort. The method speeds up lab workflows, better preserves fragile structures, and makes planning of follow-up ultrastructural studies much more targeted.

In short, low-kV SEM on Phenom XL G3, Pro G7 and STEM on Phenom Pharos desktop systems are practical means for gentle and fast imaging in life-science and materials labs – cutting down on preparation hassle, giving quick feedback, and bridging nicely to high-resolution TEM, all without requiring huge budgets or specialized infrastructure.

**Schaefer Technology GmbH**
Robert-Bosch-Str. 31
63225 Langen
+49 6103 300 98 0
info@schaefer-scientific.com
www.schaefer-scientific.com

# schaefer scientific

*For over 60 years, Schaefer Scientific has been a trusted partner for research, development, and high-tech industries across Europe. We support customers in life sciences, materials science, industry, and academia with comprehensive consulting, application expertise, sales support, and long-term service collaboration.*

**Innovative Solutions for Science and Engineering**

As an authorized distributor in the DACH-Region, we represent leading manufacturers in electron microscopy, metal and carbon sputter coaters, ion milling and polishing systems, and related technologies, such a as:

**Thermo Scientific™ Phenom Pharos™ G2 FEG SEM**

- The ultra-high-resolution desktop SEM (<2.0 nm)
- Magnification up to 2,000,000x
- With optional STEM-detector: <1.0 nm

**Thermo Scientific™ Phenom™ XL G3**

- High-resolution SEM (<9 nm)
- Magnification up to 200,000x
- Largest sample chamber in desktop format

**Thermo Scientific™ Phenom™ P-Series (Pure, Pro, ProX)**

- High-resolution SEM (≤6 nm)
- Ultrafast sample loading in < 30 seconds
- Magnification up to 350,000x

**LUXOR Au, LUXOR Pt, LUXOR C**

- Fully automated sputter coater designed for desktop and floor model SEM applications
- Sample coating with gold, platinum and carbon
- Can simultaneously coat up to 7 x 12 mm stubs

**TechnoOrg Linda SEMPrep Smart and UniMill**

- Broad-beam AR+ ion beam for SEM or TEM preparation
- Polishing or cross-sectional milling, EBSD
- Cooling and Vacuum transfer options

**ibssGroup's Mobile Cubic Asher (MCA)**

- Chamber with three TEM Holder ports
- On board plasma driving gas cylinder
- Qwk Switch TM Source provides EM chamber cleaning at SEM or TEM site

## Visit us at our booth to check out the Phenom XL G3 live in action

Schaefer Technologie GmbH
Robert-Bosch-Str. 31, 63225 Langen
Germany

schaefer-scientific.com

ThermoFisher SCIENTIFIC · LUXOR · TECHNOORG LINDA · ibss Group, Inc.

# The JEM-120i - new Generation of 120 kV TEM for life and material science

Georg Raggl

*JEOL (Germany) GmbH, Freising Germany*

The JEM-120i represents a new generation of 120 kV transmission electron microscopes (TEM) designed for applications in life sciences and materials science. The system integrates an enhanced TEM control platform with fully automated apertures, enabling continuous specimen observation without switching magnification modes or manually selecting apertures. This significantly reduces operational complexity and streamlines the workflow.

An integrated camera solution supports the entire process from specimen navigation to data acquisition. The newly developed compact design allows flexible installation and facilitates both routine operation and maintenance. In addition, extensive retrofit options ensure long-term adaptability to evolving research requirements.

For large-area investigations, a specimen plate with a high-strength, grid-free SiN supporting film is available, enabling millimeter-scale fields of view and in situ chemical treatments. The Limitless Panorama (LLP) technology combines beam scanning and stage scanning to enable automated acquisition of ultra-wide image areas without field-of-view limitations. This approach allows efficient correlation of ultrastructural details with the overall morphology of complex biological specimens.

The JEM-120i thus addresses key demands of modern TEM applications in terms of usability, flexibility, and large-area high-resolution analysis.

# Ghost Imaging with Free Electron-Photon Pairs

S. Bogdanov*[1,2], A. Preimesberger[1,2], D. Hornof[1,2], T. Spielauer[1], T. Schachinger[2], M.S. Seifner[1,2], I.C. Bicket[1,2], P. Haslinger†[1,2]

[1]*Vienna Center for Quantum Science and Technology, Atominstitut, TU Wien, Vienna, Austria*
[2]*University Service Centre for Transmission Electron Microscopy, TU Wien, Vienna, Austria*

Coincidence imaging, also known as ghost imaging, is a technique that exploits cor-relations between two particles to reconstruct information about a specimen. The particle that relays the spatial information about the object remains completely non-interacting, while the particle used to probe the object is not spatially resolved. While ghost imaging has been primarily implemented on photonic platforms [1], it be-comes particularly intriguing when applied to particles with fundamentally different properties, such as massive, charged electrons and massless, neutral photons, espe-cially considering the role of both particles as cornerstones of highly advanced mi-croscopic platforms. Utilizing a custom-built free-space cathodoluminescence setup integrated within a transmission electron microscope (see Fig. 1), we demonstrate electron–photon ghost imaging of complex patterns with a spatial resolution down to 2 µm [2]. These advances have also enabled the first experimental demonstrations of entanglement between photons and free space electrons [3],[4].

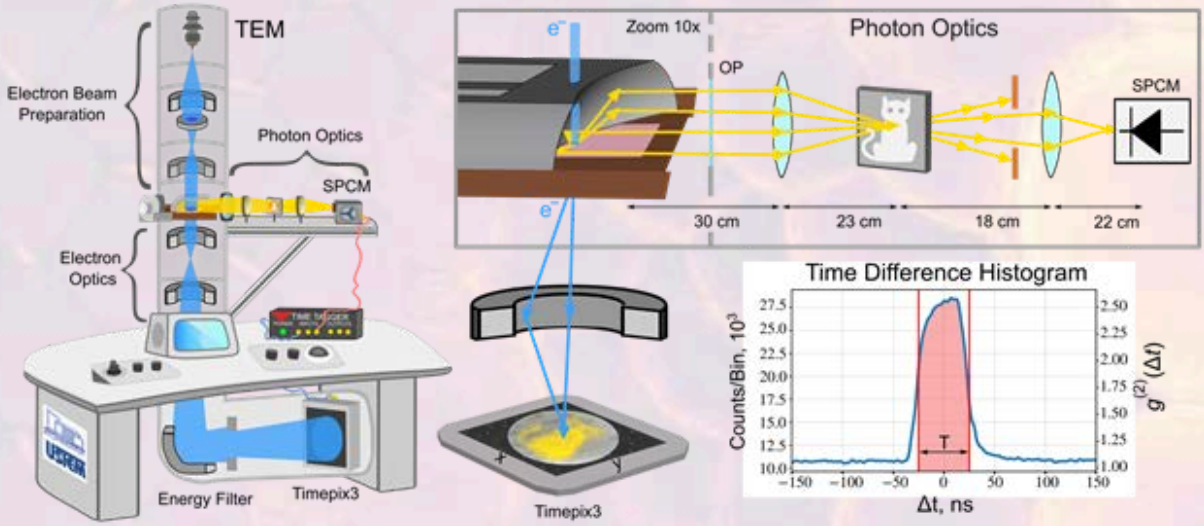


Fig. 1: Experimental setup for electron-photon pair coincidence (ghost) imaging [2].

## References

[1] D'Angelo, et al., Physical Review Letters 92, 23 (2004).
[2] S. Bogdanov, A. Preimesberger, et al., arXiv:2509.14950 (2025).
[3] A. Preimesberger, S. Bogdanov, et al., arXiv:2504.13163, (2025).
[4] J.-W. Henke, H. Jeng, M. Sivis, C. Ropers, arXiv:2504.13047 (2025).

*sergei.bogdanov@tuwien.ac.at
†philipp.haslinger@tuwien.ac.at

# Advanced multimodal Electron Microscopy for Characterization of Two-Pore Channels in Macrophages

Lena Wiesbauer[1], Emma Punzenberger[1], Julia Schatz[1], Yuliia Nazarenko[1], Ancuela Andosch[2,3], Norbert Klugbauer[4], Robert Mallmann[4], Philip Steiner[1], Susanna Zierler[1,5]

[1] *Institute of Pharmacology, Medical Faculty, Johannes Kepler University Linz, Linz, Austria*
[2] *Core Facility Imaging, Medical Faculty, Johannes Kepler University Linz, Linz, Austria*
[3] *Department of Biosciences and Medical Biology, Paris Lodron University Salzburg, Salzburg, Austria*
[4] *Institute of Experimental and Clinical Pharmacology and Toxicology, University Freiburg, Freiburg, Germany*
[5] *Walther-Straub-Institut of Pharmacology and Toxicology, LMU Munich, Munich, Germany*

Two-pore channels (TPCs), ligand-gated cation-selective ion channels located in the membranes of organelles such as endosomes, lysosomes, and endolysosomes, play a crucial role in interorganellar communication and intracellular $Ca^{2+}$ regulation and homeostasis [1]. Studies on mast cells have already revealed the importance of TPCs in communication between the endolysosomal system and the endoplasmic reticulum (ER), making them essential for $Ca^{2+}$ flux between these organelles and thus key players in mast cell degranulation [2]. However, the precise communication mechanisms and functions of TPCs in macrophages remain to be fully characterized.

Several microscopy and imaging approaches were performed to address this scientific aim. Macrophages (J774) with single (TPC1 or TPC2) or double (TPC1/TPC2) knockouts were compared to wild-type cells. Live-cell laser scanning microscopy (LSM) was used to perform quantitative lysosomal assays, endocytic uptake measurements, and vesicular trafficking analyses. Different dyes, including LysoTracker Red DND-99, LysoSensor Green DND-189, and ER-Tracker Blue-White DPX, were used to stain lysosomes or the ER and to compare their properties across the four genotypes. Furthermore, AM1-43, a fluorescent dye that integrates into the plasma membrane, was used to track endocytic uptake in the cells. Using electron microscopy and 3D TEM tomography, we performed morphometric analysis of the endolysosomal system (EN/LY), autophagolysosomes, and contact sites between EN/LY and ER. Additional approaches, such as $Ca^{2+}$ imaging, further deepened our understanding of TPC function in macrophages.

In summary, our findings showed that TPCs play a crucial role in endocytic trafficking, autophagolysosomal function, lysosomal- and $Ca^{2+}$ homeostasis. The different isoforms also revealed altered connections between the endo-/lysosomal system and the ER, underscoring the importance of these channels for interorganellar communication. Altogether, our results suggest a crucial role of TPCs in the regulation of macrophage function.

**References**

[1] Steiner, P., Arlt, E., Boekhoff, I., Gudermann, T., & Zierler, S. (2022). Two-pore channels regulate inter-organellar Ca2+ homeostasis in immune cells. Cells, 11(9), 1465.
[2] Arlt, E., Fraticelli, M., Tsvilovskyy, V., Nadolni, W., Breit, A., O'Neill, T. J., ... & Zierler, S. (2020). TPC1 deficiency or blockade augments systemic anaphylaxis and mast cell activity. Proceedings of the National Academy of Sciences, 117(30), 18068-18078.

# Optimization of dopant detection in wide band gap semiconductors using STEM EELS

Lukas Lobenwein[1], Evelin Fisslthaler[1], Aidan Arthur Taylor[2], Martin Lanius[2], Werner Grogger[1,3]

[*]*Corresponding Author: lukas.lobenwein@felmi-zfe.at*

[1]*Graz Centre for Electron Microscopy, Steyrergasse 17, 8010 Graz, Austria*

[2]*Infineon Technologies Austria AG, Siemensstraße 2, 9500 Villach, Austria*

[3]*Institute of Electron Microscopy and Nanoanalysis, Graz University of Technology, Steyrergasse 17, 8010 Graz, Austria*

Recent developments in microelectronics lead to the necessity of advancements in dopant profiling techniques with regards to sub-10 nm spatial resolution and sensitivity to dopant levels of $10^{20}$ $cm^{-3}$, while being reasonably priced and integrateable in standardized processes. STEM EELS is a promising technique to fulfil these requirements due to its ability to provide atomic resolution. Furthermore, it is a wide spread technique in academia and industry and innovations in detector systems pushed its detection sensitivity near the range of dopant concentrations typically used in semiconductor devices[1]. Nevertheless, optimum experimental and evaluation parameters are required to successfully detect these elements.

The experimental parameters include the effective collection angle, electron dose, spectrometer dispersion, beam energy, sample thickness, type of detector (charge-coupled device vs. direct electron detection), and others. The choice of the evaluation method and parameters further impacts the results. Here power-law background fitting and integration of the net edge intensity was the method of choice. The results are influenced by the placement and width of both fit and integration regions.

A highly doped Borophosphosilicate glass (BPSG) with about 4 at% Boron was used as a test sample. By using the minimum atomic fraction[2] and the signal-to-noise ratio (SNR) of the $B_K$ edge for different experimental parameters, an optimum parameter set for detecting Boron was obtained. The optimum range of the effective collection angle was found between 5 and 10 mrad (see fig.a). The optimal sample thickness lies between a t/λ value of (0.4 and 0.5). The energy dispersion should be chosen as large as possible without restricting the energy range needed for evaluation. Furthermore, a certain electron dose has to be applied to reach the required detection sensitivity (see fig.b). Finally, contour maps were created, which indicate the optimum placement and width of the integration window in terms of the SNR (see fig.c). The optimized values will be transferred to other samples with lower dopant concentrations (e.g. GaN doped with 0.2 at% Si).

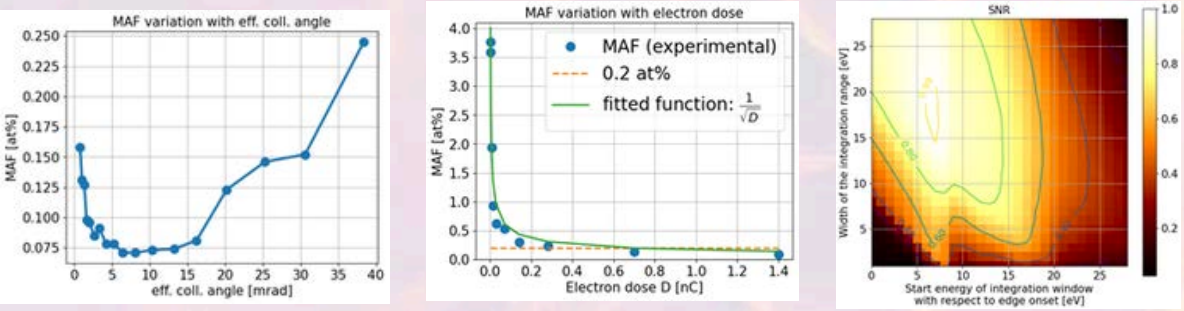


Parameter optimization for the $B_K$ edge: fig.a: Optimization of the detection sensitivity using effective collection angle. fig.b: Increase of detection sensitivity with electron dose. continuous line: fitted function, dashed line: detection sensitivity of 0.2 at% Boron, thus the intersection of both lines indicates the minimum dose needed (~0.7 nC). fig.c: Contour map for optimum placement and width of integration window (SNR normalized between 0 and 1).

**Acknowledgements**

Thanks to Martina Dienstleder and Sebastian Rauch for sample preparation. Further thanks to Austrian Research promotion agency (FFG) for the funding of the ELEVATE project (proj. No. FO999925306) and Infineon Austria for all the support

**References**

[1] Hart, J.L., Lang, A.C., Leff, A.C. et al. Direct Detection Electron Energy-Loss Spectroscopy: A Method to Push the Limits of Resolution and Sensitivity. Sci Rep 7, 8243 (2017). https://doi.org/10.1038/s41598-017-07709-4

[2] R.F. Egerton, 2011. Electron Energy-Loss Spectroscopy in the Electron Microscope. Springer US, Boston, MA. https://doi.org/10.1007/978-1-4419-9583-4_3

# Sol for ATMOSPHERE AX

**Controlled illumination for *operando* photocatalytic TEM**

*Sol is a brand-new member of the Atmosphere AX family, enabling light-driven reactions to be studied under pressurized, gaseous environments at the nanoscale. The highly-published Atmosphere AX now enables nanoscale studies for a new set of research areas.*

**Photocatalysis**
**Photochemistry**
**Photovoltaics**
**Optoelectronics**
**Plasmonics**



**Realistic Environmental Conditions**

**Well-Characterized Photoillumination**

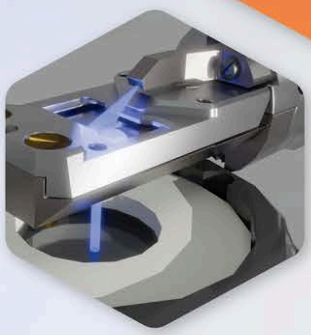

**Experimental Flexibility**

Protochips
Creating the Connected Lab

**Learn more here**

# Multi-Detector Imaging and Advanced Automation Capabilities of the Hitachi FlexSEM Platform

Sajjad Tollabimazraehno, Sales Manager,

*Analytical Instruments Videko GmbH Tribuswinkel, Austria*

The Hitachi FlexSEM 1000 is a compact scanning electron microscope (SEM) that combines multi-detector versatility with advanced automation to deliver high-quality imaging in both research and industrial environments. This work highlights the complementary capabilities of the Secondary Electron (SE), Backscattered Electron (BSE), and Ultra Variable-pressure Detector (UVD), together with the platform's fully integrated automatic alignment and optimization functions.

The SE detector provides high-resolution surface topography with strong edge contrast, enabling detailed morphological characterization at sub-micron scale. The BSE detector, fast low kV detector, offers compositional contrast based on atomic number differences, supporting rapid phase identification, inclusion analysis, and defect investigation.

A central feature of the system is the multi-functional UVD. As a variable-pressure (VP) detector, it enables stable imaging of non-conductive and insulating materials without conductive coating, minimizing charging artifacts. In addition, the UVD supports cathodoluminescence (CL) detection for defect and mineral analysis and can operate in a STEM configuration for transmitted electron imaging of thin specimens, revealing internal structure and nanoscale morphology within a compact platform.

Operational efficiency is enhanced through a comprehensive automation suite, including Auto Brightness & Contrast Control (ABCC), Auto Focus Control (AFC), Auto Stigmation/Focus (ASF), Auto Filament Saturation (AFS), and Auto Beam Alignment (ABA). The Auto Start sequence (HV-ON → ABCC → AFC) enables rapid system readiness, while the fully integrated AUTOMATIC function (AFS → ABA → AFC → ABCC) optimizes beam conditions and imaging parameters with minimal user intervention. These features significantly reduce operator dependency, improve reproducibility, and support multi-user laboratory environments.

The integration of advanced detector configurations with intelligent automation positions the FlexSEM platform as a powerful, user-friendly solution bridging conventional full-scale SEM systems and compact analytical instruments.

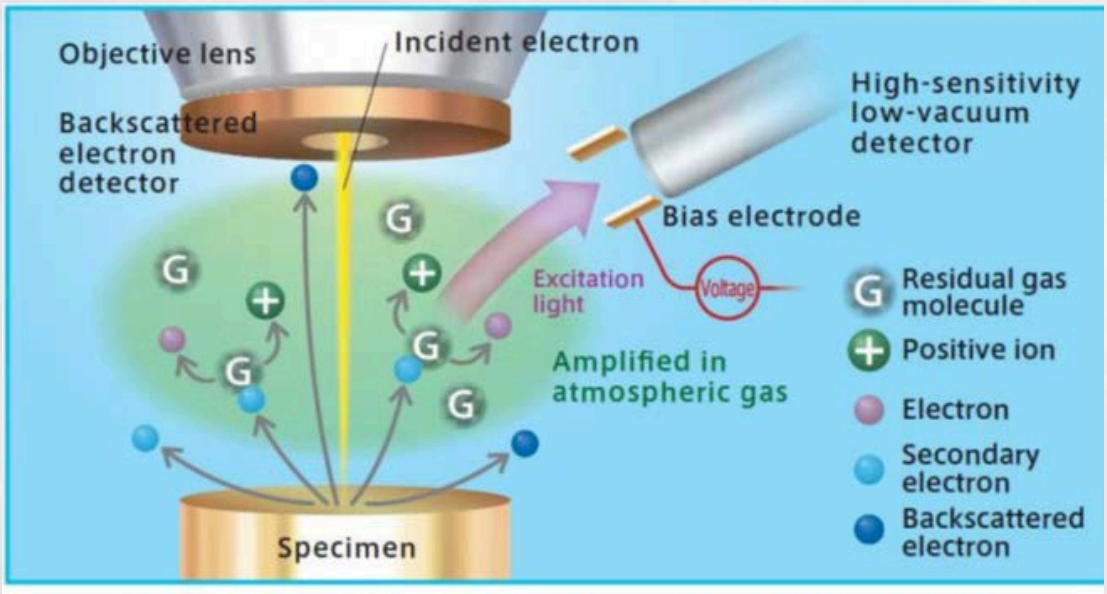


Detection principle of high-sensitivity low-vacuum detector (UVD)

# In-Situ TEM: A Nanoscale Laboratory

Bas ter Mull, Sales Manager EMEA at *Protochips*

The transmission electron microscope (TEM) has long been the gold standard for high resolution imaging, providing atomic level detail about a sample's structure. In a conventional setup, the sample is deposited onto a 3 mm copper grid which contains a layer of amorphous material, such as carbon. The sample is then inserted into the high vacuum environment of the TEM for imaging and/or elemental analysis. One significant limitation of this setup is the expectation that the sample must be stable in a high vacuum environment. In-situ transmission electron microscopy (in-situ TEM) techniques were developed to overcome this limitation, enabling samples to be imaged with TEM in non-vacuum environments, and simultaneously introduce real-time stimuli, such as temperature or electrical currents, during a TEM imaging session. Thus, users can record dynamic processes in real-world conditions at resolutions not obtained using non-TEM techniques. In-situ studies require the use of designated sample holders which protect the sample from the high-vacuum TEM column, deliver stimuli, and accurately measure signal output. The concurrent development of advanced detectors, cameras, software and designated in-situ holders has enabled researchers across diverse fields to unravel previously impossible results which range from observing viral transcription in physiological relevant, liquid environments, to changing the gas environment of catalyst particles from oxidizing to reducing during a single experiment.

State-of-the-art in-situ tools and software enable users to observe real-time reactions and behavior under a variety of conditions, such as liquid, gas and high temperatures and introduce a range of stimuli to the sample in those environments.These systems incorporate semiconductor MEMs technology into the sample support. MEMs technology enables vacuum-sensitive samples to be encapsulated between ultrathin electron transparent windows for imaging in liquid and gas, provides exceptionally low drift rates at high temperatures, and allows patterning of a variety of features such as electrical contacts. In this presentation, we will highlight the functionality of the in-situ systems developed by Protochips Inc. and demonstrate their use in conducting dynamic nanoscale studies, including thermal and electrical characterization, nanomaterial synthesis, electrochemistry, photochemistry, catalysis, corrosion, and more across a wide range of applications.

# Poster Abstracts

## Automated Particle Analysis - Top or Flop?

Harald Fitzek [1,2,*]

[1]*Graz Centre for Electron Microscopy, Steyrergasse 17, 8010 Graz, Austria;*
[2]*Institute of Electron Microscopy and Nanoanalysis, Graz University of Technology, Steyrergasse 17, 8010 Graz, Austria*

*Corresponding Author:harald.fitzek@felmi-zfe.at

As part of a laboratory exercise from WS 2023/24-SS 2025 the goal was set to test a newly acquired automated particle analysis toolbox (Horiba's Particle Finder) for Raman microscopy. The promises of the toolbox were automated particle analysis of µm-size particles using Raman spectroscopy. The possible applications range from microplastics to building materials. Can those promises the kept?

Over the course of several lab exercise samples of different common particles types were produced to test the toolbox on. In addition, two different preparation methods were tested, filtration onto an Au-coated Polycarbonate filter and embedding of the powders followed by polishing and grinding. This way a good understanding of this tools capabilities and limitations could be achieved. The figure below shows two examples of the different preparation methods and very different particle types that were used in testing.

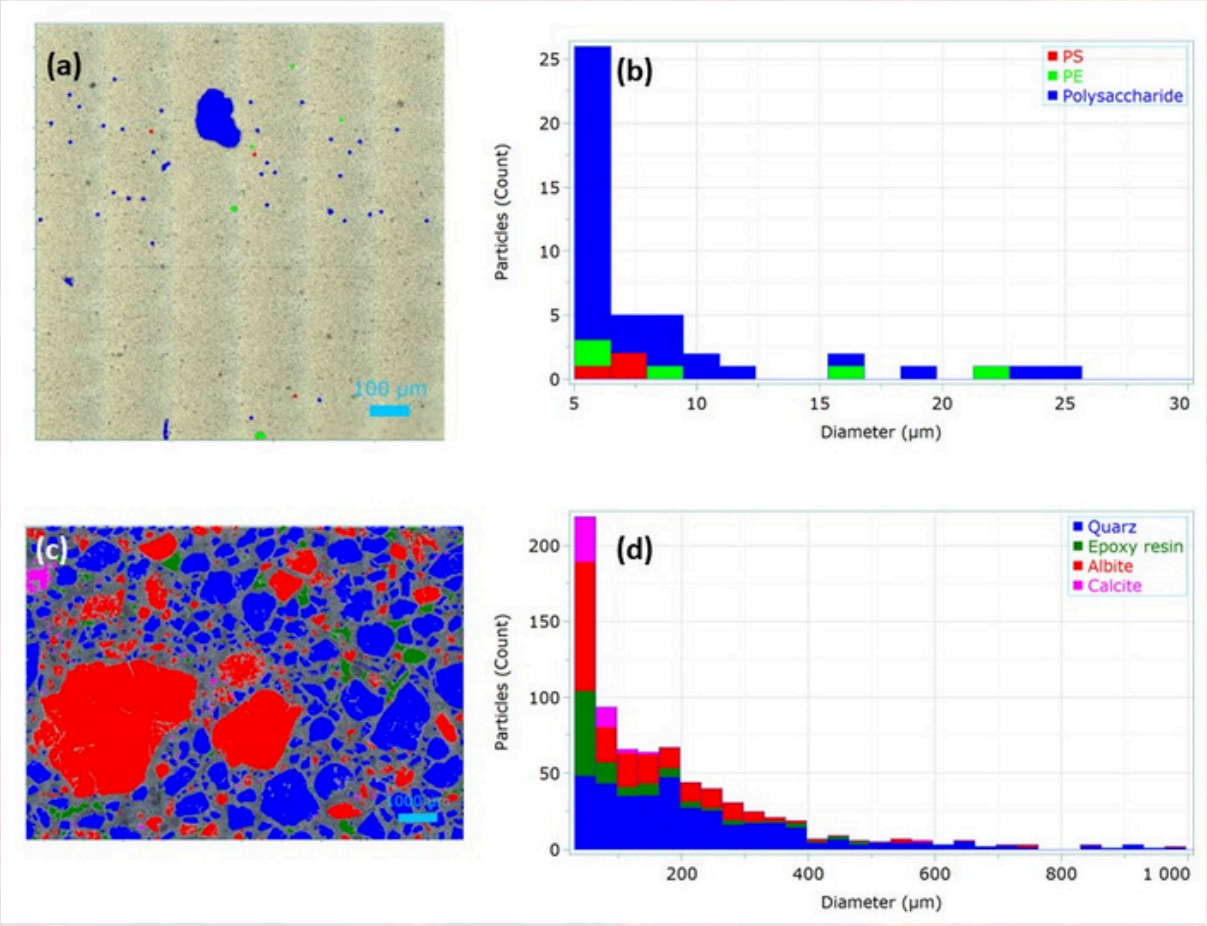


***Figure:*** Variations of automated particle analysis tested: *(a)* Light-microscopy images of microplastic on a filter with particles identified as seen in *(b)* Histogram and identification of the microplastics shown in *(a)*; *(c)* Light-microscopy images of the particles in a roof tile, the sample was embedded and polished with particles identified as seen in *(d)* Histogram and identification of the inorganic particles shown in *(c)*.

# Tescan AMBER Series

## for Materials Science

**The Tescan AMBER series brings together two advanced FIB-SEM platforms: a Xe plasma FIB-SEM and a Ga FIB-SEM, each built around our most refined ion column technologies to address the evolving needs of materials science.**

Whether the priority is analytical versatility or streamlined sample preparation, the Tescan AMBER series delivers performance aligned with your materials research goals.

### Tescan AMBER X 2

**Xe plasma FIB-SEM**

integrates the Mistral™ Xe plasma FIB column, combining high material removal rates with enhanced resolution and beam precision. It bridges the gap between Ga and conventional plasma FIB systems, enabling uncompromised TEM sample preparation alongside large-area cross-sectioning and high-throughput characterization.

### Tescan AMBER 2

**Ga FIB-SEM**

features the Orage™ 2 $Ga^+$ FIB column with higher resolution and improved beam parameters for precise ion control. These advancements make TEM lamella preparation more efficient and predictable, supporting high-quality results even for less experienced users.

# GIS free lamella preparation for in situ heating TEM

Tommaso Costanzo[1*], Sharona Horta[1], Maria Ibáñez[1]

[1]*Institute of Science and Technology Austria,Am Campus 1, 3400, Klosterneuburg, Austria*

[*]tommaso.costanzo@ista.ac.at

The general FIB procedure to protect and attach the sample to a suitable transmission electron microscopy (TEM) support, it commonly involves the use of a gas injection system (GIS). Unfortunately, the GIS deposited metal become mobile when the sample is heated for in-situ temperature dependent observations. We found the presence of platinum in the region of interest (ROI) at temperature as low as 250°C. The motion of platinum over the ROI can hinder the observation or quantification of the actual sample. For this reason, we developed a work flow that avoid the use of GIS deposited metals. In brief, we start by protecting the sample with a silicon mask. Successively, the lamella attachments are done by redepositing locally sputtered material generated by the focus ion beam (FIB). In more details, we redeposit sample material to attach the sample to the nanomanipulator nee- dle as shown in Fig. 1. Afterward, we attach the lamella to the in situ chip by making a small hole on the side pads of the lamella [2]. An SEM image of the lamella attached to a Protochip heating chip is shown in Fig. 2. In addition to avoid the platinum for protection and welding, the initial site of the lamella is prepared with a dedicated trapezoidal geometry [2]. The chosen shape allows top and bottom milling after attachment to the chip, as well as providing enough material for the GIS free attachment.

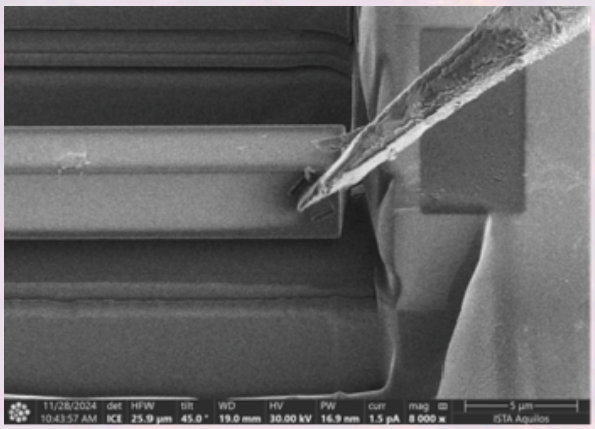

Fig. 1: Sample attachement to needle

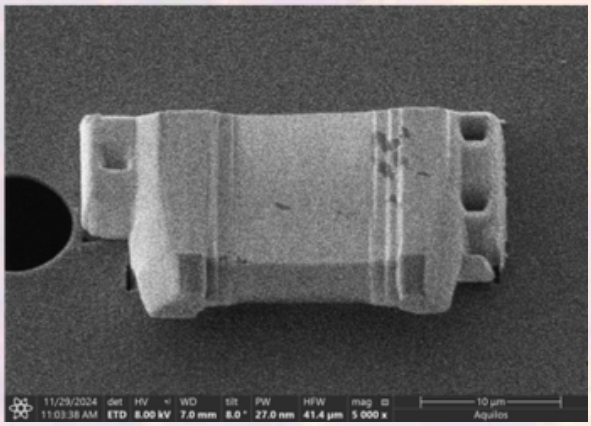

Fig. 2: Lamella attached to *in situ* chip

References:
[1] K. Wei, M. Lindley, X. Liu, S. J. Haigh, P. Xiao, P. J. Withers, A. H. Mir, G. Greaves, J. P. Martins, J. Lao, X. Zhong, Microscopy and Microanalysis, **31**, 3 (2025)
[2] T. Kleinhanns, F. Milillo, M. Calcabrini, C. Fiedler, S. Horta, D. Balazs, M. J. Strumolo, R. Hasler, J. Llorca, M. Tkadletz, R. L. Brutchey, M. Ibáñez, Adv. Energy Mater. **14,** 2400408, (2024).

# How to prepare “thin film” specimens from bulk single crystals

Elena Unterleutner[1], Ferdinand Hofer[1,2], Gerald Kothleitner[1,2] and Daniel Knez[1]

[1]*Institute of Electron Microscopy and Nanoanalysis, Graz University of Technology, Graz, Austria*

[2]*Graz Centre for Electron Microscopy (ZFE), Graz, Austria*

*elena.unterleutner@felmi-zfe.at*

One of the most important factors for quantitative TEM/STEM analysis is the development of preparation (and transfer) workflows that deliver electron-transparent specimens while preserving their native state. This step often regarded as secondary, is in fact decisive for obtaining reproducible, atomic-scale insights, particularly for single dopants and vacancies. To ensure accurate defect characterization and optimal imaging conditions, extremely thin samples are required. [[1]]

To develop and optimize defect characterization techniques, we investigate $SrTiO_3$ (STO) doped with low concentrations of Ta. Atomic-scale defect detection in complex oxides such as STO is crucial for optimizing their functional properties. The controlled introduction of dopants and vacancies enables precise tuning of electronic and magnetic behavior, making detailed knowledge of their structural and electronic configurations essential.

Here we present the workflow to achieve high quality samples one requires for such experiments, as shown in Figure 1. Starting from 500 µm thickness and resulting in regions with down to 3 nm thickness (see Figure 2) by combining mechanical thinning (wedge-polishing [[2]] and ion milling) with chemical thinning (etching).

a) b)

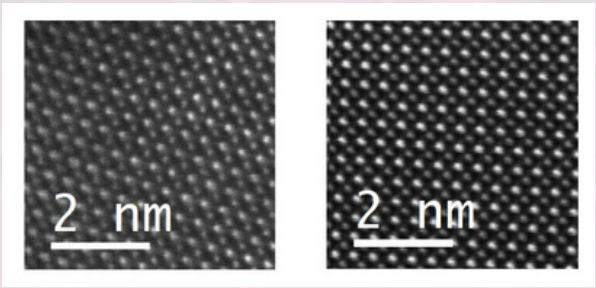


Figure 1: a) STEM HAADF atomic resolution image of $SrTiO_3$ prepared with conventional TEM sample preparation technique.
b) STEM HAADF atomic resolution image of $SrTiO_3$ prepared with refined TEM sample preparation technique presented here.

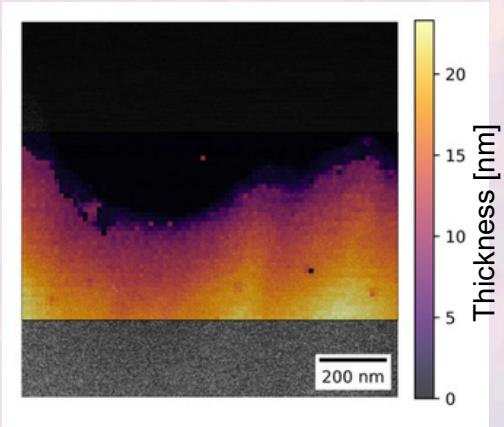


Figure 2: Thickness Map of a $SrTiO_3$ prepared with refined TEM sample preparation technique presented here, acquired with Neural Network assisted STEM PACBED analysis [3] and STEM HAADF. The thinnest regions have a thickness of approximately 3 nm.

References

[1] Mittal, Anudha, and K. Andre Mkhoyan. "Limits in detecting an individual dopant atom embedded in a crystal." *Ultramicroscopy* 111.8 (2011): 1101-1110.
[2] Voyles, P. M., J. L. Grazul, and D. A. Muller. "Imaging individual atoms inside crystals with ADF-STEM." *Ultramicroscopy* 96.3-4 (2003): 251-273.
[3] Oberaigner, Michael, et al. "Online thickness determination with position averaged convergent beam electron
diffraction using convolutional neural networks." *Microscopy and Microanalysis* 29.1 (2023): 427-436.

# Study of in-situ crystallization and phase evolution of $(AlCrTaTiNb)O_2$ high entropy oxides in atomic resolution (S)TEM

Roman Neuhauser[1], Bernhard Fickl[1], Alexander Kirnbauer[2], Tushar Gupta[1], Dominik Eder[1], Kimmo Mustonen[3], Clemens Mangler[3], Christian Rentenberger[3], Jani Kotakoski[3], Paul Mayrhofer[2], Bernhard C. Bayer[1]

[1]*TU Wien, Institute of Materials Chemistry, Vienna, Austria*

[2]*TU Wien, Institute of Materials Science and Technology, Vienna, Austria*

[3]*University of Vienna, Faculty of Physics, Vienna, Austria*

High-entropy oxides (HEOs) extend the concept of entropy engineering from metallic alloys to ionic systems, offering a pathway to unprecedented compositionally complex materials with tunable structural and functional properties. Among these, the $(AlCrTaTiNb)O_2$ system serves as a model to study how multiple cations can coexist at random occupation within a single oxide lattice and how such materials crystallize from the amorphous state or phase separate. A key challenge is however to experimentally access this element-specific structural information of such randomly elementary occupied crystalline lattices, that is the defining feature of high entropy materials.

In this work, we leverage suspended monolayer graphene films and ultrathin SiN membranes as ideal substrates for (scanning) transmission electron microscopy ((S)TEM) studies of ultrathin $(AlCrTaTiNb)O_2$ HEOs down to atomic resolution. Using these platforms, we investigate the phase evolution of this archetypical HEO system in two distinct directions: first, by tracking the in-situ crystallization process from the amorphous state, and second, by subjecting the pre-crystallized high-entropy phase to electron beam irradiation to observe its stability and dynamic response.

# QSEM

## Bring Quantum to SEM.

### Picosecond time resolution

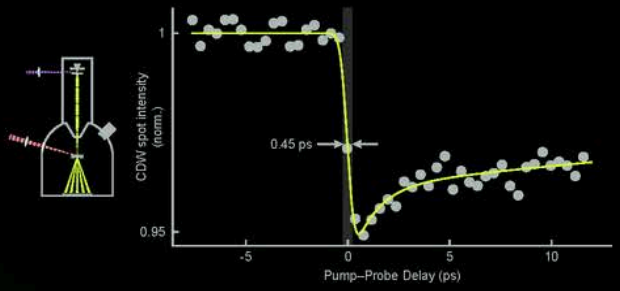


### Long-term stable photoemission

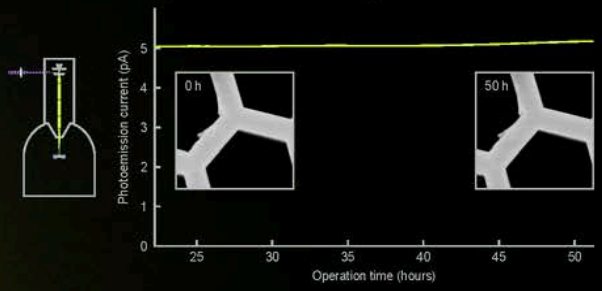


### Spatial Resolution (Continuous beam)

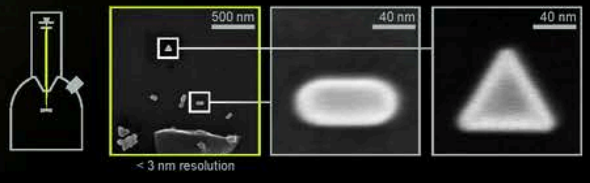


### Specifications and combinable modes

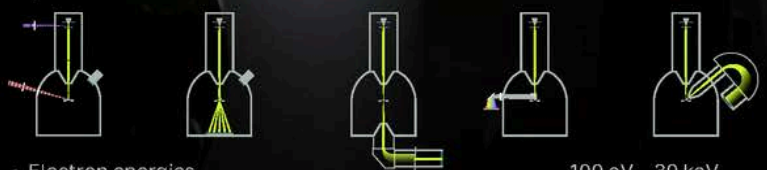

| | |
|---|---|
| • Electron energies | 100 eV – 30 keV |
| • Spatial resolution | < 3 nm (@ 20 keV) |
| • Ultra-high vacuum | < $10^{-9}$ mbar |
| • Photoemission operation | > 48 h |
| • Electron pulse duration | < 1 ps (FWHM) |

Stable ultrafast photoemission.

Laser-accessible sample space.

Energy-filtered 4D STEM.

Built to expand.

All data presented are provided courtesy of research conducted by Leon Kroß, Benjamin Schröder, Niklas Wemheuer, Claus Ropers, and Murat Sivis in the Department of Ultrafast Dynamics at the Max Planck Institute for Multidisciplinary Sciences, Göttingen.


QSEM GmbH
Hans-Adolf-Krebs-Weg 1
D-37077 Göttingen

Co-founded by:
Max Planck Society
CEOS GmbH

Prof. Dr. Claus Ropers
Dr. Murat Sivis
Dr. John H. Gaida

www.qsem.com
info@qsem.com
+49 551 270777


QSEM

# Towards Ultra-High Vacuum Operation in a TEM for Quantum-Computer-Enhanced Electron Microscopy

Martino Zanetti [1,2,3,*], Dominik Hornof [3,4], Michael S. Seifner [3,4], Philipp Haslinger [3,4], Thomas Juffmann [1,2]

[1] *VCQ, Faculty of Physics, University of Vienna, Boltzamanngasse 5, 1090 Vienna, Austria*
[2] *Max Perutz Labs, Campus-Vienna-Biocenter 5, University of Vienna, 1030 Vienna, Austria*
[3] *VCQ, Atominstitut, TU Wien, Stadionallee 2, 1020 Vienna, Austria*
[4] *USTEM, TU Wien, Stadionallee 2, 1020 Vienna, Austria*

** martino.zanetti@univie.ac.at*

Quantum electron microscopy is an emerging research field at the intersection of electron microscopy, quantum optics, and nanophotonics. Free electrons can serve as powerful quantum probes, on par with photons in their ability to carry and transfer quantum information, generate entanglement within and with a specimen, and reveal previously inaccessible details on nanoscale quantum phenomena [1].

However, quantum experiments are generally highly sensitive to decoherence arising from interactions with residual gas particles, making ultra-high vacuum (UHV) conditions sometimes essential. UHV environments are also required in transmission electron microscopes (TEMs) for the investigation of contamination-sensitive materials [2, 3]. In our project, we aim to combine a trapped-ion quantum computer with a TEM to realise Quantum-Computer-Enhanced Electron Microscopy (QCEM) (www.qcem.info). In this scheme, coherent interactions between free electrons and a trapped ion require vacuum conditions beyond the standard TEM operation [4].

Although UHV-TEM systems have previously been realised [2,3, 5-7], achieving base pressures in the $10^{-9}$ mbar range or better typically involves significant financial investment, long implementation times, and close collaboration with manufacturers.

We present a cost-effective, minimally invasive modification to the vacuum system of a JEOL JEM-2100F to reduce the base pressure at the sample position to below $5 \times 10^{-9}$ mbar. Our approach is to integrate two additional 50 L/s NEG-ion pumps mounted on flanges near the sample region, with no structural modifications to the microscope. The NEG pumps are integrated into the microscope workflow through controlled activation and regeneration cycles compatible with standard TEM operation.

This work represents a practical step toward enabling the realisation of QCEM, and the concept enables a relatively rapid implementation at a moderate cost, which can, in principle, be adapted to any TEM that provides suitable flange access to the sample chamber.

References

1. Garcìa de Abajo F.J. et al., ACS Photonics 12, 9, 4760–4817 (2025)
2. MORE-TEM, https://more-tem.univie.ac.at/ (accessed on 2026.02.23)
3. Leuthner G.T. et al., Ultramicroscopy 203, 76 (2019)
4. Pescoller E. et al., 10.48550/arXiv.2601.11446 (2026)
5. Heinemann K. and Poppa H, Journal of Vacuum Science and Technology A 4, 127 (1986)
6. Mishima T. and Osaka T., Surface Science 395, L256-260 (1998)
7. Malac M. et al., Micron 163, 103362 (2022)

# Transmission Electron Microscopy of Polymer-Electrolyt-Membranes

S. Schwarz[(a)]*, M. Binder[(a)], L. Anker[(a)], D. Wuketich[(b)] and T. Lauer[(b)]

*(a) USTEM - University service centre for transmission electron microscopy, TU Wien, Stadionallee 2/057-02, 1020 Vienna*

*(b) IFA - Institute of Powertrain and Automotive Technology, TU Wien, Getreidemarkt 9, 1060 Vienna*

**corrsponding author: sabine.schwarz@tuwien.ac.at*

Fuel cells are one of the most important ways to reduce CO2 emissions from transport worldwide to improve and preserve the environment for the future.

As part of the PEMLife project [1], research is being conducted into aged fuel cells in comparison with non-aged material, and various parameters of these cells are being characterised for use in technical and scientific predictions.

Simulations are one of the most important tools in science and have become indispensable in research. To obtain accurate results from these simulations, empirically determined parameters must be found to feed these simulations.

One of the most powerful tools for obtaining parameters on a micro- and nanometre basis is transmission electron microscopy (TEM) [2], [3]. Size parameters such as layer thickness, grain size, particle size, chemical composition (e.g. analysis using energy-dispersive X-ray analysis), as well as information about the crystal structure (crystal lattice, phase, amorphous, crystalline or nanocrystalline structures) can be determined. Images for the preparation and TEM images are shown in Fig.1 and Fig. 2.

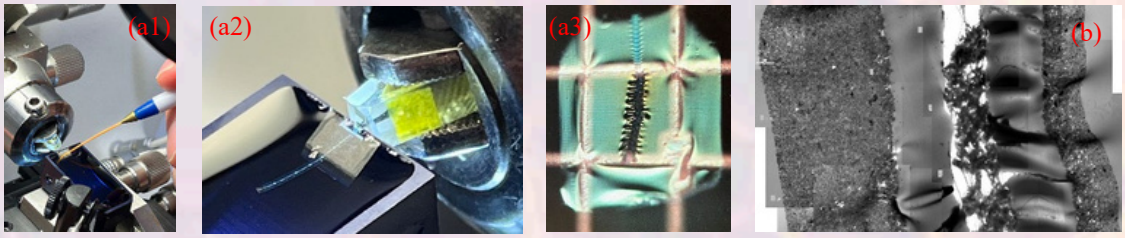


Fig. 1: (a) Cutting thin electron transparentsheets of PEM-layers for TEM investigationby ultramicrotomy.TEM overview of the PEM-layer (b) consisting of a cathodic catalyst layer (left), a membrane (center) and a catalyticlayer (right).

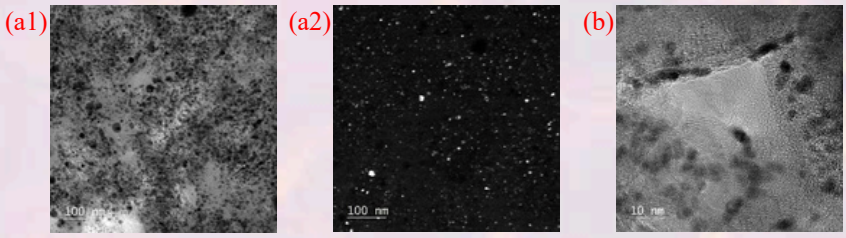


Fig. 2: TEM bright (a1) and dark (a2) field images of particles in theCCL layer. A HRTEM image of the anode catalyst layer is shown in (b).

References

[1] PEMLife, FFG No. 47180439. V. Shokhen, L. Strandberg, M. Skoglundh, B.

[2] Wickman, Fuel cell electrode degradation followed by identical location transmission electron microscopy, J. Mater. Chem. A, 2023, 11, 21029.

[3] P. Henry, L. Guétaz, N. Pélissier, P. Jacques, S. Escribano. Structural and chemical analysis by transmission electron microscopy of Pt-Ru membrane precipitates in proton exchange membrane fuel cell aged under reformate, Journal of Power Sources 275 (2015) 312-321.

# Mapping optical properties of distinct dislocations in GaN based electronic devices

Michael Stöger-Pollach[1,2], Ze Scales[3]

[1] *University Service Centre for TEM, TU Wien, Stadionallee 2, 1020 Wien*
[2] *Institute for Solid State Physics, TU Wien, Wiedner Hauptstraße 8-10, 1040 Wien*
[3] *Infineon Technologies Austria, Siemensstraße 2, 9500 Villach*

GaN exhibits excellent electronic properties for high power electronic devices, but it cannot be manufactured free of lattice defects. For electronic devices reliability and expected lifetime are crucial parameters driven by the density of distinct types of these dislocations. Consequently, it is important to understand how which type of lattice defect influences the overall performance and how the types of lattice defects can be characterized on an industrial scale. Typically, the defect density is in the range of 6 billion per cm$^2$, but only a fraction of them is critically.
In the present work we investigate electrically characterized dislocations by using low voltage valence electron energy loss spectrometry (LV-VEELS) and cathodoluminescence (CL). Using low beam energies prevents the sample from beam damage and avoids relativistic effects altering both, the VEELS and the CL spectrum, respectively. The electrical characterization was done by means of electron beam induced current (EBIC) and electron channelling contrast imaging (ECCI), both using a scanning electron microscope (SEM), prior to sample preparation employing focused ion beam (FIB).

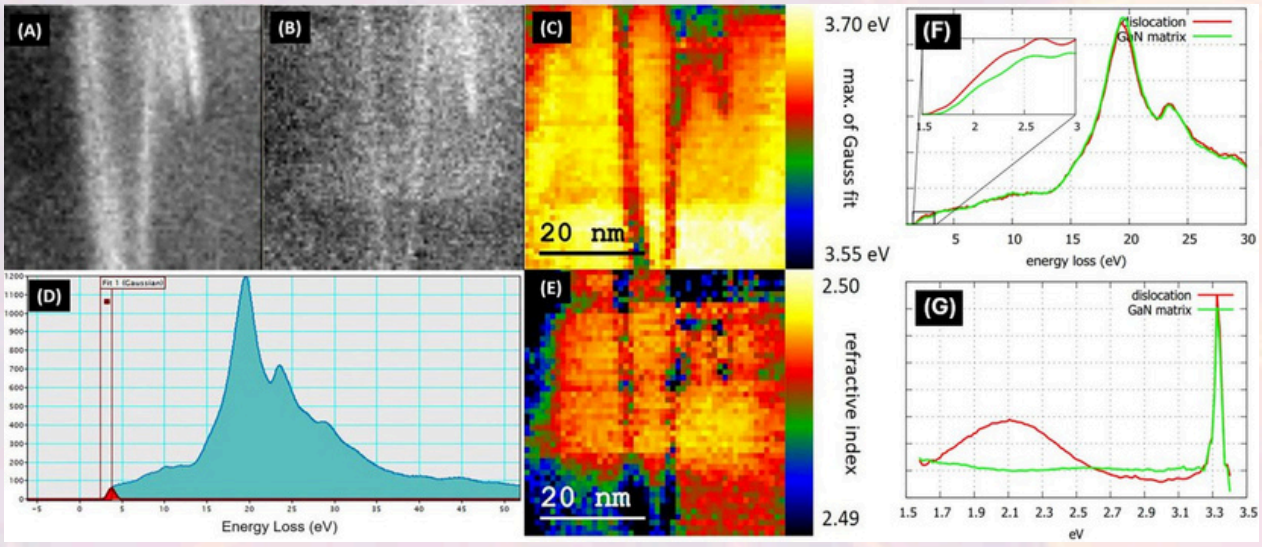


(A) Stain fields of the dislocations, (B) Z-contrast, (C) bandgap measured via VEELS, (D) measurement of inelastic signal onset, (E) refractive index determined via KKA, (F) VEELS spectra of matrix and defect, (G) CL spectra of same defect and matrix region

Electrically active defects show a significant yellow band emission at ~2eV, both in VEELS and CL. The reason for this is found in gap states due to enrichment of impurity atoms in the affected dislocations. For this purpose, chemical analysis was also performed using 200 keV EELS.

# Controlling stacking-fault-enriched ω phase formation in commercial-purity Titanium via oxygen and shear strain

Qiulin Qu[1*], Yong Huang[1], Zhuo Chen[1], Zaoli Zhang[1]

[1] *Erich Schmid Institute of Materials Science, Austrian Academy of Sciences, 8700 Leoben, Austria*
**qiulin.qu@oeaw.ac.at*

This study investigates the competitive and synergistic effects between dissolved oxygen and strain-induced defects in commercially pure titanium processed by high-pressure torsion (HPT). By varying the oxygen content (0, 0.14, 0.36, and 1.60 wt.%) and the applied shear strain (γ = 0, 5.9, 23.4, 261.7), we conducted comprehensive transmission electron microscopy (TEM) analysis to reveal the formation of the ω phase and its internal defect structures. Results show that ω phase formation is driven by shear strain but suppressed by oxygen, which acts as a drag point defect. Within the ω phase, we observed stacking faults with a displacement vector of 1/2<0001>, aligned along its prismatic planes. Based on the orientation relationships ($(0002)_\alpha||(11\text{-}20)_\omega$, $[11\text{-}20]_\alpha||[0001]_\omega$) and the defects present in the α phase, we propose a mechanism: pre-existing dislocations and stacking faults in the α-Ti matrix not only serve as preferred nucleation sites for the ω phase but also propagate into its interior, transforming into the observed stacking faults. These intrinsic planar defects contribute to the stabilization of the nanoscale ω phase. Our work clarifies the interaction and competition between interstitial oxygen and shear strain during the formation and evolution of defect-rich ω phases. The proposed nucleation and stabilization model offers a new perspective for understanding nanoscale pathways in stress-induced phase transformations in Ti alloys.

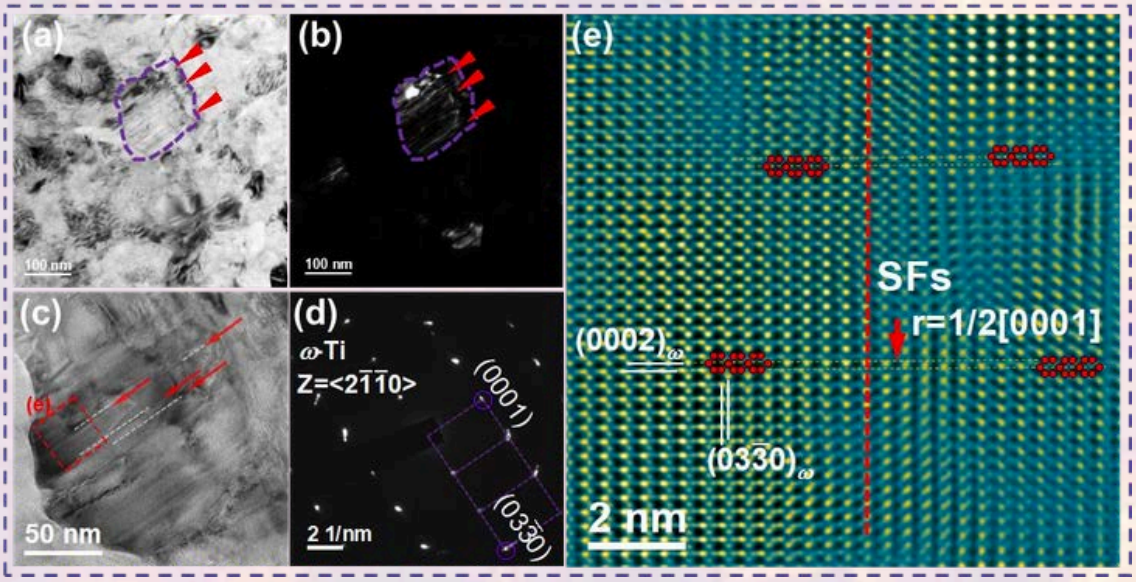


Figure 1. For the 0.36 wt.% Ti with 10 turns HPT rotation specimen: (a) The bright field image; (b) The dark field image of the ω phase formed using $(0001)_\omega$ diffraction spots, corresponding to (a); (c) The low magnification TEM image of the ω phase in (a); (d) The selected aera electron diffraction pattern of the ω grain in (c); (e) The high-resolution TEM image of the stacking fault within the ω grain.

**Acknowledgment**

This work is financially supported by the Austrian Science Fund (FWF) Grant 10.55776/P36581.

From Eye to Insight

Leica MICROSYSTEMS

# Ultramicrotome UC Enuity


- Experience the cutting edge of automation and precision
- Produce thin or ultra-thin sections for EM sample preparation.
- UC Enuity, the next generation ultramicrotome saves you valuable time and resources through its automated setup functions, providing state-of-the-art sectioning quality.

danaher.

# Quantitative Assessment of Charge Transfer in Potassium-Intercalated Graphite by Core-Loss EELS

Alexandra Wagner, Christian Kramberger, Andreas de Hartog and Thomas Pichler

*Faculty of Physics, University of Vienna, Vienna*

Graphite intercalated compounds (GICs) allow controlled tuning of the electric properties of graphite by either n-doping or p-doping. One of the most prominent examples of GICs is Li intercalated Graphite, which is the basis for Li batteries. Li might be replaced with K as component for charge transfer in batteries for geo strategic reasons.

Charge transfer in GICs can be assessed by analysing the modifications of the π* and σ* features in the carbon K-edge core-loss EEL spectra in comparison to pristine graphite. Changes in the Fermi level are reflected in the relative peak intensities and fine structure.

Preliminary measurements of $KC_8$ revealed changes in the C1s and K2p core-loss EEL spectrum after the sample was kept under standard TEM vacuum conditions for some time. Specifically, the π* peak intensity increased, while the σ* feature decreased in intensity and developed an additional excitation, that was not present in the initial spectrum of $KC_8$. As K is highly reactive toward both $O_2$ and $H_2O$, even trace amounts of residual gases present under traditional TEM vacuum conditions are sufficient to induce oxidation of K to KOH, which switches the doping of the material from n-type to p-type.

Further analysis of this effect has been conducted with the pioneering ultra-high vacuum MORE-TEM. Under these conditions the doping is stable for two to three days. Controlled in-situ laser annealing and deintercalation are done with the customized IDES @ MORE-TEM system.

**Acknowledgment**

This project has received funding from the European Research Council (ERC) under the European Union's Horizon 2020 research and innovation program (MORE-TEM ERC-SYN project, grant agreement No 951215). This work was supported by the Vienna Doctorate School of Physics.

# edXTrace: Improved Quantitative EDXS in TEM via Absorption and Detector-Shadowing Corrections

M. Oberaigner[1], N. Grogger[1], J. Lammer[1], D. Knez[2], G. Haberfehlner[2], G. Kothleitner[1,2], W. Grogger[1,2]

*[1]: FELMI, Graz University of Technology, Steyrergasse 17, Graz, Austria*
*[2]: ZFE, Graz Centre for Electron Microscopy, Steyrergasse 17, Graz, Austria*

Over the past two decades, energy-dispersive X-ray spectrometry (EDXS) in TEM has advanced significantly with the introduction of large-area silicon drift detectors (SDDs) and multi-detector setups. These systems achieve very large solid angles, enabling single-atom sensitivity. However, their size fundamentally alters the TEM geometry, making conventional specimen tilting ineffective and introducing significant detector shadowing. As a result, X-ray absorption by both the specimen and the specimen holder must be considered for accurate quantitative EDXS.

We developed edXTrace, a Python-based ray-tracing tool to model X-ray absorption and shadowing effects in arbitrary detector–specimen geometries. The software allows flexible definition of detector configurations, specimen shapes, and holder components, including their 3D geometry and material composition (Fig 1a). Once the scene is defined, edXTrace computes energy-dependent shadowing, effective solid angles, and quantitative absorption corrections for each detector. These corrections account for absorption in both the specimen and holder components and are provided via HDF5 output files, along with visualization images of detector shadowing.

edXTrace improves quantitative EDXS by providing reliable absorption corrections. Its effect and the errors arising from neglecting detector shadowing are demonstrated using a NiO film. As shown in Fig. 1b, the uncorrected Ni/O ratio varies significantly at high tilt angles, whereas absorption-corrected values remain stable, highlighting the improved accuracy of quantification.

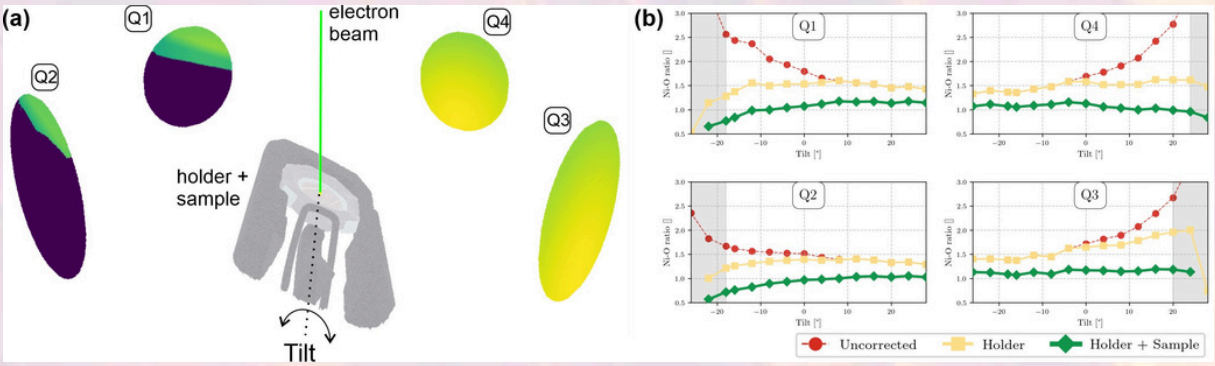


Fig 1: EDXS quantification of a NiO film over a tilt series: (a) experimental geometry; (b) comparison of uncorrected and corrected Ni/O ratios at different specimen tilts.

**Acknowledgment**

The authors acknowledge funding from “ESTEEM3” (European Union’s Horizon 2020 research and innovation program under grant agreement No 823717) and “IMPRESS” (European Union's Horizon Europe framework program for research and innovation under grant agreement No 101094299).

# Unravelling the enamel-steel interface using electron microscopy: From oxide scale to mechanical interlocking

Philipp Kürnsteiner[1], Martin Krenn[1], Liam Brown[1], Andreas Muhr[2], Reza Sharif[2], Thomas Steck[2], Heiko Groiss[1,*]

[1]*Christian Doppler Laboratory for Nanoscale Phase Transformations, ZONA, Johannes Kepler University Linz, Altenberger Straße 69, 4040 Linz, Austria, Linz*

[2]*voestalpine Stahl GmbH, voestalpine Straße 3, 4020 Linz, Austria, Linz*

[*]*heiko.groiss@jku.at*

Steel enamelling is a common coating used for products such as kitchen appliances, ovens, heat exchangers or chemical reactors. The durability of such coatings depends critically on their adhesion to the steel substrate. The enamelling process involves several stages, including surface preparation, enamel application and finishing at high temperatures. During firing in air atmosphere, an oxide scale forms on the steel surface, which must be dissolved in the liquid enamel to ensure good adhesion. Understanding both the formation and subsequent dissolution of this oxide layer is therefore crucial for elucidating the interfacial mechanisms that govern enamel-steel adhesion.

In this study, we investigated various steels grades including die cast DC04EK, DC06EK, dual phase DP450 and open coil OC material. To track oxide scale evolution, we interrupted the enamelling process at specific temperatures ranging from 300°C to 820°C. The oxide layer thickness and surface coverage were monitored during heating. At temperatures above 700 °C, the dissolution of the oxide in the viscous enamel layer was then examined. To preserve the native structure of the interfaces between enamel, oxide and steel for high-resolution analysis, we have developed a careful sample preparation procedure. Advanced electron microscopy techniques were employed to visualize oxide dissolution at high lateral resolution, allowing us to monitor the involved diffusion processes from the base material into the enamel. The dissolution of elements from the steel into the enamel contributes to increased surface roughness and the formation of undercuts at the steel surface, promoting mechanical interlocking and enhanced enamel adhesion.

This comprehensive toolbox for analysing the precise steel-enamel interface enables direct comparisons between interface processes for different steel grades and firing temperatures. This is the basis for the development of improved enamelling steels and optimized coating processes.

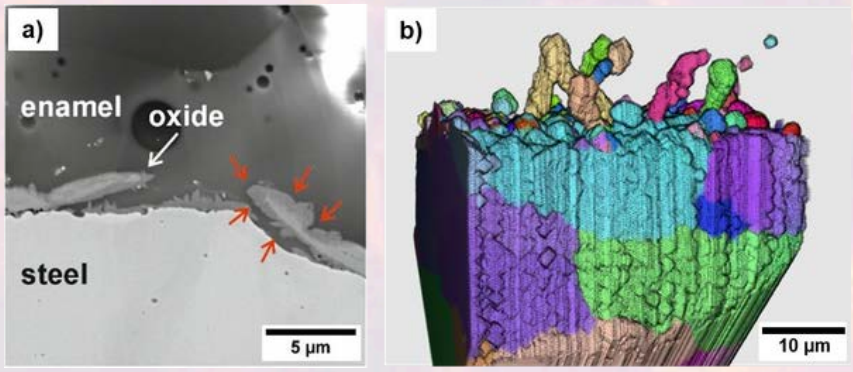


a) Dissolution of the oxide scale, investigated via SEM at an interface between DC04steel and the enamel coating interrupted at 750°C. A region of the interface is depicted where theenamel penetrates beneath the scale layer, causing it to dissolve from both sides. The associated interdiffusion region is marked by red arrows. b) Plasma FIB tomography of an enamel-steel interface of a DC04, fully formed at 820°C. The 3D reconstruction of the steel interface is shown, revealing the interface steel anchors that facilitate enamel adhesion.

# Analysis and Classification of Non-Exhaust Particle Emissions by Combining Microscopy, Spectroscopy and Machine Learning.

Niko Koch[1], Hartmuth Schröttner[1,2] and Manfred Nachtnebel[2]

*[1]: FELMI, Graz University of Technology, Steyrergasse 17, 8010 Graz, Austria*
*[2]: ZFE, Graz Centre for Electron Microscopy, Steyrergasse 17, 8010 Graz, Austria*

Over the past decades, EU regulations have successfully reduced particulate matter (PM) emissions from vehicle exhaust systems. As a result, exhaust-related PM emissions have reached comparatively low levels, while non-exhaust sources – namely tyre, brake, road, and rail abrasions – have remained largely unchanged and now dominate traffic-related PM emissions. Within the TU Graz Leadproject NExT (Non-Exhaust Emission Topics), which focuses on the assessment and reduction of particle emissions from abrasion processes, this work addresses the detailed analysis and characterization of microscopic wear particles obtained from test benches which simulate real-world emissions.

To meet this challenge, testing methodologies and automated single-particle analysis workflows are being developed. The central analytical platform is a correlative RISE (Raman Imaging and Scanning Electron Microscopy) system combining scanning electron microscopy (SEM), energy-dispersive X-ray spectroscopy (EDX), and confocal Raman microscopy. Automated SEM feature analysis enables detection and morphological characterization of thousands of individual particles, while EDX provides elemental composition and Raman spectroscopy adds complementary molecular information.

The resulting multidimensional datasets are evaluated using Python-based machine learning approaches to enable automated classification, clustering, and statistical analysis of the heterogeneous particle mixture. The overarching objective is the development of standardized and automated characterization procedures tailored to abrasion emissions, thereby supporting the goal of the NExT project.

**Acknowledgment**

The authors gratefully acknowledge Graz University of Technology for (co-)financing this work through the Lead Project NExT (Non-Exhaust Topics)

Quantum Design

qd-europe.com

# Electron Microscopy

## Sample preparation and measurement

- High-resolution compact & tabletop SEM
- In situ TEM/SEM/µXCT
- Sputter & carbon coaters
- Cryo preparation system
- FusionScope – correlative microscopy platform
- Electron diffraction



HITACHI Inspire the Next

Quorum

ELDIGO

DENS solutions

# Towards Integrating a Trapped-Ion Quantum-Bit in a Transmission Electron Microscope

D. Hornof[1,2], M. Zanetti[3,4], N. Jungwirth[5], M. S. Seifner[1,2], P. Schindler[5], T. Juffmann[3,4], P. Haslinger[1,2]

*[1]VCQ, Atominstitut, TU Wien, Stadionallee 2, Vienna, 1020, Austria*
*[2]USTEM, TU Wien, Stadionallee 2, Vienna, 1020, Austria*
*[3]VCQ, Faculty of Physics, University of Vienna, Boltzmanngasse 1, Vienna, 1090, Austria*
*[4]Max Perutz Laboratories, University of Vienna, Dr. Bohr Gasse 9, Vienna, 1030, Austria*
*[5]Department of Experimental Physics, University of Innsbruck, Technikerstraße 25, Innsbruck, 6020, Austria*

In electron microscopy, the pursuit of atomic-scale resolution for imaging biological [1] samples and soft-matter systems [2] is perpetually constrained by beam-induced sample degredation. While classical approaches attempt to optimize the trade-off between dose efficiency and image quality, they remain fundamentally limited by the physical interactions between electrons and the sample. Quantum technologies, however, present a transformative opportunity by enhancing information extraction per electron without increasing exposure [3], thereby breaking through classical constraints.

In this work, we integrate for the first time a trapped-ion qubit into a transmission electron microscope, leveraging the strong Coulomb interaction between swift electrons and $Ca^+$ ions [4], along with the precise control and readout capabilities of trapped $Ca^+$ ions [5]. By harnessing quantum coherence and controlled interactions, this hybrid approach seeks to advance the capabilities of low-dose imaging, improving the analysis of radiation-sensitive samples while minimizing damage. For this purpose, we customize a transmission electron microscope to provide the required ultra-high-vacuum integrity and adapt the $Ca^+$ trap design, including laser cooling and state readout/manipulation, to the geometric constraints of the microscope's pole-piece gap.

References

[1] Kato, K. et al. "High-resolution cryo-EM structure of photosystem II reveals damage from high-dose electron beams." Communications Biology 4.1 (2021): 382.
[2] VandenBussche, E. J. and Flannigan, D. J. "Reducing radiation damage in soft matter with femtosecond-timed single-electron packets." Nano letters 19.9 (2019): 6687-6694.
[3] Okamoto, H. et al. "Entanglement-assisted electron microscopy based on a flux qubit", Appl. Phys. Lett. 104, 062604 (2014)
[4] Pescoller, E. et al. "Coupling free electrons to a trapped-ion quantum computer", arxiv:2601.11446 (2026)
[5] Gulde, Stephan, et al. "Implementation of the Deutsch–Jozsa algorithm on an ion-trap quantum computer." Nature 421.6918 (2003): 48-50.

**Acknowledgment**

This research is funded by the Gordon and Betty Moore foundation, the FFG-project AQUTEM and the Austrian Cluster of Excellence Quantum Science Austria (quantA).

# Reliable Texture Analysis in Wrought Aluminum Alloys via EBSD and MTEX

Moritz Theissing[1,2], Vitesh Shah[3], Georg Falkinger[3], Stefan Mitsche[1,2], Gerald Kothleitner[1,2]

[1]*Institute of Electron Microscopy and Nanoanalysis, Graz University of Technology, Graz, Austria*
[2]*Graz Centre for Electron Microscopy, Graz, Austria*
[3]*AMAG rolling GmbH, Ranshofen, Austria*

The microstructure of wrought aluminum alloys plays a critical role in determining their macroscopic properties. Electron backscatter diffraction (EBSD) provides crystallographic orientation data at individual scan points, enabling the evaluation of grain structure, internal deformation, and crystallographic texture. Texture components are defined by specific orientations, such as the Cube orientation (0,0,1), within a prescribed tolerance angle [1]. Given the strong influence of texture on material behavior, this work focuses on the reliable investigation and analysis of crystallographic texture in aluminum alloys.

EBSD measurements were performed on AA2024 and AA8079 alloys in both deformed and annealed states. The influence of EBSD step size on the measured texture fraction was assessed, showing that below a certain step size further refinement does not significantly alter the calculated fractions. The effect of tolerance angle selection was also examined, as overlapping texture components can reduce evaluation clarity and depend on the components considered. Orientation noise was investigated in the context of recently introduced spherical indexing methods [2], which substantially reduce this source of error. Additionally, a comprehensive texture evaluation workflow was implemented using the MATLAB toolbox MTEX [3], including the determination of recrystallized fractions, texture maps, pole figures (PFs), and orientation distribution functions (ODFs).

Overall, this study presents a systematic approach to crystallographic texture evaluation in aluminum alloys, enabling more reliable assessments of its influence on material properties.

References

[1] Lenthe, W. C., Singh, S., & De Graef, M. (2019). A spherical harmonic transform approach to the indexing of electron back-scattered diffraction patterns. Ultramicroscopy, 207, 112841.

[2] Engler, O., Zaefferer, S., & Randle, V. (2024). Introduction to texture analysis: macrotexture, microtexture, and orientation mapping. CRC press.

[3] Bachmann, F., Hielscher, R., & Schaeben, H. (2010). Texture analysis with MTEX–free and open source software toolbox. Solid state phenomena, 160, 63-68.

# Modifying 2D materials using swift heavy ions

N. Ravindran[1,2,*], S. Dibeh[1,2], A. Niggas[3], F. Vukovic[3], V. Zobac[1], R. Wilhelm[3], and T. Susi[1]

[1]*University of Vienna, Faculty of Physics, Vienna, Austria*
[2] *University of Vienna, Vienna Doctoral School in Physics, Austria*
[3]*TU Wien, Institute of Applied Physics, Vienna, Austria*
**corresponding author: nandhini.ravindran@univie.ac.at*

When ions with mega-electron-volt (MeV) kinetic energies hit free-standing 2D materials such as molybdenum disulphide and its combination into van der Waals heterostructures, several physical processes can occur depending on the irradiation energy and dose. The ions typically create pores, the size of which depends on the kinetic and potential energy of the impinging ions. Study of ion interaction with solid surfaces opens paths to atomic-scale structural modification of materials, where imaging at the atomic scale can elucidate the influence of ion parameters on the pore structure [1].

In recent studies of highly charged ion irradiation of free-standing 2D materials and their heterostructures, it was realised that material order plays a significant role. In the case of graphene facing the ion beam, apparently it absorbed all the potential energy while shielding the underlying $MoS_2$ layer. By contrast, a single layer of $MoS_2$ facing the ions gets perforated, but when there are two or more layers, the second or third layer shows reduced or no damage [2].

$MoS_2$ flakes grown on silicon wafers by chemical vapour deposition (CVD) were transferred onto a single-layer graphene-coated transmission electron microscopy (TEM) grids. For this study, we made sure that the $MoS_2$ side is on top of graphene facing the ion beam. Three freestanding $MoS_2$ on graphene van der Waals heterostructures were irradiated at 4.8 MeV/u amu at charge states of $Au^{25+}$, $Au^{54+}$, $Au^{58+}$ and at a fluence of $5\times10^{10}$ ions/cm$^2$ per sample. To characterize the samples both before and after ion irradiation, we imaged them at atomic resolution using an aberration-corrected scanning transmission electron microscope Nion UltraSTEM100 [3]

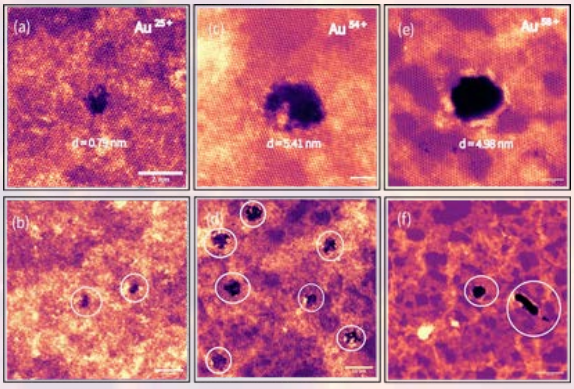


(a)-(f) STEM-MAADF images of $MoS_2$/Graphene. Pores in $MoS_2$ after irradiation with highly energetic ions at different charge states. (Top row) Pores on the lattice at a 16 nm field of view (FOV). (Bottom row) Pores at a 64 nm FOV.

The pore density closely matches the applied ion fluence, indicating a pore creation efficiency in $MoS_2$ of approximately unity. The mean pore diameter of the irradiated samples were 1.5  0.4 nm for $Au^{25+}$, 4.7  0.5 nm for $Au^{54+}$ and 4.4  0.4 nm for $Au^{58+}$. The charge of the ion increases the pore sizes even in case of swift heavy ions. Graphene remains intact even after swift heavy ion impact, consistent with previous findings for highly charged ions.

Through this research, we hope to build a systematic understanding of the interaction between very high-energy ions and the lattice of 2D materials and their heterostructures. This can enable the modification of 2D materials with controlled pore sizes for further studies and various applications.

References

1. Schwestka, J. et al., ACS Nano 14(8), 10536-10543 (2020).
2. R. Ritter, et al., Applied Physics Letters 102(6), 063112 (2013).
3. Mangler, C. et al., Microsc. and Microanal 28(S1) (2022).

# Capturing the respiratory chain in action with time-resolved cryo-EM

Kaitlyn Kiernan and Leonid Sazanov

*Institute of Science and Technology Austria*

The respiratory chain plays a crucial role in generating metabolic energy for cellular life. It is powered by four large membrane protein complexes that harness redox chemistry to power proton translocation across the mitochondrial membrane and drive ATP synthesis. Respiratory enzymes undergo many conformational transitions to tightly coordinate electron transfer to proton pumping. Decades of research have uncovered the basic principles of this process, but most structural insights have come from static snapshots that fail to represent the dynamic nature of these molecular machines. To address this, we have implemented time-resolved cryo-EM to visualize transient structural states of the largest enzyme of the respiratory chain, respiratory complex I (NADH:ubiquinone oxidoreductase). We have constructed a device enabling controlled substrate delivery and rapid freezing of cryo-EM grids on the millisecond timescale. This approach allows us to trap short-lived conformational states during turnover and resolve precisely how complex I couples electron transfer from NADH to quinone with proton pumping. Ultimately, this work will advance our understanding of mitochondrial bioenergetics and establish a broadly applicable approach for probing the structural dynamics of large, membrane-bound molecular assemblies in action.


**SCIENCE SERVICES – Ihr Partner für Mikroskopie und Laborbedarf**

Seit nun 50 Jahren, seit 1976, bietet SCIENCE SERVICES zuverlässige Lösungen für die Probenpräparation in Mikroskopie und Ultrazentrifugation. Wissenschaftliche und industrielle Labore weltweit schätzen unsere Expertise und langjährige Zusammenarbeit.

Unser Sortiment umfasst über 20.000 Produkte ausgewählter Spezialhersteller, mit denen uns langjährige Partnerschaften verbinden. Unser Fokus liegt auf Lösungen für die Material- und Lebenswissenschaften im Bereich TEM, REM, Kryo-EM und CLEM.

Ein interdisziplinäres Team aus Wissenschaftlern, Technikern und Anwendungsspezialisten sichert fundierte Beratung und zuverlässige Unterstützung.

## 50 JAHRE SCIENCE SERVICES

Profitieren Sie von regelmäßigen Rabatten, Aktionen und Anwendungsinformationen!

Nichts verpassen und gleich anmelden unter: www.scienceservices.de/newsletter und folgen Sie uns auf linkedIn (#scienceservices)

Newsletter

LinkedIn

SCIENCE SERVICES 50 YEARS - EST. 1976 -

SEIT 50 JAHREN
IHR KOMPETENTER
PARTNER

Info@ScienceServices.de
www.ScienceServices.de

# $Ca^{2+}$-Induced Conformational Changes in Mammalian ATP Synthase

Anton Kavaleuski and Leonid Sazanov

*Institute of Science and Technology Austria*

Elevated $Ca^{2+}$ concentrations induce the opening of a non-specific channel in the inner mitochondrial membrane known as the permeability transition pore (PTP).Although the molecular entity of the PTP remains formally unresolved, most current studies agree that ATP synthase underlies pore formation.

In this work, we used cryo-EM to extensively compare the conformations adopted by native murine ATP synthase and the enzyme incubated with 1 mM $Ca^{2+}$, revealing structural changes that provide a mechanistic explanation for how ATP synthase may contribute to PTP opening.

From models reaching 2.3 Å resolution, we identify distinct structural features specific to the $Ca^{2+}$-treated enzyme, including displacement of the β-barrel in a catalytic subunit and a pronounced shift of the peripheral stalk. These conformational rearrangements are consistent with the proposed mechanism of signal propagation from $Ca^{2+}$ binding at the catalytic site toward the membrane region of ATP synthase.

Another major finding is the identification of a binding dwell (ATP-waiting) conformation that has not previously been structurally characterized in mammalian ATP synthase. This conformation is also associated with $Ca^{2+}$ treatment; however, its relevance to PTP formation remains unclear.

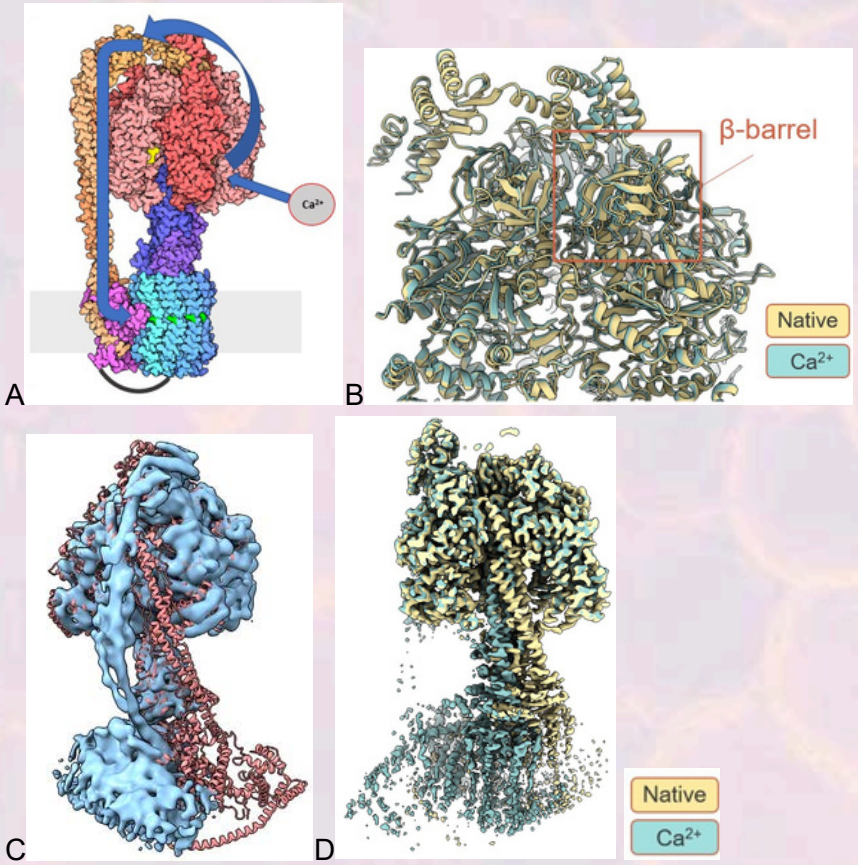


**Figure 1.** (A) Proposed pathway of signal propagation leading to PTP opening. (B) Displacement of the β-barrel in a catalytic subunit. (C) Shift of the peripheral stalk in $Ca^{2+}$-treated ATP synthase (blue). (D) ATP synthase in the binding-dwell conformation (blue).

# In-situ atomic-resolution observation of the anisotropic decomposition in TaN

Xiaoming Liu[1*], Zhuo Chen[1], Yong Huang[1], Qiulin Qu[1], Zaoli Zhang[1]

[1] *Erich Schmid Institute of Materials Science, Austrian Academy of Sciences, 8700 Leoben, Austria*

**xiaoming.liu@oeaw.ac.at*

The service life of transition-metal nitride thin films is critically limited by their tendency to decompose under extreme conditions. Previous studies have generally suggested that decomposition proceeds through a gradual structural transformation between different phases, accompanied by nitrogen loss [1,2]. Here, using in-situ high-resolution transmission electron microscopy and quantitative measurements combined with theoretical analyses, we carefully investigate the decomposition behaviour of a rock-salt TaN film at the atomic scale under electron-beam irradiation. The results reveal that TaN decomposes directly into metallic Ta without forming the intermediate hexagonal $TaN_2$ phase. Furthermore, when irradiated along the $[001]_{TaN}$ direction, TaN exhibits a stronger tendency toward structural transformation, while most nitrogen remains within the irradiated Ta product. In contrast, irradiation along the $[110]_{TaN}$ direction promotes nitrogen loss from TaN but suppresses the structural transformation. The observed decoupling between structural transformation and nitrogen depletion is primarily attributed to the orientation-dependent decomposition of TaN crystals. These findings provide new insights into the anisotropic decomposition behaviour of transition-metal nitrides and establish a framework for tailoring the stability and composition of non-stoichiometric nitride systems.

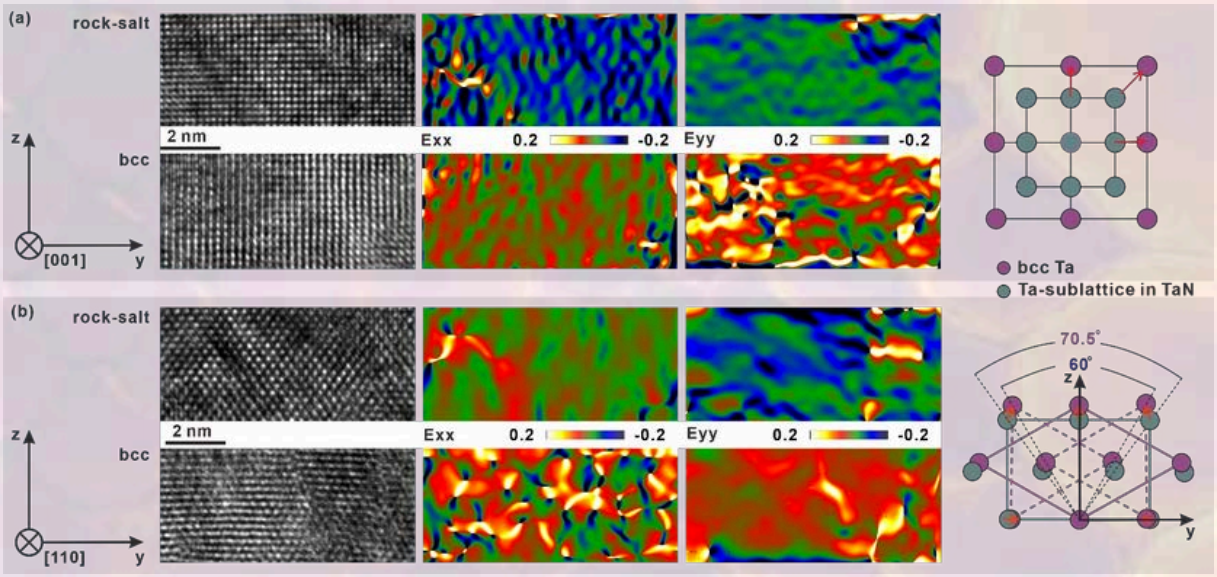


Figure 1. (a, b) HRTEM images, corresponding strain maps by GPA, and schematic illustrations showing the transformation pathways of rock-salt TaN into bcc Ta along the [001]TaN and [110]TaN directions, respectively.

References

[1] W. Ernst; J. Neidhardt; H. Willmann; B. Sartory; P.H. Mayrhofer; C. Mitterer, Thin Solid Films, 2008, 517, 568-574.

[2] P.K. Tripathy, Journal of Materials Chemistry, 2001, 11(5), 1514-1518.

**Acknowledgment**

This work is financially supported by the Austrian Science Fund (FWF 10.55776/PAT1946623). We would like to sincerely thank Univ.-Prof. Dr. Christian Mitterer and Mag. Velislava Terziyska (Montanuniversität Leoben) for their assistance with thin-film deposition.

# Selective defect creation in 2D hexagonal boron nitride via ultra-low energy $Ar^+$ irradiation

Shrirang Chokappa[1,2,*], Manuel Längle[1], Vladimir Zobač[1], Jacob Madsen[1], Diana Propst[1,2], David Lamprecht[1,3], Philipp Irschik[1,2], Clemens Mangler[1], Toma Susi[1], and Jani Kotakoski[1]

[1]*University of Vienna, Faculty of Physics, Boltzmanngasse 5, 1090 Vienna, Austria*
[2]*University of Vienna, Vienna Doctoral School in Physics, Boltzmanngasse 5, 1090 Vienna, Austria*
[3]*Institute for Microelectronics, TU Vienna, Gußhausstraße 27-29 / E360, 1040 Vienna, Austria*
** Contact email: shrirang.chokappa@univie.ac.at*

In recent years, point defects in hexagonal boron nitride (hBN) have received increasing attention for being excellent hosts for single photon emitters (SPE) at room temperature [1,2]. SPEs are a growing research area that have potential applications in quantum communication and information technology, quantum simulations, as well as photonics [3], and introduces the question of whether defect creation in hBN can be controlled. But, so far, no conclusive results have been reported correlating the exact defect structure and the quantum emission [4,5]. According to simulations using time dependent density functional theory (TDDFT), an $Ar^{+1}$ ion in a head-on collision with nitrogen requires 34.5 eV to successfully knock it out from the hBN lattice, and 45.5 eV to successfully knock out a boron atom, indicating the possibility of selective defect creation.

In this experimental study, freestanding monolayer hBN samples were prepared using the electrochemical delamination method and were subjected to 150 eV $Ar^+$ ion irradiation. Using our interconnected ultra-high vacuum system [6], the irradiation effects were directly characterized via scanning transmission electron microscopy (STEM) without exposing the samples to ambient conditions. Large area semi-automated STEM image acquisition [7] was performed to acquire hundreds of images of hBN before and after the irradiation. The data analysis was carried out with the help of a semi-autonomous convolutional neural network (CNN) defect identification software. The intrinsic defect density was found to be 0.023 $nm^{-2}$ with a roughly 1:1 ratio in B:N single vacancies, but ca. 40% of the boron single vacancies were found to be filled by Si atoms. After irradiation, we found a defect density of 0.243 $nm^{-2}$ with a roughly 85:15 ratio in B:N single vacancies and a 3:1 and 6:1 ratio of single to double and single to triple vacancies, respectively. Here we also observe that a large number of the vacancies have been filled by Si and C atoms. Overall, we show a high defect creation probability at this ion energy and demonstrate that such an irradiation already provides selectivity in the defect types created.

References

1. Tran et al., Nature Nanotech. 11, 37-41 (2016)
2. Grosso et al., Nature Comms. 8, 705 (2017)
3. Liu et al., Nano Mat.Science 3, 291-312 (2021)
4. Tawfik et al., Nanoscale 9, 13575-13582 (2017)
5. Gale at al., ACS Photonics 9, 2170-2177 (2022)
6. Mangler et al., Micro. and Microanal. 28 S1, 2940-2942 (2022)
7. Mittelberger et al., Micro. and Microanal. 23 S1, 809-817 (2017)

# Hematene lattice parameter variation as a function of thickness

Maximilian Melchior[a], Jana Dzibelova[a], Anastasiia Nihei[b], Rico Friedrich[b], Jani Kotakoski[a]

[a]*University of Vienna, (Vienna),Austria,*
[b]*TU Dresden, (Dresden), Germany*
*Contact email:maximilian.melchior@univie.ac.at*

Hematene ($\alpha$-$Fe_2O_3$) is a two-dimensional non-van der Waals material, first successfully exfoliated in 2018 [1]. Contrary to its bulk counterpart, this iron oxide phase exhibits photocatalytic activity in its low-dimensional form, making it interesting for various applications [1, 2]. As the thickness approaches a few atomic layers, interatomic distances are modified due to the accommodation of dangling bonds. First-principles calculations indicate lateral stretching of exfoliated [001] planes up to 2% [3]. This contribution aims to experimentally investigate and quantify the change in the lattice parameters of hematene.

Thickness measurements are performed using four-dimensional scanning transmission electron microscopy (4D-STEM). Position averaged convergent electron beam diffraction (PACBED) is sensitive to material thickness and tilt. The collected PACBED patterns are matched with a library of abTEM-simulated datasets of known thickness and tilt [4, 5]. The calibration of the convergence angle using graphene enables the determination of the lattice parameters directly from the PACBED data.

In order to validate the results, thickness is also determined by electron energy loss spectroscopy (EELS) using the log-ratio model [6]. The custom-made SiN grids (Silson Ltd) used in STEM are compatible with atomic force microscopy (AFM), which is also available in the University of Vienna CANVAS system [7] and allows for a careful calibration of the mean free path. This approach ensures a robust estimate of the number of hematene layers.

References

1. A. Puthirath Balan, S.Radhakrishnan, C.F. Woellner et al., Nature Nanotech 2018,13, 602–609
2. J. Dzíbelová, et al., Applied Materials Today 2023, 34, 101881
3. R. Friedrich, et al., Nano Letters 2022, 22, 989-997
4. C. Ophus, et al., Appl. Phys. Lett. 2017, 110, 063102
5. J.Madsen, T.Susi, Open Research Europe 2021, 1:24
6. K. Iakoubovskii, et al., Microsc. Res. Tech. 2008, 71, 626-631
7. C Mangler, et al., Microscopy and Microanalysis 2022, 28 (S1), 2940–2942

# Tracing metal losses in ferronickel production: a multiscale structural study

Tamara Đorđević[1,2], Sabine Schwarz[1] and Michael Stöger-Pollach[1]

*[1]E057-02 USTEM, Vienna University of Technology, Stadionallee 2, 1020 Vienna, Austria*
*[2]Department of Mineralogy and Crystallography, University of Vienna, Josef-Holaubek-Platz 2, 1090 Wien, Austria*
*e-mail: tamara.dordevic@tuwien.ac.at*

The laterite Ni-smelting operations at Euronickel Industries, Vozarci, North Macedonia, have produced large amounts of smelting waste deposited near the smelter. Previous bulk mineralogical (powder X-ray diffraction), chemical (X-ray fluorescence), and scanning electron microscopy (SEM) investigations of electric furnace slags (EFS) derived from laterites of different localities were reported by Đorđević et al. (2024). These EFS are predominantly composed of crystalline olivine-like phases, pyroxene-like phases and spinel-like oxides, all embedded within an amorphous silicate glass matrix. Locally, the slags contain intermetallic ferronickel particles ranging in composition from pure Fe through $Fe_7Ni_3$ to $Ni_3Fe$, occurring as microscale metal droplets.

To optimize metal retention protocols for critical and strategic elements, we investigated the nanoscale distribution and speciation of nickel (Ni), cobalt (Co), and chromium (Cr) using transmission electron microscopy (TEM). Both finely dispersed slag powders (ethanol-suspended) and focused ion beam (FIB)-extracted TEM lamellae from distinct microstructural domains were analyzed. TEM imaging reveals the coexistence of crystalline silicate phases (forsterite), spinel-type oxides (Mg-bearing chromite), amorphous glass domains and finely dispersed crystalline ferronickel particles together with Fe–Ni sulfides.

Energy electron-loss spectroscopy (EELS), combined with energy-filtered TEM (EFTEM), enabled phase mapping and determination of metal oxidation states. ELNES analysis of the Fe-L edge reveals distinct spectral features corresponding to $Fe^0$ in metallic alloys, $Fe^{2+}$ in silicates, and mixed $Fe^{2+}/Fe^{3+}$ states in spinel-type oxides, allowing nanoscale discrimination of redox-dependent partitioning. Selected area electron diffraction (SAED) patterns from metal-bearing particles confirm the crystallographic identification of $Fe_7Ni_3$ alloy in both micro- and nano-inclusions. Furthermore, SAED combined with Fe-L edge EELS distinguishes two structurally distinct Fe-sulfide phases: pyrrhotite-type sulfide with Fe:S~1:1 isostructural with hexagonal mineral troilite and Ni-bearing Fe-sulfide ($Fe_{5.5}Ni_{2.5}S_7$) isostructural to the cubic mineral pentlandite.

Nanoparticles (<50 nm) of ferronickel alloy are also widespread within the sulfides and in the glass matrix and likely represent early-stage metal nucleation during smelting. Notably, Fe, Ni, and Co are hosted in multiple forms: structurally incorporated within silicates and spinels, alloyed in intermetallic particles, and present in sulfide inclusions. Cr is predominantly structurally incorporated within spinel-group oxides. The nanoscale proximity and occasional textural association between spinel particles and ferronickel nanospheres suggest possible interfacial processes influencing metal segregation.

This research was funded by the Scientific & Technological Cooperation (WTZ- project PL 14/2024 of the Austria's Agency for Education and Internationalization-ÖAD).

References

Đorđević, T., Tasev, G., Aicher, C., Potysz, A., Nagl, P., Lengauer, C.L., Pędziwiatr, A., Serafimovski, T., Boev, I., Boev, B. (2024). J. Appl. Geochem., 170, 106068–106081.

# Establishing a Workflow for 3D reconstruction with the Katana from ConnectomX for serial block face Scanning microscopy (SBF-SEM)

Lena Reberz, Magdalena Knapp, Ute Rothbächer, Anna Seybold

*Institute of Zoology, University of Innsbruck, Austria*

Serial block face has advanced the automated acquisition of 3D Volume microscopy inside the scanning electron microscope (SEM)[3]. A removable ultra microtome for the SEM that can section and image samples reproducibly and reliably is a valuable addition to our Electron Microscopy facility. For that we established an SBF-SEM workflow at the University of Innsbruck using the Katana ultramicrotome from ConnectomX[2] installed in the Tescan Clara SEM.

This workflow integrates the sample preparation resin embedding and block trimming, the Pin preparation, the automated serial sectioning and image acquisition with optimised SEM conditions, stack alignment and three-dimensional reconstructions via FIJI[5].

For the fixation and staining specific Volume EM protocols have been tested as well as conventional protocols. The samples in resin were then trimmed, and the sample was cut out in a $1mm^3$ cube. This cube was then adhered with conductive resin to a pin. For the smoothing of the resin sample surface special parts were made to hold the significantly smaller Katana pins. The pins where sputtered with a 20nm gold coat and where then ready for imaging. In the SEM the Low Vacuum setting was chosen to reduce charging. The imaging was done using the Gatan OnPoint BSE detector[4] for fast and high resolution imaging. The cutting thickness and all imaging parameters were gradually optimized for the samples to achieve good resolution and consistent images throughout the stack. The resulting data sets were then processed via the FIJI insert TrackEM2[1]. This workflow was successfully applied to different biological samples like the papillae of Phallusia mammillata larvae, heart cells of salmons or the adhesive organs of Macrostomum lignano.

This implementation highlights the different important technical points to apply, from sample preparation to the final 3D reconstruction, and help others who are looking into establishing SBF-SEM.

References

1. Cardona A, Saalfeld S, Schindelin J, Arganda-Carreras I, Preibisch S, Longair M, Tomancak P, Hartenstein V, Douglas RJ. TrakEM2 Software for Neural Circuit Reconstruction. PLOS ONE. 2012;7(6):e38011. doi:10.1371/journal.pone.0038011

2. ConnectomX. https://www.connectomx.com/

3. Lippens S, Kremer A, Borghgraef P, Guérin CJ. Chapter 4 - Serial block face-scanning electron microscopy for volume electron microscopy. In: Müller-Reichert T, Pigino G, editors. Methods in Cell Biology. Vol. 152. Academic Press; 2019. p. 69–85. https://www.sciencedirect.com/science/article/pii/S0091679X19300536. doi:10.1016/bs.mcb.2019.04.002

4. OnPoint BSE Detector. [accessed 2026 Feb 24]. https://www.gatan.com/products/sem-imaging-spectroscopy/onpoint-bse-detector

5. Schindelin J, Arganda-Carreras I, Frise E, Kaynig V, Longair M, Pietzsch T, Preibisch S, Rueden C, Saalfeld S, Schmid B, et al. Fiji: an open-source platform for biological-image analysis. Nature Methods. 2012;9(7):676–682. doi:10.1038/nmeth.2019

# Bridging EFTEM with MRI to Quantify Iron in the Human Brain

Stefan Ropele[1], Luca Schmid[1], Nina Schlögl[1], Robert Reimer[1], Michael Stöger-Pollach[2], Sowmya Sunkara[1], Snjezana Radulovic[1], Walter Goessler[3], Gerd Leitinger[1]

*[1]Medical University of Graz, Gottfried Schatz Research Center, Austria;*
*[2]Technical University of Vienna, University Service Centre for TEM, Austria;*
*[3]University of Graz, Analytical Chemistry, Austria*

There are several ways of visualizing iron in the human brain. Most of the iron is stored in ferritin's iron core, and these cores can be visualized on iron (L-) maps using energy filtered transmission electron microscopy (EFTEM). Magnetic Resonance Imaging (MRI) allows iron quantification by applying $R_2$* mapping. $R_2$* is strongly dependent on the paramagnetic properties of ferritin. However, the relationship between magnetic configuration of the iron core in ferritin is still incompletely understood and could influence the accuracy of iron quantification using MRI. It is generally believed that most of the signal from $R_2$* mapping is picked up from the iron cores of ferritin, and not from cytoplasmic iron.

We aimed to use small brain samples of human donors in order to relate the $R_2$* signal with numbers of ferritin and total iron content. For this, we combined iron mapping using electron microscopy with $R_2$* mapping using quantitative fMRI, and determined the total iron content using mass spectrometry [1]. The number of ferritin cores was determined from iron maps of postmortem brain samples from six deceased human subjects. The mean iron content of adjacent human samples were obtained using mass spectrometry, and quantitative MRI at 3 Tesla was used for $R_2$* mapping of the same samples. Analyses focused on three gray matter regions: the frontal cortex, putamen, and globus pallidus. The post mortem intervals of the human donors had ranged from 6 to 24 hours. We demonstrated that autolysis led to a rapid degradation of ferritin iron cores, with fewer than one-third remaining detectable via EFTEM after 24 hours postmortem. The degradation followed a single-exponential decay pattern, suggesting that approximately 94% of the total brain iron is stored in ferritin in fresh tissue. However, $R_2$* relaxation rates did not follow this degradation pattern but instead correlated strongly with total iron content as measured by mass spectrometry. This signifies that $R_2$* mapping-derived magnetic susceptibility for iron appeared to be independent of the structural and magnetic organization of the ferritin iron core and shows a linear relationship with total iron content.

grant sponsor: FWF, grant 10.55776/P29370; ethics votum Medical University of Graz, 28-549 ex 15/16

References

[1] Ropele S., et al. Magn Reson Med. 2025 Dec 31. doi: 10.1002/mrm.70241

# Structural and Plasmonic Evolution in Mixed-Dimensionality Bismuth/Graphene Heterostructures

Tushar Gupta,[1] Kenan Elibol,[2,3] Michael Stöger-Pollach,[4] Kimmo Mustonen,[2] Clemens Mangler,[2] Jannik C. Meyer,[2,5] Jani Kotakoski,[2] Dominik Eder,[1] Bernhard C. Bayer,[1,2,*]

*[1]Institute of Materials Chemistry, Technische Universität Wien (TU Wien), Getreidemarkt 9/165, A-1060 Vienna, Austria (www.nanobayer.com)*

*[2]University of Vienna, Faculty of Physics, Boltzmanngasse 5, A-1090 Vienna, Austria*

*[3]Max Planck Institute for Solid State Research, Heisenbergstrasse 1, 70569 Stuttgart, Germany*

*[4]USTEM, Technische Universität Wien (TU Wien), Wiedner Hauptstrasse 8-10, A-1040 Vienna, Austria*

*[5]Institute of Applied Physics, Eberhard Karls University of Tuebingen, Auf der Morgenstelle 10, D-72076 Tuebingen, Germany*

*bernhard.bayer-skoff@tuwien.ac.at*

Mixed-dimensional heterostructures of low-dimensional bismuth (Bi) with two-dimensional (2D) graphene are of interest in a variety of application fields ranging from nanoelectronics, next-generation batteries, (photo-)catalysis to plasmonics. We here explore the evolution of morphology and structure of low-dimensional Bi/graphene heterostructures by high-resolution (scanning) transmission electron microscopy ((S)TEM). To this end, we physical vapour deposit (PVD) low-dimensional Bi nanostructures onto suspended monolayer graphene membranes. This enables us to study intrinsic Bi/graphene interactions, in contrast to prior work that utilized Bi on itself supported graphene. We find that Bi deposited onto room temperature graphene consists of grains formed by irregular shaped β-Bi crystals with β-Bi[001]^graphene(001) texture crystals and β-Bi nanorods with β-Bi[2-21]^graphene(001) texture. Importantly, both texture types show rotational van-der-Waals epitaxy with the supporting graphene. The room temperature depositions grow via an initial amorphous β-Bi[2-21]-like state into a closed film of β-Bi structure. For higher graphene temperatures of 150 °C to 250 °C during deposition, we find formation of amorphous Bi nanoparticles (NPs) at much reduced coverage due to Bi reverse desorption at these temperatures. While the room temperature deposited Bi films remain static under the electron beam in the (S)TEM, the amorphous Bi NPs from higher temperature depositions exhibit electron beam induced in situ crystallisation in the TEM. In parallel to observing their structural evolution during this crystallisation, this also enables us to probe the evolution of plasmonic features of Bi NPs via (valence) electron energy loss spectroscopy ((V)EELS), suggesting a link between crystallisation state and Bi NP surface plasmon (SP) energy.

References

T. Gupta et al.: Structural and Plasmonic Evolution in Mixed-Dimensionality Bismuth/Graphene Heterostructures, ACS Appl. Mater. Interfaces, asap, https://doi.org/10.1021/acsami.5c20752

# SEM study of metalloid buffering in As- and Sb-rich tailings, Lojane, North Macedonia

Katharina Vacek[1] and Tamara Đorđević[2,1]

[1]*Department of Mineralogy and Crystallography, University of Vienna, Josef-Holaubek-Platz 2, 1090 Vienna, Austria*

[2]*E057-02 USTEM, Vienna University of Technology, Stadionallee 2, 1020 Vienna, Austria*

*E-mail: k.vacek16@gmx.at*

Legacy flotation tailings, which are a by-product of historical mining activities, are increasingly recognised as both a potential source of strategic raw materials and a significant environmental liability. The former Sb–As–Cr mine at Lojane in North Macedonia is one of the region's largest sites of arsenic (As)- and antimony (Sb)-rich tailings. These tailings originate from processing hydrothermal vein-type mineralisation within ophiolitic units of the Vardar Zone (Đorđević et al. 2019).

In order to elucidate the retention mechanisms of Sb and As in secondary minerals, we conducted a detailed scanning electron microscopy (SEM) investigation of these tailings. Unlike previous studies (Đorđević et al. 2019) which were limited to small volumes of surface material, our sampling strategy included vertical profiling throughout the tailings to enhance the spatial representation of mineral phases.

In addition to the dominant primary sulphide minerals such as realgar ($As_4S_4$), pararealgar ($As_4S_4$) and stibnite ($Sb_2S_3$), we identified three principal sinks of Sb and As formed by the weathering of the primary phases. These occur as secondary oxide matrices that act as pore-filling and grain-coating, cement-like phases. All three matrices exhibit heterogeneous compositions, but differ significantly in their As, Sb, Fe and S content. The Fe-rich phase contains 5–15 at% Fe, 15–25 at% As, 2-5 at% S and less than 20 at% Sb, whereas the Fe-poor phase contains less than 10 at% Fe, 10–20 at% As, 2-5 at% S and 15–30 at% Sb. In contrast, the S-rich phase with up to 20 at% S contains less than 5 at% Fe, 10-30 at% As and 10-20 at% Sb.

The Fe-rich phase most likely represents Sb-bearing Fe-As oxyhydroxides (scorodite-like or poorly crystalline Fe–As gels) formed during oxidative weathering, acting as an important sink that temporarily immobilizes As. The Fe-poor, Sb-rich phase is consistent with mixed Sb-As oxides, indicating redistribution of metalloids during oxidation and controlling antimony mobility under oxic conditions. The S-rich phase reflects partially oxidized As-Sb sulphide relics (realgar–stibnite intergrowths), representing the primary metalloid source that progressively releases As and Sb during weathering and thus sustains secondary mineral formation and buffering processes.

These compositional patterns imply that, during oxidation and hydrolysis As and Sb are mobilised from primary sulphides, subsequently incorporating them into more stable secondary oxide matrices. Our results show that these cement-like phases act as dynamic sinks for the sequestration of these metals, thereby partly buffering their release into the surrounding environment.

T. Đorđević acknowledges the financial support of the Austrian Science Fund (FWF) [Grant: P 36828-N].

References

Đorđević, T., Kolitsch, U., Serafimovski, T., Tasev, G., Tepe, N., Stöger-Pollach, M., Hofmann, T. and Boev, B. (2019): Can. Mineral., 57, 10–21.

# Direct-Write Fabrication of Ultrathin Nb–N–O Memristive Devices by Focused Electron Beam Induced Deposition

Sabrina Menhart[1], Sven Barth[2], Harald Plank[3]

[1] *Institute of Electron Microscopy and Nanoanalysis, Graz University of Technology, 8010 Graz, Austria*
[2] *Physics Institute, Goethe-Universität, 60438 Frankfurt am Main, Germany*
[3] *Graz Centre of Electron Microscopy, 8010 Graz, Austria*

Over the past decade, additive direct-write nanomanufacturing has emerged as a powerful approach for the localized synthesis of functional materials with minimal constraints on substrate choice or geometry. Among the available nanoscale techniques, Focused Electron Beam Induced Deposition (FEBID) has gained increasing attention due to its capability to directly synthesize nanostructures from precursor molecules with nanometer-scale precision. While FEBID is now widely recognized for the fabrication of complex 3D architectures, its potential for the direct synthesis of functional electronic materials in planar device geometries remains relatively unexplored. In particular, beam-written materials for memristive devices represent a promising route toward highly localized neuromorphic hardware elements and may ultimately enable adaptive networks extending even into three dimensions.

Here, we investigate the feasibility of synthesizing Nb-based memristive materials using FEBID from a $Nb(NMe_2)_3(N\text{-}t\text{-}Bu)$ precursor. First, we confirm that the precursor enables reliable deposition of Nb-containing structures. A systematic parameter study is then performed to identify process windows allowing the fabrication of sub-nanometer-flat, homogeneous deposits, which are essential for integration in memristive devices. The intrinsic electrical properties of the resulting Nb–N–O material are subsequently evaluated using multi-electrode test structures. In this context, the influence of post-growth treatments, including electron beam curing, $H_2O$-assisted purification, and ambient exposure, is examined. It is found that the electrical behavior remains largely stable across these processing conditions, indicating robust conduction pathways within the material.

Based on these findings, stacked Au–(Nb–N–O)–$Co_3Fe$ devices are fabricated with progressively reduced active layer thicknesses. While intermediate thicknesses (≈ 50–15 nm) exhibit stable conduction behavior with only minor processing dependencies, clear memristive characteristics emerge when the active layer thickness is reduced to the sub-5 nm regime. In such geometries, the devices show reproducible hysteretic I–V behavior following a short conditioning phase during the first measurement cycles. In contrast to purely ohmic conduction, a non-linear transport characteristic is observed. This suggests field-assisted conduction through defect states within the ultrathin Nb–N–O layer, consistent with trap-mediated transport mechanisms. Within this picture, charge transport is governed by the filling and emptying of localized defect states, giving rise to non-linear current–voltage behavior and the formation of dynamically evolving conductive pathways across the ultrathin layer, as commonly observed in amorphous nanogranular materials.

These results demonstrate that FEBID enables the direct synthesis of Nb-based memristive materials and provides a promising starting point for further research towards nanoscale memristive devices and beam-written neuromorphic architectures, both in planar and future 3D device designs.

# Nanoscale investigation of degradation processes in historical daguerreotype plates

Soňa Borovská[a,b], Zuzana Šupolová[a,b], Valentina Ljubic Tobisch[a], Leon Ploszczanski[d] ,Janka Blaško Križanová[b], Wolfgang Kautek[c]

[a] *TU Wien, X-Ray Center, Vienna, Austria*
[b] *Academy of Fine Arts and Design in Bratislava, Department of Conservation and Restoration, Bratislava, Slovakia*
[c] *University of Vienna, Department of Physical Chemistry, Vienna, Austria*
[d] *Boku University, Institute of Physics and Materials Science, Vienna, Austria*

The daguerreotype, introduced by Louis Jacques Mandé Daguerre in 1839, was the first commercially successful photographic process and represents a major cultural and technological achievement [1]. Daguerreotypes are unique images formed on silver-plated copper plates sensitized with halogens, producing Ag-Hg amalgam nanoparticles. Over time, these delicate surfaces undergo various degradation phenomena that affect both structural integrity and visual quality [2–4]. Understanding these processes at the nanoscale is essential for developing effective conservation strategies [5–6]. This study investigates degradation features on historical daguerreotype plates from diverse provenances and conservation histories.

During this study, multiple historical daguerreotype plates were analysed. The daguerreotypes exhibited diverse stated of degradation, including corrosion, nanoparticle alternation, delamination and effects from previous cleaning interventions. The plates originated from different environments and were housed under varying conditions. Analytical techniques included scanning electron microscopy (SEM) with energy-dispersive X-ray spectroscopy (EDX), micro X-ray fluorescence (μXRF) and optical microscopy, allowing detailed characterization of surface morphology, elemental composition, and corrosion products.

SEM and μXRF analyses revealed heterogeneous corrosion patterns, including localized degradation caused by leaching from deteriorated cover glasses. Plates that had undergone previous cleaning showed altered surface chemistry and increased vulnerability to further degradation. Comparison between housed and unhoused specimens demonstrated the protective role of original framing. Elemental mapping also showed migration and redistribution of Ag and Hg nanoparticles, with delamination observed in severely degraded zones.

Nanoscale insights from multimodal microscopy highlight the complex interaction between original material composition, environmental exposure, and past conservation interventions. These findings stress the importance of conservation approaches that account for both original manufacturing techniques and subsequent handling. Future research will focus on non-invasive diagnostic tools and refined preservation strategies based on a deeper understanding of daguerreotype degradation mechanisms.

References

1. L. J. M. Daguerre, Historique et Description des Procedes du Daguerreotype et du Diormama,Paris, 1839.
2. A. E. Schlather, P. Gieri, M. Robinson, S. A. Centeno, and A. Manjavacas, “Nineteenth-century nanotechnology: The plasmonic properties of daguerreotypes,” Proc Natl Acad Sci U S A, 2019, 116, 13791–13798.
3. D. Q. Balbas, B. Cattaneo, R. Fontana, J. Striova, A. Cagnini, P. Belluzzo, S. Rossi, Sensors, 2023, 23, 1-15.
4. V. Ljubić Tobisch, K. Hradil, K. Whitmore, C. Streli, P. Wobrauschek, W. Kautek, J. Cult. Herit., 2024, 70, 223–230.
5. P. Ravines, R. Wiegandt, C. M. Wichern, Surface Engineering, 2007, 24, 138-146.
6. E. Da Silva, M. Robinson, C. Evans, A. Pejović-Milić, D. V. Heyd, J. Anal. At. Spectrom., 2010, 25, 654–661.
6. Project PHELETYPIA, “The impact of early photography and electrotyping media on the creationof images and contemporary art", Heritage 2020-060 PHELETYPIA, Heritage Science Austria grant program of the Austrian Academy of Sciences.

# Detection of Micro- and Nanoplastic (MNP) in winter wheat plants

Ilja Ortner [1], R. Markolin [1], C. Mayrhofer [2], T. Rath [3], J. Drausinger [4], C. Pichler-Rohrhofer[5], J. Rattenberger [1,2]

*[1]Institute of Electron Microscopy and Nanoanalysis (FELMI), Graz University of Technology, Steyrergasse 17, 8010 Graz, Austria*
*[2]Graz Centre for Electron Microscopy (ZFE), Steyrergasse 17, 8010 Graz, Austria*
*[3]Institute for Chemistry and Technology of Materials, Graz University of Technology, Stremayrgasse 9, 8010, Graz, Austria*
*[4]Lebensmittelversuchsanstalt (LVA), Zaunergasse 1-3, 1030 Wien, Austria*
*[5]Versuchsanstalt für Getreideverarbeitung (VG), Prinz-Eugen-Strasse 14, 1040 Wien, Austria*

Introduction

Micro- and nanoplastics, ranging from 1 nm to 5 mm in size, are among the most discussed pollutants in our society. This is hardly surprising, given that the weekly human consumption can be as high as 5 g - which is equivalent to the weight of a credit card [1]. However, the exact intake pathways are not yet fully understood and remain subject of current research.

The ACR-strategic project MicroPIC (Microscopy For Plastics In Cereals) is dedicated to the controlled contamination and observation of MNP in winter wheat by using a variety of vibrational spectroscopy analyses (FT-IR and Raman spectroscopy) and electron microscopic (EM) methods (SEM, TEM).

Methods

A routine for the controlled contamination of winter wheat plants during germination and growth with Polystyrene (PS) MNP was formulated. Since most spectroscopic methods are deficient in the required resolution needed for such observations and due to the weak contrast for organic specimens in EM, the introduced PS-MNP were labelled with gold NP for contrast enhancement [2].

At various growth stages different plant parts (root, seedling, shoots) were analyzed for micro- and nano plastic deposits.

Results and outlook

Paired with different sample preparation approaches (microtomy, ion beam slope cutting) the observation of the presence and position of MNP clusters in winter wheat roots and shoots was feasible with low vacuum scanning electron microscopy (LV-SEM) in conjunction with energy-dispersive X-ray spectroscopy (EDX).

However, to what extent MNP impact the quality of winter wheat and whether MNP will also find its way into the grain of corn needs to be discovered through follow-up research

We would like to express our sincere thanks to Thomas Rath from the ICTM, the LVA and VG teams and ACR and BMWET for financial support (SP-2023-06).

References

[1] Gruber et al., Expo Health 15, 33–51 (2023)
[2] Obare et al., Nano Lett 1, 601–603 (2001)

# Mechanical and elemental differences of bone at the implant interface in response to osteosynthesis implants in trained and untrained rats

Sara Kobinger, Gerhard Sinn, Thomas Bretschneider, Leon Ploszczanski, Helga C. Lichtenegger

Following orthopaedic surgery, physical exercise plays a crucial role in recovery and rehabilitation. While the general effects of exercise on bone are well understood, its specific influence on bone healing at the implant site has only recently been investigated. Building on studies that explored mineral particle orientation and thickness, this work aims to provide information about the mechanical and elemental properties at the bone-implant interface during different stages of healing.

Male rats received femoral implants of either a bioresorbable magnesium alloy (ZX00) or titanium. Animals underwent either a post-surgery treadmill exercise protocol or unrestricted cage movement. Rats were killed at two, four, and six weeks following implantation and bone was extracted, dehydrated and embedded. Regions of interest were defined at the immediate bone–implant interface and in mature bone remote from the implant. Nanoindentation with a Berkovich indenter (Oliver–Pharr analysis) provided hardness and local stiffness, and energy-dispersive X-ray spectroscopy (EDX) quantified elemental composition, focusing on calcium (Ca).

Across groups, mature bone showed higher hardness and stiffness than interface bone. In titanium-implanted samples, exercised rats exhibited greater hardness and elastic modulus at weeks 2 and 6 than non-exercised controls. Indicating exercise-enhanced stiffening during early and intermediate healing. In contrast, magnesium-implanted bones showed no consistent exercise effect. This may reflect spatiotemporal heterogeneity associated with degradation and remodeling near the interface. Ca in weight % increased over time in titanium samples from the 2 to the 6 weeks samples. Differences between interface and mature bone were modest for titanium, but more pronounced for magnesium. At the interface, Ca content correlated with elastic modulus for titanium implants within significance at $\alpha$ = 0.05, while magnesium showed this trend as well (Mg: $R^2$ = 0.35, $p$ = 0.072; Ti: $R^2$ = 0.39, $p$ = 0.038). No such correlation was observed in mature bone, suggesting that early-stage stiffness correlates with mineralization at the interface but not in established bone.

# Electron-Enabled Nanoparticle Diffraction

Stefan Nimmrichter[1], Dennis Rätzel[2,3], Isobel C. Bicket[3,4], Michael S. Seifner[3,4], Philipp Haslinger[3,4]

[1]*Naturwissenschaftlich-Technische Fakultät, Universität Siegen, Walter-Flex-Straße 3, 57068 Siegen, Germany*

[2]*ZARM, Unversität Bremen, Am Fallturm 2, 28359 Bremen, Germany*

[3]*Vienna Center for Quantum Science and Technology, Atominstitut, TU Wien, Stadionallee 2, 1020 Vienna, Austria*

[4]*University Service Centre for Transmission Electron Microscopy, TU Wien, Wiedner Hauptstraße 8-10/E057-02, 1040 Wien, Austria*

Matter-wave interferometry is a phenomenon which has been utilized and studied in electron microscopy since the early days of electron optics, with the development of phase contrast imaging, electron diffraction, electron holography, etc. When an electron diffracts off of a crystal lattice, it enters a superposition state of eligible Bragg diffraction components; due to momentum conservation, the crystalline sample must receive an equal and opposite superposition of momentum transfers. In theory, this results in an entangled electron-sample state. Typically, however, the sample is extremely large relative to the electron and is held fast in a sample holder, and this reciprocal momentum transfer is unobservable [1].

We present a proposal [2] to establish a system where such momentum kicks would be resolvable, to enable probing of the matter-wave properties of the sample as well as the free electron. A crystalline silicon nanoparticle is levitated in the sample plane, then released from its trap to enter free-fall. A single electron impacts the nanoparticle and undergoes Bragg diffraction. The nanoparticle receives a momentum transfer from the diffraction and is allowed to continue free-falling for a fixed amount of time before recapture and measurement of its position, X. In synchrony, the position of the electron, x, is measured. Assuming perfect measurement resolution, we calculate the resulting interference pattern for a quantum interaction, where the nanoparticle can behave as a quantum wave (Fig. 1a), or for the case where it behaves as a classical grating aperture (Fig. 1b) for different recapture times, t. The quantum scenario presents additional fringes visible at specific recapture times. Such an experiment provides a test of the matter-wave behaviour of high mass nanoparticles, with an efficient duty cycle and a short interference time, and would allow access to electron-sample entanglement in a transmission electron microscope.

References

[1] P. Schattschneider and S. Löffler, “Entanglement and decoherence in electron microscopy,” Ultramicroscopy, vol. 190, pp. 39–44, Jul. 2018, doi: 10.1016/j.ultramic.2018.04.007.

[2] S. Nimmrichter, D. Rätzel, I. C. Bicket, M. S. Seifner, and P. Haslinger, “Electron-Enabled Nanoparticle Diffraction,” Phys. Rev. Lett., vol. 135, no. 17, p. 173601, Oct. 2025, doi: 10.1103/3bvs-ymd7.

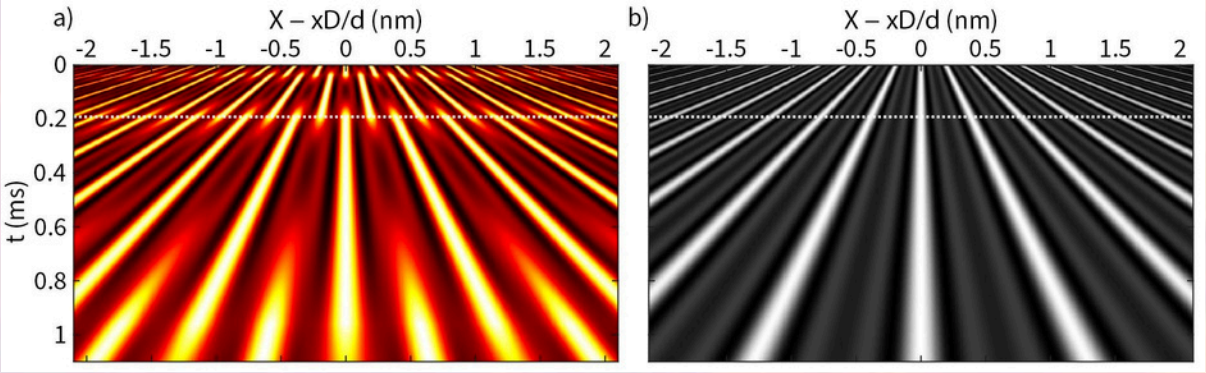


Fig. 1: Calculated interferogram between a) an electron and a silicon nanoparticle evolving in time after a Bragg diffraction event and b) diffraction assuming a classical grating aperture.

## Why does the processing of biological samples for TEM still take so long?

Magdalena Knapp, Elio Hobmayer, Lena Reberz, Peter Ladurner, Anna Seybold

*University of Innsbruck, Department of Zoology, Electron Microscopy*

Usually, several hours are needed for a chemical fixation process and additional days are needed to have a fully embedded sample ready to be cut into ultrathin slices to later be imaged with a transmission electron microscope. Although several scientists have tried to speed up these processes using various methods and devices in the past decades, today these long procedures are still the most widespread. Sample processing involves the fixation, dehydration, infiltration and polymerisation with the goal for the samples to be as close as possible to their natural state. Why is it still common that each of these processes takes so long although there are faster methods that yield similar or even better results? The chemical reactions that occur while fixing the sample are usually extremely fast, so a faster diffusion of the fixing agents through the tissue would shorten the fixation process. Also, there are the beliefs that more viscous solutions like resin require a longer duration to diffuse through the sample and that an oven temperature higher than 60°C damages the sample and/or the resin. Here we show, using flatworms as a model system, that all major processing steps – fixation, dehydration, infiltration and polymerisation – can be substantially shortened while still yielding samples suitable for transmission electron microscopy.

# Cell Wall Characterization by TEM and FIB-SEM in Streptofilum: Member of a Putative new Class of Basal Streptophyta

Andreas Holzinger[1], Pierre-Henri Jouneau[2], Clarisse Uwizeye[3], Denis Falconet[3], Eric Marechal[3], Klaus Herburger[4]

[1]*University of Innsbruck, Department of Botany, Sternwartestrasse 15, 6020 Innsbruck, Austria.*
[2]*Laboratoire Modélisation et Exploration des Matériaux, CEA, UGA, Grenoble, France*
[3]*Laboratoire de Physiologie Cellulaire et Végétale, CNRS, CEA, INRAE, UGA, Grenoble, France*
[4]*University of Rostock, Institute of Biological Sciences, 18059 Rostock, Germany*

The genus *Streptofilum*, first described by Mikhailyuk et al. 2018 [1], has a unique architecture of the cell coverage composed of scales and polysaccharides, distinct from other streptophyte green algae [1,2]. Its phylogenetic position falls outside all known algal classes, potentially representing a new class within the basal Streptophyta [3]. These algae are key to understanding the evolution towards vascular plants. Here we investigated the composition of *Streptofilum capillatum* cell coverage by comprehensive microarray polymer profiling CoMPP and in situ-localization via carbohydrate binding module (CBM) 3a specifically targeting cellulose, indicating that the unique cell wall scales are partially composed of cellulose. This is supported by monosaccharide analysis suggesting high amounts of glucose in scales. Transmission electron microscopy (TEM) after high pressure freeze fixation – freeze substitution (HPF-FS) shows high electron density in the distinct scales, suggesting a component reacting strongly with $OsO_4$ or Ur-acetate in the substitution medium (Fig 1A-C). Focused ion beam scanning electron microscopy (FIB-SEM) using a Zeiss Crossbeam 550 with Atlas 5 software provided 3D insight into the arrangement of the unique scales (Fig. 1D-E). Taken together these results further corroborate that the extracellular matrix (ECM) has unique features, previously not described in any members of Streptophyte green algae. The structures and chemical composition of scales are also distinct from scales described in the early diverged Streptophyte *Mesostigma* [4].

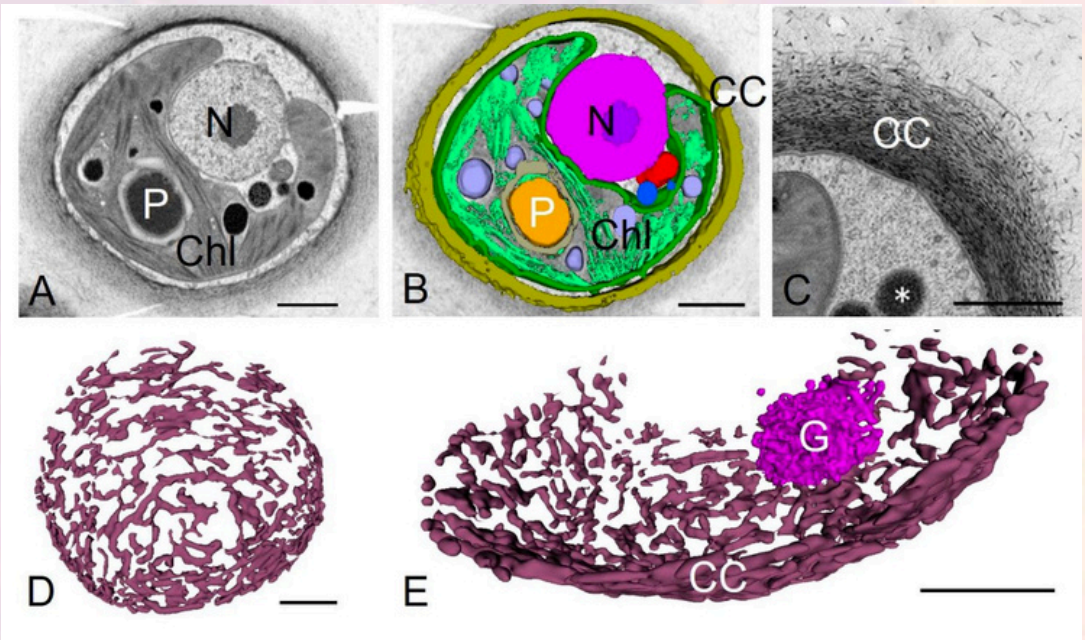


Figure 1 TEM and FIB-SEM reconstructions of *Streptofilum capillatum*. A overview of cross section, B color coded segmented structures, C conventional TEM of scales in the cell coverage, D 3D reconstruction of the batchy arrangement of scales, D scale packages and Golgi body. Scale bars 1 µm. Abbreviations: Chl chloroplast, P pyrenoid, N nucleus, CC cell coverage, G golgi body

References

[1] Mikhailyuk et al. (2018) Protist doi: 10.1016/j.protis.2018.03.002; [2] Glaser et al. (2025) Environ Microbiol doi: 10.1111/1462-2920.70033; [3] Bierenbroodspot et al. (2024) Curr Biol doi: 10.1016/j.cub.2023.12.070; [4] Domozych et al. 1992 Protoplasma 167:19-32.

# Electron microscopy and trams: Towards a friendly coexistence

Thomas Schachinger[1*], Ulrich Bette[2], Thomas Brückl[3], Thomas Mallits[4], Stephanie Manz[5], Andreas Randacher[3], Wolfang Emmer[6], Ernst Schmautzer[6], Karl Tiran[7], Rudolf Mörk-Mörkenstein[4]

[1]*TU Wien, USTEM, Wiedner Haupstraße 8-10, 1040, Vienna, Austria*
[2]*IfB Institut für Beeinflussungsfragen, Konrad-Adenauer-Str. 57, 42111, Wuppertal, Germany*
[3]*WIENER LINIEN GmbH & Co KG, I64 Anlagenmanagement, Erdbergstraße 202, 1030, Vienna, Austria*
[4]*IES Institut f. Elektrotechnik u. Sicherheitswesen Ziviltechniker GmbH, Gastgebgasse 27, 1230, Vienna, Austria*
[5]*TU Wien, Atominstitut Quantummetrology, Stadionallee 2,1020, Wien, Austria*
[6]*ESC Engineering & Services GmbH,Nikolaiplatz 4, 8020, Graz, Austria*
[7]*SV-Büro Tiran, Fettinger-Gasse 6/10, 8430, Leibnitz, Austria*
[*]*thomas.schachinger@tuwien.ac.at*

Electron microscope (EM) imaging capabilities are reduced upon exposure to environmental disturbances like mechanical vibrations and slowly varying magnetic fields, which necessitates stringent threshold limits on these environmental factors, e.g., ≤25-100 nT for magnetic fields [1]. EM labs, often situated at universities, are traditionally found in- or close-to city centres with rather "extreme" electromagnetic conditions. Tram lines, representing an efficient and powerful public transport mode, are DC powered, contributing to that large scale low-frequency, magnetic field fluctuations found in dense urban areas (~400 nT @ 50 m), and by that potentially diminishing imaging- and analytical performance of EMs, see Fig. 1a. Even though there are compensation systems at the instrument side available, they exhibit reduced damping factors when it comes to strong field gradients, are costly and difficult to retrofit. Similar on the tram side, battery- and ground-level power supply based systems can reduce the field emissions but they are also costly and demand specialized tramcars.

An effective and economic solution is a passive system that strongly reduces the area of the current loop produced by the catenary and the rails using a special arrangement of bypass cables and additional supply points on the catenary [2,3], see Fig. 1b. By adopting this approach to the dense urban setting of Vienna simulations and calibration tests show that a maximum field of 20 nT per tram at a distance of 100 m should be achievable, see Fig. 2a/b.

This "Viennese" variant of a passive field reduction system for tram lines may guarantees that urban public transport demands no longer interfere with researchers' desire for electromagnetic quietness.

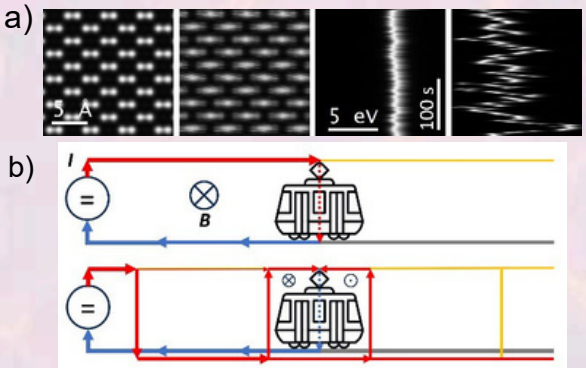


Fig. 1: a) TEM image distortions and energy shifts caused by near-DC magnetic fields and b) tram field reduction system principle.

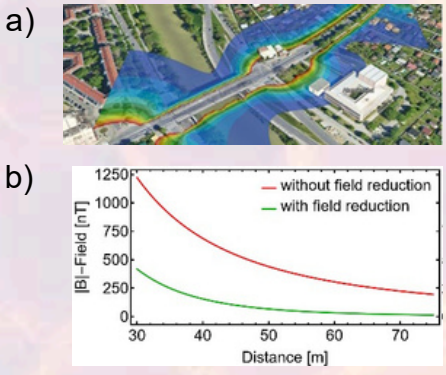


Fig. 2: a) 3D-FEM simulation result for the new "Linie 18" extension (blue: <20 nT), b) field distribution as a function of distance to rails.

References

[[1] Muller et al., Ultramicroscopy 106, 1033–1040 (2006).

[2] Pieter Kruit et al., eb Elektrische Bahnen 118, 100-108 (2020) Heft 6.

[3] Ulrich Bette et al., eb Elektrische Bahnen 118, 8-18 (2020) Heft 1.

# Inflammation in Diabetes: Correlative Electron Microscopy of the Endocrine Pancreas

Kerstin Hingerl[1], Melisa Malovcic[1], Dominique Pernitsch[1], Lea Bogensperger[3], Thomas Pieber[4,5], Barbara Ehall[4,5], Dagmar Kolb[1,2]

*[1]Core Facility Ultrastructure Analysis| Medical University of Graz, Austria.*
*[2]Gottfried Schatz Research Center for Cell Signaling, Metabolism and Aging, Division of Cell Biology, Histology and Embryology| Medical University of Graz, Austria.*
*[3]Machine Learning for Medicine & Protein Design | University of Zurich University of Zürich, Switzerland.*
*[4]Division of Endocrinology and Diabetology, Medical University of Graz, Austria.*
*[5]The Center for Biomarker Research in Medicine GmbH, Graz, Austria*

The established **scanning transmission electron microscopy (STEM)** technology enables detailed investigation of the mechanisms by which immune cells penetrate pancreatic tissue. STEM imaging, combined with the **ATLAS software platform**, allows the acquisition of large-scale, high-resolution datasets that provide comprehensive overviews of the tissue architecture while simultaneously preserving nanoscale structural detail. This approach makes it possible to analyze both the spatial organization of pancreatic islets and the interactions between immune cells and resident tissue cells. All images were acquired at a resolution of **1 nm**, enabling precise visualization of subcellular structures and cellular interfaces.

Based on the light microscopy results reported by **Barbara Ehall,** we were able to characterize structural changes occurring in pancreatic islets during the progression toward a diabetic state. Through systematic analysis of the imaging datasets, we identified **five distinct stages of islet alteration**, including several intermediate stages that reflect gradual transitions in tissue morphology and immune cell infiltration. These stages provide a framework for understanding the structural progression of islet destruction during disease development.

To further investigate the direct interactions between immune cells and pancreatic cells, selected samples were transferred from the **scanning electron microscope (SEM)** to the **transmission electron microscope (TEM)** for higher-resolution ultrastructural analysis. This workflow enabled the visualization of the so-called **"deadly kiss"**, describing the intimate contact between immune effector cells and their target cells within the pancreatic tissue. At this level of resolution, the physical interface between attacking immune cells and pancreatic cells becomes clearly visible, revealing morphological features associated with immune-mediated cytotoxicity.

The ability to directly observe these cellular interactions provides important insights into the mechanisms underlying immune-mediated damage in pancreatic islets and contributes to a better understanding of the structural events that accompany the progression toward diabetes.

# AI-Assisted Live-Cell Volume-CLEM and Cryo-EM Analysis for Biomedical Research

Ancuela Andosch[1,2], Philip Steiner[3], Lena Wiesbauer[3], Emma Punzenberger[3], Julia Schatz[3], Heiko Groiss[4], Alexey Minenkov[4], and Susanna Zierler[3,5,6]

*[1]Department of Biosciences and Medical Biology, Paris Lodron University Salzburg, Austria*
*[2]CF Imaging, Center for Medical Research, Faculty of Medicine, Johannes Kepler University Linz, Austria*
*3Institute of Pharmacology, Faculty of Medicine, Johannes Kepler University Linz, Austria*
*[4]Center for Surface and Nanoanalytics, Johannes Kepler University Linz, Austria*
*[5]Walther Straub Institute of Pharmacology and Toxicology, Ludwig-Maximilians-Universität München, Germany*
*[6]Clinical Research Institute for Inflammation Medicine, Johannes Kepler University Linz, Austria*

The interdisciplinary project “AI-Assisted Live-Cell Volume-CLEM and Cryo-EM Analysis for Biomedical Research” aims to develop and establish an AI-driven workflow for correlative light and electron microscopy (CLEM) of living cells combined with cryo-electron microscopy (cryo-EM). This integrated approach enables comprehensive, high-resolution, and correlative analyses of immune cells at both the functional and ultrastructural levels. The workflow correlates live-cell confocal laser scanning microscopy (CLSM) with advanced EM techniques. It includes high-pressure freezing (HPF), cryo-substitution, focused ion beam-scanning electron microscopy (FIB-SEM), and cryo-EM. This combination allows precise localization of transmembrane proteins, detailed physiological investigations, and high-resolution 3D visualization of immune cell architectures. A key innovation lies in the application of AI-based segmentation for ultrastructural datasets, which facilitates automated interpretation of complex 3D volumes obtained via FIB-SEM tomography. This significantly improves the efficiency and accuracy of identifying distinct subcellular features. Furthermore, high-quality cryo-sample preparation and imaging by cryo-transmission electron microscopy (cryo-TEM) enable qualitative assessment of near-native biological specimens, minimizing fixation and contrast artifacts and ensuring a realistic representation of cellular ultrastructure. This interdisciplinary approach, linking expertise and infrastructure from the Institute of Pharmacology, the Department of Dermatology and Venerology, the Center for Surface and Nanoanalytics (ZONA), and the Institute for Machine Learning at JKU Linz, will foster and expand unique research capabilities within the university’s biomedical and technological landscape.

# Speeding Up 2D Analytical in situ Transmission Electron Microscopy: Direct Electron Detection EELS for Nanostructural Precipitate Evolution in Aluminum Alloys

Evelin Fisslthaler*[1], Martina Dienstleder[1], Moritz Theissing[1,2], Daniel Knez[2]

*evelin.fisslthaler@felmi-zfe.at*

[1]*Graz Centre for Electron Microscopy, Steyrergasse 17, 8010 Graz, Austria*

[2]*Institute of Electron Microscopy and Nanoanalysis, Graz University of Technology, Steyrergasse 17, 8010 Graz, Austria*

A key challenge in advancing modern alloys is the revelation of the dynamics of precipitate formation. The elemental properties of these complex materials are governed by processes on the micro- and nanoscale that are often triggered by different types of heat treatments and minuscule changes of the composition of the alloy. By using MEMS-based in situ TEM holder systems and aberration corrected transmission electron microscopes, researchers can directly observe the formation and evolution of nanoscale precipitates. [1,2] They can subject their samples to precisely defined temperature ramps, and track the fate of different types of precipitates by imaging different stages of the evolution of one sample area. Concomitant analytical analysis with electron energy-loss spectroscopy (EELS) and energy dispersive x-ray spectroscopy (EDXS) is extremely valuable to understand the details of the various states of precipitate formation, as structures are changing rapidly and interdependently. However, commonly the speed of these techniques is not sufficient to use them for 2D mapping directly during the in situ experiments, due to the pixel times necessary to get adequate spectra for the identification of all components. Direct Electron Detection EELS (DED EELS) cameras like the K2 from Gatan offer new and more efficient possibilities to capture EELS datasets with both high speed and high quality, resulting in elemental maps taken at frame rates that allow a live view of the chemical evolution of the precipitates of the alloy system.

This study demonstrates the application of DED EELS in conjunction with high-resolution STEM as a method capable of capturing chemical changes in a complex Al-Mg-Si alloy during an in situ STEM heating experiment.

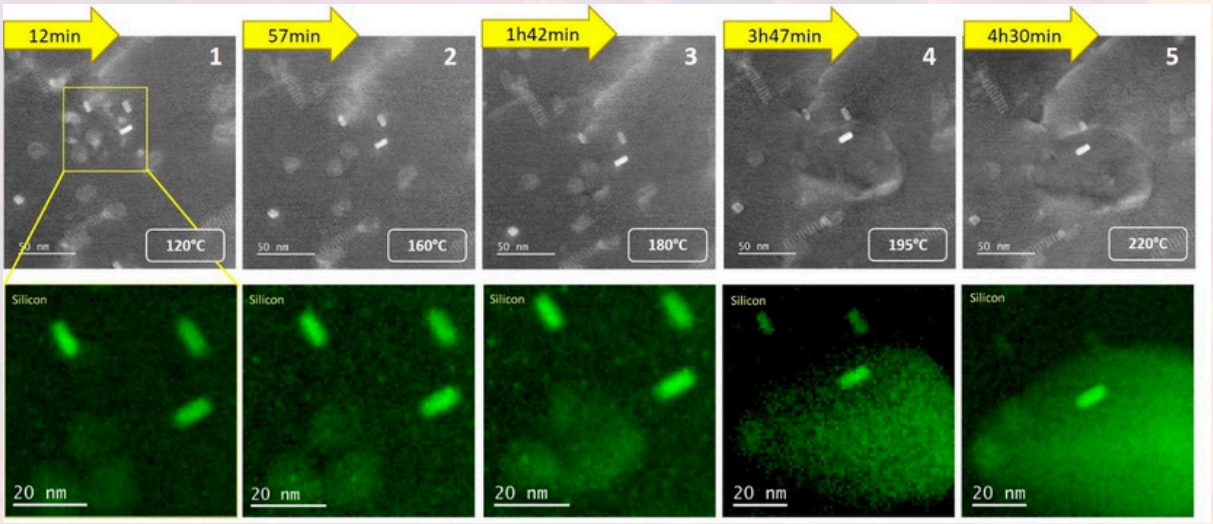


Figure 1: Evolution of nanoscale precipitates in an Al-Mg-Si alloy during *in situ* STEM heat treatment illustrated by STEM imaging (ADF, top row) and DED EELS nanoscale analysis of the $Si_K$ edge (bottom row) (total time for each map was 5min 20s). Reproduced from [3]

References

[[1] Sunde, Wenner, Holmestad, J. Microsc. 2020, 279, 143, doi: 10.1111/jmi.12845

[2] Liu, Malladi, Xu, Chen, Tichelaar, Zhuge, Zandbergen, Sci. Rep. 2017, 7: 2184, doi:10.1038/s41598-017-02081-9

[3] Fisslthaler, Dienstleder, Lammer, Theissing, Knez, Adv. Eng. Mater, 2025, 27, 2500716, doi.org/10.1002/adem

# Color formation in the blue shark, *Prionace glauca*

Viktoriia Kamska[1], Frederik Mollen[2], Stefan Redl[3], Michael Blumer[4], Emeline Raguin[5], Clemens Schmitt[5], Mason Dean[1]

*[1]Department of Infectious Diseases & Public Health, City University of Hong Kong, Kowloon, Hong Kong;*
*[2]Elasmobranch Research, Bonheiden, Belgium;*
*[3]Institute of Neuroanatomy, Medical University Innsbruck, Austria;*
*[4]Institute of Anatomy, Medical University Innsbruck, Austria;*
*[5]Max Planck Institute of Colloids and Interfaces, Potsdam, Germany.*

Blue is a rare color in nature. As there are no stable blue pigments in living organisms, natural blue color is mainly produced by structural coloration, where microscopic structures scatter light to create a blue appearence. Using various microscopic techniques, we find that inside the dermic scales, the socalled denticals, guanine crystal bearing cells, together with melanosomes are responsible for the creation of the characteristic brilliant blue hue of the blue sharks back and side. The stability of the guanine crystals during sample preparation seems to depend on different factors, not solely relying on general ultrastructural preservation.

# Measurement and Classification of Degradation Effects in Organic Photovoltaics using STEM Techniques

Philipp Christ*[,1], Julia Hönigsberger[2], Georg Haberfehlner[1], Martina Dienstleder[1], Gerald Kothleitner[1], Thomas Rath[2], Gregor Trimmel[2] and Daniel Knez[1]

*philipp.christ@felmi-zfe.at;

[1]Institute of Electron Microscopy and Nanoanalysis (FELMI), Graz University of Technology, Steyrergasse 17, 8010, Graz, Austria;

[2]Institute for Chemistry and Technology of Materials (ICTM), Graz University of Technology, Stremayrgasse 9, 8010, Graz, Austria

Organic photovoltaics (OPV) offer a versatile and cost-effective pathway for solar energy conversion. However, solar irradiation can also induce degradation in the constituent materials, compromising device efficiency [1]. Understanding these mechanisms is essential for long-term stability. A schematic of such an OPV cell is shown in Figure 1a. We employ advanced STEM EELS and EDX in combination with machine learning assisted evaluation strategies to analyse the degradation on the nanoscale. Our investigations show that the halogenated active layer (AL) in an OPV serves as a trigger for degradation. By comparing halogenated and non-halogenated OPV cross-section samples - cut via plasma FIB - we map chemical divergencies. Figure 1b shows a HAADF image of such an OPV cross-section sample with an EELS-elemental map in Figure 1c corresponding to the highlighted AL region in (b) revealing the morphology of the phases within the blend.

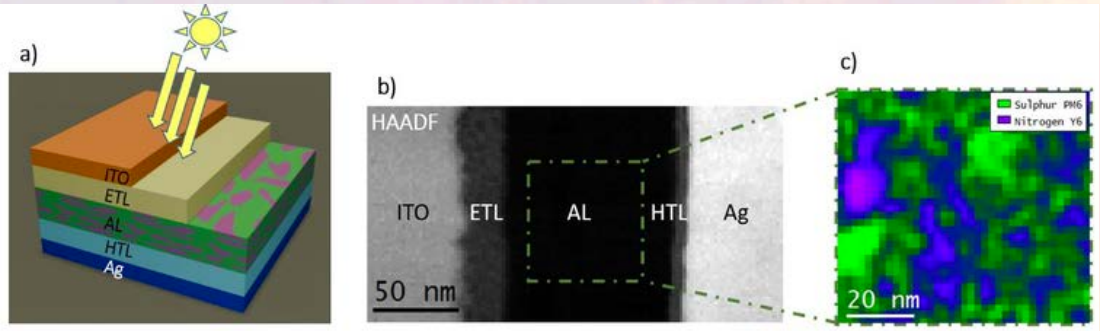


Figure 1: An OPV cell consists of several layers [1]. In a), a schematic structure is shown with the ITO and Ag electrodes, the electron and hole transport layers (ETL and HTL) and the AL in the middle, which consists of the two polymers PM6 and Y6. A first HAADF image is shown in b) with the same layer structure. Finally, c) shows a phase separation of the AL created using STEM-EELS elemental mapping.

4D-scanning confocal electron diffraction (SCED) is further employed to analyze structural changes and molecular stacking within the AL [3]. We correlate the structural data with the local differences in the absorption capacity of the AL, a quantity that is directly related to the efficiency of the organic solar cells. This is achieved spatially resolved using Kramers-Kronig Analysis (KKA) applied on monochromated STEM-EELS data [2]. Experimental measurements in conjunction with appropriate simulations provide information about molecular changes caused by degradation. We further show that the adverse effects of beam damage and carbon contamination can be minimized by performing STEM measurements at cryogenic temperatures (-170 °C), enhancing the fidelity of results, particularly for 4D-SCED and KKA.

References

1. Tang Haoran and et al. “Interface Engineering for Highly Efficient Organic Solar Cells”. In: Advanced Materials (July 2023). doi: 10.1002/adma.202212236.
2. M. Stöger-Pollach, A Laister, and Peter Schattschneider. “Treating retardation effects in valence EELS spectra for Kramers-Kronig analysis”. In: Ultramicroscopy 108 (May 2008), pp. 439–44. doi: 10.1016/j.ultramic.2007.07.003.
3. Mingjian Wu, Daniel Stroppa, and Erdmann Spiecker. “Dose-Efficient Structure Mapping of Nano-Crystallites in Organic Solar Cells with Fast 4D-SCED Experiments Using Hybrid Pixel Detector”. In: Microscopy and Microanalysis 29. Supplement1 (July 2023), pp. 1752–1753. issn: 1431-9276.

# Detachment Strategies for 3D-Nanoprinted FEBID Structures for untethered Microbots using Polyphtalaldehyde (PPA)

Philipp Kinast, Ilja Ortner and Robert Winkler

*Institute of Electron Microscopy and Nanoanalysis (FELMI), TU Graz, Austria*

In recent years, 3D-printing of nanostructures produced by focused electron beam induced deposition (3D-FEBID) has undergone significant development, which opens up a wide range of applications.[1] Typically 3D-FEBID structures adhere strongly to the substrates on which they are fabricated.[2] For applications such as untethered microbots, reproducible detachment processes are inevitable.

Therefore, a sacrificial polymer layer of Polyphtalaldehyde (PPA) is spin coated on a Si-wafer. The material PPA typically decomposes at medium low temperatures.[3] This property is used to release the 3D-printed nanostructures from the substrate by heating the wafer to an adequate temperature. A schematic for this detachment strategy is shown in figure 1a. Exact and reproducible strategies for the coating and decomposition procedure are discussed as well as implications of the heat treatment on the properties of the printed materials.

The 3D-FEBID nanostructures are further printed directly onto the polymer layer. Figure 1b shows a sample of a tripod printed directly on PPA with diameters around 75 nm, proving the printability and ability of PPA to withstand electron beams without disruptive electrical charging.

The main advantages of a thermal sacrificial layer like PPA are, that on the one hand no wet chemicals are needed and on the other hand the delicate nanostructures are neither touched mechanically nor exposed to any other kind of physical impact.

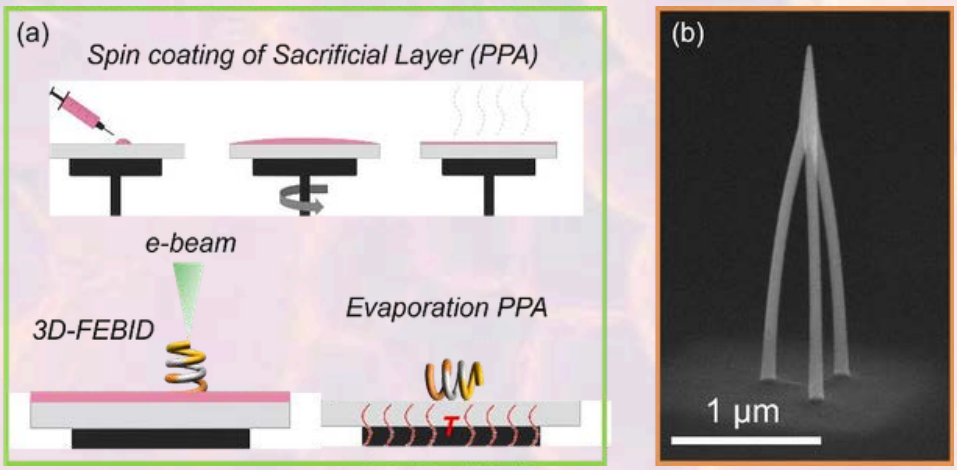


*Figure 1: (a) schematic of detachment strategy; (b) 3D-FEBID $PtC_X$ tripod directly printed onto PPA.*

References

(1) Reisecker, V.; Winkler, R.; Plank, H. A Review on Direct-Write Nanoprinting of Functional 3D Structures with Focused Electron Beams. Adv. Funct. Mater. 2024, 34 (46), 2407567. https://doi.org/10.1002/adfm.202407567.

(2) Plank, H.; Winkler, R.; Schwalb, C. H.; Hütner, J.; Fowlkes, J. D.; Rack, P. D.; Utke, I.; Huth, M. Focused Electron Beam-Based 3D Nanoprinting for Scanning Probe Microscopy: A Review. Micromachines2019, 11 (1), 48. https://doi.org/10.3390/mi11010048.

(3) Holzner, F. Thermal Scanning Probe Lithography Using Polyphthalaldehyde, ETH Zurich, 2013, p 1 Band. https://doi.org/10.3929/ETHZ-A-009756918.

# Metrological Optimization and Simulation of Spin Resonance Spectroscopy in Transmission Electron Microscopy

S. Beltrán-Romero[1,2], M. Gaida[3], S. Löffler[2], S. Nimmrichter[4], D. Rätzel[1,2,5], P. Haslinger[1,2]

[1] *Vienna Center for Quantum Science and Technology, TU Wien, Atominstitut, Vienna, Austria*
[2] *University Service Centre for Transmission Electron Microscopy, TU Wien, Vienna, Austria*
[3] *Institute for Complex Quantum Systems and Center for Integrated Quantum Science and Technology, Ulm University, Albert-Einstein-Allee 11, D-89069 Ulm, Germany*
[4] *Naturwissenschaftlich-Technische Fakultät, Universität Siegen, Walter-Flex-Str. 3, 57068 Siegen, Germany*
[5] *ZARM, Unversität Bremen, Bremen, Germany*

Recent advances in Transmission Electron Microscopy (TEM), including aberration correction, cryogenic stabilization, and ultrafast electron pulses, have pushed spatial and temporal resolutions to unprecedented levels. However, extending this precision to the detection of single spins and their magnetic dynamics remains a significant challenge. We present a comprehensive theoretical and computational framework for Spin Resonance Spectroscopy (SRS) in TEM, such as nuclear (NMR) or electron spin resonance (ESR), enabling state-selective spin imaging at the nanoscale. By capturing both elastic and inelastic scattering processes between free-space electron probes and microwave-driven spin systems, we describe the resulting magnetic phase shifts and deflection angles imprinted on the electron wave function. We demonstrate through simulations that these phase shifts from individual spins are detectable in both image and diffraction modes.

To determine the precision limits of this technique, we quantify measurement sensitivity using Classical Fisher Information (CFI) and compare it against the Quantum Fisher Information (QFI) and the Helstrom bound. Our findings identify optimal imaging conditions, specifically the effects of defocus and beam width, to maximize the signal-to-noise ratio. We find that while standard diffraction and imaging measurements can approach quantum-limited performance for classical dipoles, orbital angular momentum (OAM)-resolved detection is required to restore sensitivity when electron backaction from a quantum spin becomes significant. This work lays the foundation for spin resonance spectroscopy with the atomic resolution of TEM, as well as for future experiments in quantum spin research and nanoscale material characterization.

References

[1] Antonín Jaroš, Michael S. Seifner, Johann Toyfl, Benjamin Czasch, Santiago Beltrán-Romero, Isobel C. Bicket, and Philipp Haslinger, Sensing spin precession with free electrons, ACS Nano (2026), 10.1021/acsnano.5c13351, pMID: 41556847, https://doi.org/10.1021/acsnano.5c13351.

[2] Santiago Beltrán-Romero, Stefan Löffler, Dennis Rätzel, and Philipp Haslinger, Simulating microwave-controlled spin imaging with free-space electrons, arXiv:2602.20852 [quant-ph] (2026).

[3] Santiago Beltran-Romero, Michael Gaida, S. Nimmrichter, Dennis Rätzel, and Philipp Haslinger, Quantum Metrology of Spin Sensing with Free Space Electrons, arXiv:2509.14982 [quant-ph] (2025).

# Towards manipulating Electron-Photon Pairs with Digital Micromirror Devices

Alexander Becker[1,2], Alexander Preimesberger[1,2], Sergei Bogdanov[1,2], Isobel C. Bicket[1,2]and Philipp Haslinger[1,2]

*[1]University Service Centre for Transmission Electron Microscopy (USTEM), TU Wien, Austria*
*[2]Atominstitut, TU Wien, Austria*

In recent years, the advent of time resolved direct electron detectors has made it possible to study electrons together with the Cathodoluminescence (CL) photons they produce on a single particle level [1,2,3]. Results from our group have shown that the position and momentum correlations produced by transition radiation can go beyond classical physics [4]. It has therefore become evident, that to fully capture the physics of such electron-photon pairs, we need more fine-grained control over the photon measurement.

Modern adaptive optics, in particular Digital Micro-mirror Devices (DMD) and phase-shifting spatial light modulators (SLM) promise a high degree of precision and flexibility [5]. As a first step, we are in the process of implementing a DMD as a programmable optical mask, making variable automated measurements possible. To ensure that the requirements mentioned above and optical specifications are satisfied, a series of tests was performed. By adapting a pre-existing Python library to the given setup, we are able to display arbitrary patterns. To examine contrast and diffraction efficiency we used a simple test setup, consisting of a laser, lenses, DMD and a camera. By collecting several diffraction orders, we were able to transmit photons with an efficiency of approximately 50% while maintaining a contrast of >95%. While better performance should still be achievable with a refined setup, these baseline values are already sufficient to be practically useful. . This would greatly simplify otherwise challenging experiments such as [6] and enable more complex protocols that would not be possible with fixed transmission masks.

References

[1] N. Varkentina, Y. Auad, S.Y. Woo, A. Zobelli, L. Bocher, J.-D. Blazit, X. Li, M. Tencé, K. Watanabe, T. Taniguchi, O. Stéphan, M. Kociak, L.H.G. Tizei, Science Advances 8, eabq4947, (2022).

[2] A. Feist, G. Huang, G. Arend, Y. Yang, J.-W. Henke, A.S. Raja, F.J. Kappert, R.N. Wang, H. Lourenço-Martins, Z. Qiu, J. Liu, O. Kfir, T.J. Kippenberg, C. Ropers, Science 377, 777 (2022).

[3] A. Preimesberger, D. Hornof, T. Dorfner, T. Schachinger, M. Hrtoň, A. Konečná, and P. Haslinger, Phys. Rev. Lett. 134, 096901 (2025).

[4] A. Preimesberger, S. Bogdanov, I.C. Bicket, P. Rembold, P. Haslinger, arXiv:2504.13163.

[5] S. M. Popoff, L. Malosse, R. Gutiérrez-Cuevas, Y. Bromberg, J. Commre, M. Glanc, R. Galicher, and M. W. Matthès, arXiv:2311.17496.

[6] P. Rembold, S. Beltrán-Romero, A. Preimesberger, S. Bogdanov, I. C. Bicket, N. Friis, E. Agudelo, D. Rätzel, and P. Haslinger, Quantum Sci. Technol. 10, 045003 (2025).

# 3D Imaging of Optical Modes in Dielectric Nanocavities

Michael S. Seifner,[1,4] Anne Sofie Darket,[2,4] Ali N. Babar,[2,4] Babak Vosoughi Lahijani,[2,4] Rasmus E. Christiansen,[3,4] Ole Sigmund,[3,4] Elizaveta Semenova,[2,4] Søren Stobbe,[2,4] Philip T. Kristensen,[2,4] Shima Kadkhodazadeh[1,4]

*[1]DTU Nanolab, DTU, Fysikvej 307, 2800 Kgs. Lyngby, Denmark*
*[2]DTU Electro, DTU, Ørsteds Plads 343, 2800 Kgs. Lyngby, Denmark*
*[3]DTU Construct, DTU, Koppels Allé 404, 2800 Kgs. Lyngby, Denmark*
*[4]NanoPhoton, DTU, Ørsteds Plads 345A, 2800 Kgs. Lyngby, Denmark*

Recent advances in dielectric optical cavities aim to achieve efficient sub-wavelength light confinement for enhanced light-matter interactions in optoelectronics and quantum technologies [1]. However, their development requires three-dimensional (3D) characterization methods that overcome the limitations of existing techniques, including spatial resolution.
Here, we demonstrate 3D mapping of optical modes in topology-optimized dielectric nanocavities using multi-orientation electron energy-loss spectroscopy (EELS) combined with tomographic reconstruction. In a silicon bowtie nanocavity [2], we experimentally resolve multiple polarized resonant modes that show strong agreement with numerical calculations. In particular, the mode of interest (MOI) in the telecommunications-wavelength regime (~1550 nm) is observed to be tightly confined at the cavity bridge (see Figure 1).

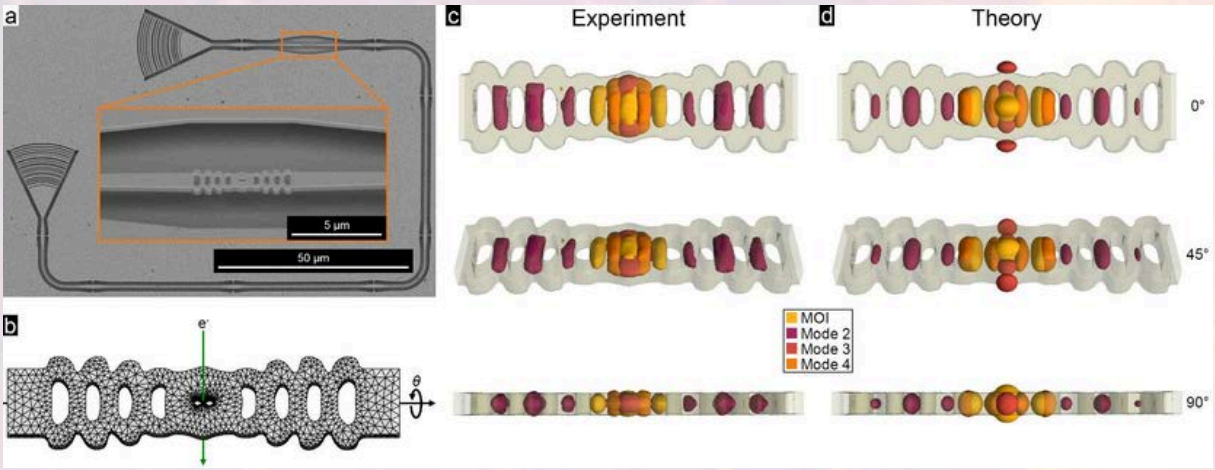


Figure 1: (a) Scanning electron microscopy (SEM) image of the fabricated waveguide-coupled optical cavity. (b) Schematic illustration of the experimental approach. (c) Isosurface renderings at various sample tilt angles obtained from tomographic reconstructions of the MOI and additional modes (Modes 2-4), showing strong agreement with the theoretically calculated mode profiles presented in (d).

These results demonstrate the potential of free-electron spectroscopy combined with tomography for 3D mapping of optical modes in nanophotonic structures. Furthermore, the integrated waveguide architecture provides a pathway for optical coupling into the system, enabling electron energy-gain spectroscopy that may enhance signal strength and support a deeper understanding of the underlying physical phenomena [3].

References

[1] A. González-Tudela, A. Reiserer, J. J. García-Ripoll, F. J. García-Vidal Nat. Rev. Phys. 2024, 6, 166.
[2] G. Dong, A. N. Babar, R. E. Christiansen, S. E. Hansen, S. Stobbe, Y. Yu, J. Mørk Laser Photonics Rev. 2025, e00895.
[3] F. J. García de Abajo Rev. Mod. Phys. 2010, 82, 209.

# Correlative in situ SEM-DIC and EBSD microscopy for quantitative analysis of strain localization during bending of AA6xxx alloys

Florian Zrim*[1], Stefan Mitsche[1], Georg Falkinger[2], Angela Thum[2]

**Corresponding Author: florian.zrim@felmi-zfe.at;*
*[1] Graz Centre for Electron Microscopy (ZFE), Steyrergasse 17, 8010 Graz, Austria*
*[2] AMAG rolling GmbH, Lamprechtshausenerstrasse 65, 5282 Ranshofen, Austria*

Understanding deformation and damage initiation in AA6xxx alloys requires experimental methods capable of resolving strain localization at the microstructural scale while maintaining statistically representative sampling areas. In situ scanning electron microscopy (SEM) digital image correlation (DIC) is well suited for this purpose, though it necessitates balancing high spatial resolution with a field of view large enough to capture global bending dynamics.

This work presents an in situ SEM-DIC methodology that enables strain measurements across the full 1 mm thickness of industrially rolled AA6xxx samples while retaining sufficient spatial resolution to resolve individual grains. A custom three-point bending setup integrated into the SEM allows time-resolved imaging during deformation. High-resolution µDIC is achieved using nanoscale surface patterning based on silica nanoparticles, with emphasis on pattern quality and imaging conditions required for reliable strain extraction at large fields of view.

The large analysed area enables statistical evaluation of strain distributions across hundreds of grains. Quantitative measurements of the strain field are used to characterize strain localization and its evolution during bending, providing a robust description of deformation heterogeneity. In situ observations reveal pronounced strain accumulation at grain boundaries, second-phase particles, and within shear bands spanning multiple grains, with localized high-strain regions frequently preceding surface damage.

Correlation with electron backscatter diffraction (EBSD) data is explored using a geometric transformation between datasets using DefDAP [1]. While a definitive relationship between crystallographic texture and strain localization remains inconclusive, qualitative agreement between strain hotspots and microstructural features demonstrates the capability of the methodology used.

The results highlight the advantage of capturing the entire sample thickness during in situ SEM-DIC, enabling the observation of macro-scale shear bands while simultaneously allowing for statistically meaningful microstructural analysis. This approach provides a powerful tool for investigating deformation heterogeneity and early damage processes in structural alloys.

References

[1] M. Atkinson, R. Thomas, P. Crowther, D.T. Fullwood, J. Quinta da Fonseca, A. Harte. MechMicroMan/DefDAP: v0.93.4. 2022.

# Probing Quantum Correlations in Joint Electron-Photon States

Alexander Preimesberger[1,2], Sergei Bogdanov[1,2], Isobel C. Bicket[1,2], Phila Rembold[2] and Philipp Haslinger[1,2]

*[1] University Service Centre for Transmission Electron Microscopy (USTEM), TU Wien, Austria*
*[2]Atominstitut, TU Wien, Austria*

Since the introduction of time-resolved direct electron detectors to transmission electron microscopy (TEM), there has been a growing interest in studying the correlations between an electron and the cathodoluminescence (CL) photons it produces [1,2,3]. Recent studies using coincidence measurements in both continuous [4] and discrete variables [5] have shown correlations that exceed the classical limits for separable states, thus demonstrating quantum entanglement between free electrons and photons. We present our continuous-variable approach [4], showing how ghost imaging [6], a method adapted from photonic quantum optics, can be used to demonstrate entanglement and even EPR-like behaviour of the joint electron-photon state.

For this purpose, we generate correlated electron-photon pairs via transition radiation from 200 keV electrons passing a 50 nm monocrystalline silicon membrane. We detect the CL photons in a time-resolved manner, using a custom parabolic mirror and a single-photon counter. Employing a Timepix3 based direct electron detector we are able to determine which photons arrive in time with a corresponding electron. These electron-photon pairs exhibit precise (anti-)correlations in momentum and position. Placing a known absorptive mask in the photon beam path while measuring the electron in imaging and diffraction mode allows us to extract the joint position and momentum uncertainties of the electron–photon pair. We use these measurements to evaluate entanglement criteria such as the MGTV inequality [7] and the Reid-EPR bound [8].

We hope that these results will help to make entanglement available as a resource for electron microscopy, enabling novel measurement schemes inspired by photonic quantum optics.

References

[[1] A. Feist, G. Huang, G. Arend, Y. Yang, J.-W. Henke, A.S. Raja, F.J. Kappert, R.N. Wang, H. Lourenço-Martins, Z. Qiu, J. Liu, O. Kfir, T.J. Kippenberg, C. Ropers, Science 377, 777 (2022).
[2] N. Varkentina, Y. Auad, S.Y. Woo, A. Zobelli, L. Bocher, J.-D. Blazit, X. Li, M. Tencé, K. Watanabe, T. Taniguchi, O. Stéphan, M. Kociak, L.H.G. Tizei, Science Advances 8, eabq4947, (2022).
[3] A. Preimesberger, D. Hornof, T. Dorfner, T. Schachinger, M. Hrtoň, A. Konečná, and P. Haslinger, Phys. Rev. Lett. 134, 096901 (2025).
[4] A. Preimesberger, S. Bogdanov, I.C. Bicket, P. Rembold, P. Haslinger, arXiv:2504.13163.
[5] J.-W. Henke, H. Jeng, M. Sivis, C. Ropers, arXiv:2504.13047.
[6] M. J. Padgett and R. W. Boyd, Philos. Trans. R. Soc. A 375, 20160233, (2017).
[7] S. Mancini, V. Giovannetti, D. Vitali, P. Tombesi, Phys. Rev. Lett. 88, 120401 (2002).
[8] M. D. Reid, Phys. Rev. A 40, 913 (1989).

# Atomic Contrast or Illusion? Imaging Single-Photon Emitters in hBN

David Lamprecht, Shrirang Chokappa, Alissa M. Freilinger, Barbara Maria Mayer, Maximilian Melchior, Jana Dzíbelová, Darwin Lorber, Luiz H. G. Tizei, Mathieu Kociak, Clemens Mangler, Lado Filipovic, Jani Kotakoski

*TU Vienna, Institute of Microelectronics*

Identifying the atomic origin of single-photon emitters in hexagonal boron nitride (hBN) is often treated as a problem of sufficient resolution. Annular dark-field scanning transmission electron microscopy (ADF-STEM) is therefore often used to assign specific atomic defects based on column intensity variations, even in near-bulk hBN flakes. In practice, this approach assumes that atomic-resolution contrast is interpretable and trustworthy under conditions optimized for optical studies.

Here, we challenge this assumption by systematically probing the limits of ADF-STEM defect identification in multilayer hBN using a combination of multislice simulations and experimental data. Even under ideal aberration-free conditions, we find that boron–nitrogen column contrast collapses beyond ~17 atomic layers, while single substitutional carbon atoms become invisible at substantially smaller thicknesses. Vacancy-type defects persist slightly longer, but also fall below reliable detectability well within the thickness range commonly used in photonic studies.

More critically, we show that small residual non-centrosymmetric aberrations – most notably threefold astigmatism – can generate artificial column-to-column contrast that is indistinguishable from genuine mass–thickness contrast. Standard image post-processing often amplifies this artifact, increasing the risk of false-positive defect assignment. By deliberately detuning the aberration correction, we demonstrate a “magic trick”: nitrogen-dominated columns can be made to appear boron-dominated and vice versa, under otherwise realistic imaging conditions (see Fig.1).

Finally, by correlating these findings with thickness-dependent cathodoluminescence measurements, we expose a fundamental trade-off between optical signal strength and atomic-scale interpretability. Our results highlight that atomic-resolution images of single defects in thicker hBN samples may look convincing while being fundamentally misleading. We therefore argue for extreme caution when correlating STEM contrast with single-photon emission, and emphasize the necessity of complementary techniques, knowledge of common artifacts, and realistic expectations of what ADF-STEM imaging can reveal.

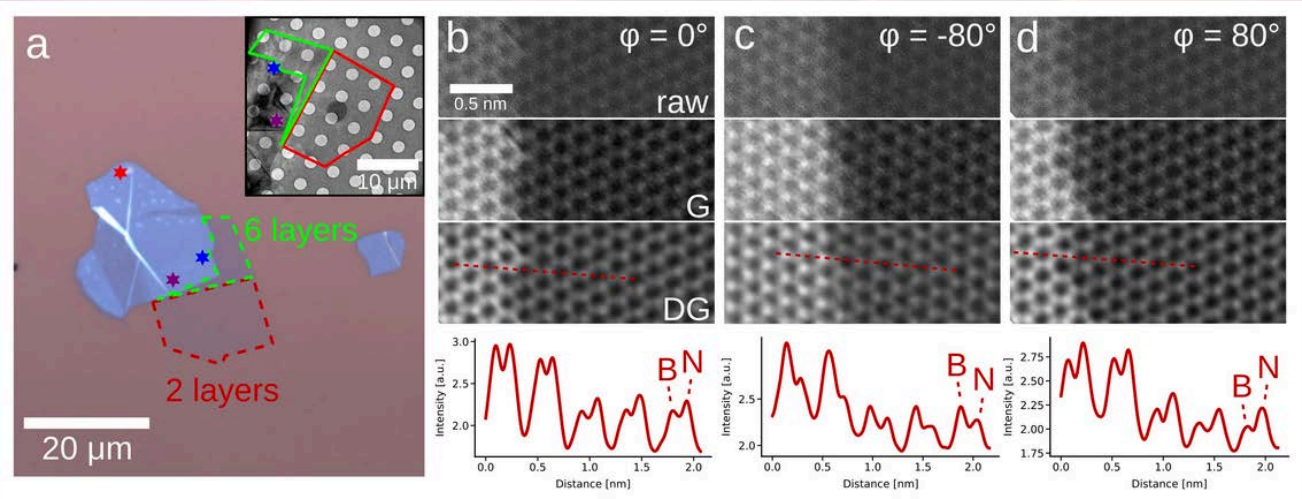


Fig.1: **a** Optical microscopy image of a flake with different layer numbers. **b** Atomic scale ADF-STEM image of astep between mono and bi-layer without detuning of threefold astigmatism. **c** Same area with 132 nm threefold detuning, reversing the BN contrast. **d** Same area with detuning turned by 180°, enhancing BN contrast.

We thank our sponsors for their financial support to enable this event